Transponder Tunability and Waveband Switching in Reconfigurable Optical Networks

by Onur Turkcu

2003, B.S. Degree in Electrical and Electronics Engineering,
Boğaziçi Üniversitesi, İstanbul, Türkiye

2005, M.S. Degree in Telecommunications & Computers,
The George Washington University, Washington, DC USA

A Dissertation submitted to

The Faculty of
The School of Engineering and Applied Science
of the George Washington University
in partial satisfaction of the requirements
for the degree of Doctor of Philosophy

August 31, 2009

Dissertation directed by

Suresh Subramaniam
Professor of Engineering and Applied Science

The School of Engineering and Applied Science of The George Washington University certifies that Onur Turkcu has passed the Final Examination for the degree of Doctor of Philosophy as of June 25, 2009. This is the final and approved form of the dissertation.

Transponder Tunability and Waveband Switching
in Reconfigurable Optical Networks

Onur Turkcu

Dissertation Research Committee:

Suresh Subramaniam, Professor of Engineering and Applied Science,
Dissertation Director

Hermann J. Helgert, Professor of Engineering and Applied Science,
Committee Member

Milos Doroslovacki, Associate Professor of Engineering and Applied Science,
Committee Member

Hyeong-Ah Choi, Professor of Engineering and Applied Science,
Committee Member

Dr. Sashi Thiagarajan, Principal Engineer, Ciena Corp., Linthicum, MD,
Committee Member

Acknowledgments

First and foremost, I would like to thank my thesis advisor Prof. Suresh Subramaniam for his invaluable guidance throughout this dissertation. It was a wonderful learning experience for me. I had the great opportunity to discuss any part of my research with him in great detail and he always made time for any question I had.

I wish to thank my committee members Prof. Hermann J. Helgert, Prof. Milos Doroslovacki, Prof. Hyeong-Ah Choi, and Dr. Sashi Thiagarajan for their advice and constructive criticism. They enlightened me a lot with the courses I have taken from them. I am grateful to Prof. Helgert for creating the opportunity for me to join George Washington University as a Masters student. I would additionally like to thank our Department Chair, Prof. Can Korman for his continuous help throughout my education. It was a pleasure to work as a teaching assistant at the ECE Department.

I acknowledge the support of the National Science Foundation in the research conducted in this thesis.

I also would like to thank my friends Arush Gadkar, Majid Al-Naimi,and Amir Askarian at the Optical and Wireless Networks Laboratory for the research environment they created which was both motivating and fun.

Finally, I would like to give my special thanks to my family for all their support during my doctoral education. I would not be here without them.

Abstract of Dissertation

Transponder Tunability and Waveband Switching in Reconfigurable Optical Networks

We investigate the blocking performance of all-optical reconfigurable networks with constraints on reconfiguration brought by Reconfigurable Optical Add/Drop Multiplexers (ROADMs) and tunable transponders. Considering a fully reconfigurable ROADM and limited tunable transponders at each ROADM port, we develop an analytical model to calculate call blocking probability in a network of arbitrary topology for two different models for transponder sharing within a node: Share-Per-Link and Share-Per-Node. In such a configuration, limited tunable transponders determine the set of wavelengths that can be added/dropped at a reconfigurable node. A lightpath can only be established if a transponder on both ends can tune to the same available wavelength along the route. We call this as *wavelength termination constraint*. The number of transponders (as many as ports) and the waveband size (the range of wavelengths over which a transponder is tunable) are the key parameters of the model assuming that wavebands are randomly assigned to transponders. We also present a heuristic algorithm for assigning wavebands to transponders at each node and modify the analytical model to approximate the performance of the algorithm. We present simulation results to validate our model and also show results for Share-Per-Link and Share-Per-Node models with various sets of parameters. We show that limited tunable transponders give the same performance with widely tunable transponders in terms of blocking. We also show that transponder wavelength/waveband assignment to limited tunable transponders is an important factor determining the blocking. We then show several algorithms for transponder wavelength/waveband assignment considering different kinds of traffic models (e.g., non-uniform traffic). With simulation results, we show that these algorithms improve the blocking performance of the network significantly. We then consider O-E-O conversions enabled in the network by the use of limited tunable transponders. Using two limited tunable transponders, first to drop a wavelength and then to add another wavelength at a node, a lightpath can be established on different wavelengths along its route. We call this technique *multihopping*. We develop several routing and wavelength assignment algorithms for fixed and alternate routing in order to find the nodes to do the

O-E-O conversions if necessary. Using a graph model, these algorithms determine the best route on which the transponder and wavelength resources are the least exhausted. Finally, we investigate the waveband switching technique to reduce the switching costs of the network. In waveband switching, wavelengths are grouped and switched together as a waveband. We solve an optimization problem to find the minimum total number of wavebands required in a ring network. We show by numerical analysis that the sizes of switches can be reduced by a large amount using waveband switching compared to wavelength switching. Overall, this dissertation provides a detailed analysis on the performance of reconfigurable optical networks and investigates several design methods to improve the performance and reduce the cost.

Table of Contents

List of Figures

List of Tables

List of Acronyms

FT	Fixed Transponder
FOADM	Fixed Optical Add-Drop Multiplexer
LTT	Limited Tunable Transponder
MG-OXC	Multi-Granular Optical Cross-Connect
OADM	Optical Add-Drop Multiplexer
O-E-O	Optical-Electrical-Optical
ROADM	Reconfigurable Optical Add-Drop Multiplexer
SPL	Share-Per-Link
SPN	Share-Per-Node
TEF	Tunable Edge Filter
WB	Wavelength Blocker
WDM	Wavelength Division Multiplexing
WSS	Wavelength Selective Switch
WTT	Widely Tunable Transponder

Chapter 1

Introduction

The demand for faster and at the same time cheaper communications has resulted in continuously evolving communication networks. First starting with copper wires, the technology long ago enabled the use of glass wires (i.e., fiber optic cables) as communication medium. There are currently fiber optic networks built all over the world covering landmasses as big as countries. Optical networks are used as the backbone of most telecommunication networks today due to their high capacity to carry information. The high capacity of an optical fiber is efficiently utilized by the Wavelength Division Multiplexing (WDM) technology in which multiple users are multiplexed onto the same fiber to efficiently utilize the whole bandwidth available. Each user occupies a separate frequency band, called *wavelength*. WDM networks have been widely used in the lowest level of communication networks hierarchy (a common hierarchy is IP/ATM/SONET/WDM). Tse in [1] mentioned that the data demand for AT&T's backbone network had tripled over the last four years. AT&T's network has more than a half million fiber miles operating at a 40 gigabit-per-second (Gbps) transport capacity. They project the IP traffic to be 5600 percent greater than today in 2018 and AT&T is aiming to achieve 114 Gbps capacity on each wavelength transporting a total capacity of 17 Tbps over a single strand of optical fiber.

The optical circuit (*lightpath*) establishment requires not only the selection of routes but also the selection of the wavelengths on which the lightpath is to be set up. This problem is known as the Routing and Wavelength Assignment (RWA) problem. In the absence of wavelength conversion capability, a lightpath traverses each fiber link along its path on the same wavelength. However, wavelength conversion brings the ability to change the wavelength of the lightpath by wavelength converters along the path. Therefore, a lightpath does not require to be wavelength-continuous end-to-end.

At the source node of a lightpath, the assigned wavelength has to be added on the

fiber while at the destination node it has to be dropped. The add/drop functionality of optical nodes is provided by components called Optical Add/Drop Multiplexers (OADM). They add/drop certain wavelengths and bypass the others. With OADMs, optical-electrical-optical (O-E-O) conversion is not necessary [2]. Most of today's optical networks are still either point-to-point WDM links or *static (non-reconfigurable)* networks wherein lightpaths connecting edge nodes and carrying client traffic are statically provisioned up front using Fixed Optical Add-Drop Multiplexers (FOADMs) that allow specific wavelengths to be added/dropped at nodes. While such a solution incurs relatively low capital expenditures (CapEx), the operational expenditures (OpEx) involved in reconfiguring the network are quite high. Any change in the lightpath topology requires manual reconfiguration employing additional equipment and personnel. This is not only time-consuming and costly, but also error-prone.

The companies who build and operate such networks also face the problem of designing their networks such that the capacity is efficiently utilized and also providing a cheaper but more flexible service. By flexible service we mean the adaption of the network to changes in data demands easily without incurring significant additional costs. Recent advances in optical technology and corresponding decreases in equipment costs together with increasing traffic demand have made carriers to look into deploying *agile* or *reconfigurable optical networks*. In such networks, the network can be remotely and quickly reconfigured under software control to dynamically adapt to changes in traffic demands. Thus, a network operator may, for instance, be able to create a new lightpath originating at an arbitrary port on a source node, following an arbitrary route, and terminating at an arbitrary destination port on an arbitrary wavelength – all at the click of a button. Such flexibility in network operation is obviously very desirable for carriers, but the flexibility comes at the price of increased CapEx. The OpEx is potentially reduced but the amount of reduction is unclear and carriers have thus far been largely unwilling to make the up-front investment.

Such reconfigurability in a network does not require any pre-planning for the carriers, and lightpaths can be established or torn down within a matter of seconds whenever wanted. The key technology enabling reconfigurability in an optical network is the Reconfigurable Optical Add-Drop Multiplexer (ROADM). Different from FOADMs, ROADMs

do not permanently add/drop the same wavelengths but they can be remotely configured to add/drop different wavelengths at different times. Allowing the bypass traffic to pass through without O-E-O conversion reduces the overall equipment costs and also loosens the capacity bottleneck caused by electrical signal processing [3]. ROADMs enable carriers to offer a flexible service and provide significant savings in OpEx and CapEx [4].It is pointed out in [1] that ROADMs have driven huge costs out of networks more than any other technological advance.

There are several papers in the literature describing various ROADM architectures and technologies [2, 5]. We review the three main ROADM architectures and the corresponding technologies in Section 1.1. ROADM types may differ in wavelength granularity and channel bandwidth. Another important factor is whether they have wavelength specific (colored) or colorless add/drop ports [5]. Different types also have different connectivity capabilities. Connectivity specifies how many optical links a ROADM can support. Accordingly, ROADMs can be classified as 2-degree ROADMs or multiple degree ROADMs. 2-degree ROADMs are most commonly used in ring networks while higher degree ROADMs can be used to physically connect mesh networks. In [4], it is shown that multiple-degree ROADMs enabling interconnection of several ring networks can reduce network cost (CapEx) significantly. A similar categorization of ROADMs is done in [3], and they are compared according to their wavelength routing capabilities. ROADM applications in metro and regional networks and some future network architectures depending on ROADMs are discussed in [6].

In order to achieve full reconfigurability, ROADMs are used in conjunction with tunable transceivers (transponders). Tunable transceivers are required to transmit/receive the added/dropped wavelengths at each ROADM port. They utilize tunable filters and lasers to terminate the drop wavelengths and to launch the add wavelength signals.[1]

[1]Transponders incorporate additional electrical/demultiplexing functions over transceivers; we use the term transponders to represent both.

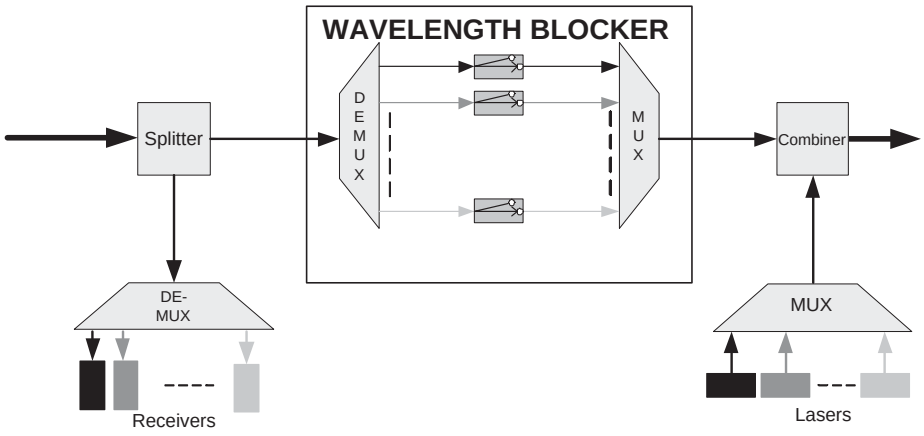

Figure 1.1: A ROADM using the broadcast-and-select architecture.

1.1 Reconfigurable Optical Add-Drop Multiplexers

OADMs have the capability to be remotely reconfigured to add or drop different wavelengths at different times. Such flexibility frees the network operator from extensive preplanning and allows the offering of flexible services to customers, such as *lambda on demand*. ROADMs are built on three different architectures: Broadcast-and-Select, Demux-Switch-Mux and Wavelength Selective Switch (WSS).

In Fig. 1.1, a ROADM using the broadcast-and-select architecture is shown. This architecture consists of a drop module, an add module and a Wavelength Blocker (WB) in between. In the drop module, the incoming fiber is divided into two equivalent signals by a coupler with one of them going to the drop port and the other toward the express path. WB blocks the desired wavelength that is to be dropped and a wavelength is added on the express path from the add ports by using another coupler [5]. A demultiplexer/multiplexer is used in the drop/add port. With this configuration, the ports are colored. In order to have colorless ports, the demultiplexer and the multiplexer need to be replaced with a splitter and a combiner respectively [2, 5]. This architecture has a lower cost but the insertion loss increases with the number of wavelengths dropped [5]. WB is built based on liquid crystal (LC) or MEMS technologies but LC is the lower cost solution. These ROADMs are 2-degree and they cannot be upgraded to support multiple degrees.

ROADMs using the Demux-Switch-Mux architecture use Arrayed Waveguide Gratings (AWGs) for multiplexing and demultiplexing together with switches and attenuators as in

Fig. 1.2. Add/Drop switching follows after demultiplexing the incoming signal. This architecture is built on Planar Lightwave Circuit (PLC) technology. All of the components in this ROADM are integrated on a chip and it is smaller in size. ROADMs in this configuration can drop each wavelength to their specific (colored) ports. However, with the addition of optical switches in the add/drop channels a colorless solution can be obtained. This architecture is also not degree upgradeable [2].

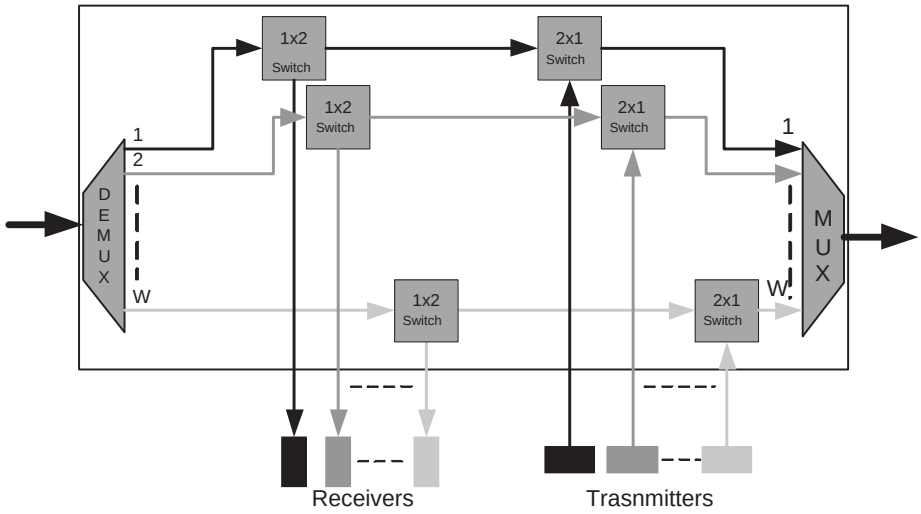

Figure 1.2: A ROADM in demux-switch-mux architecture.

ROADM using the WSS architecture is the most attractive solution today due to its full reconfigurability (i.e., colorless ports). ROADMs using this architecture are mostly built on MEMS technology but with recent advances, WSS architectures have been built with LC technology as well. A MEMS spatial switching element is used to switch any wavelength to any of the ports as in Fig. 1.3. The first WSS module handles switching to the drop ports while the second WSS module switches wavelengths from the add ports to the output fiber. Optical branching is easier in WSS ROADMs; it can support up to 8 degrees. A hybrid architecture consisting of one WSS module with colorless drop ports and colored add ports or vice versa is proposed in [7].

In terms of wavelength granularity, WB ROADMs may have a channel spacing as low as 25 GHz, whereas PLC-based ROADMs have 100GHz, and WSS ROADMs have 50 to 100 GHz channel spacing.

Another factor determining reconfigurability is the transponders used at the add/drop

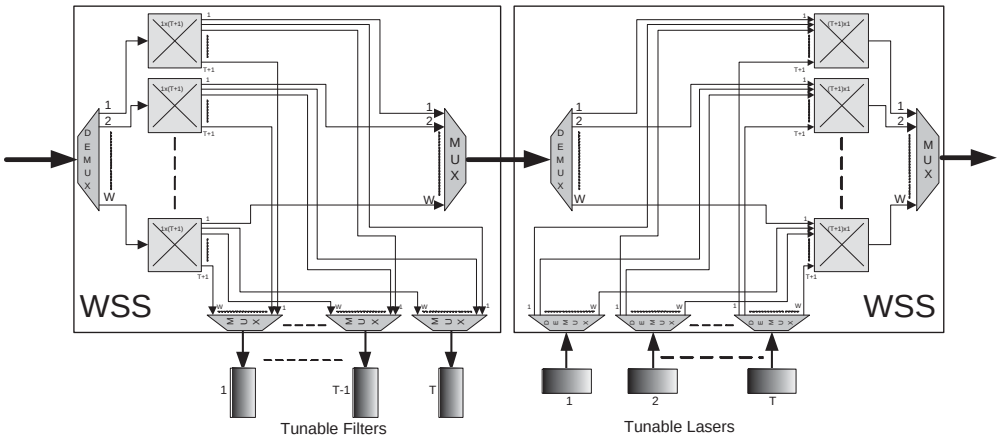

Figure 1.3: A ROADM using the wavelength selective switch architecture.

ports. We can classify the transponders into three categories: (1) Fixed Transponders (FT), (2) Limited or Narrowly Tunable Transponders (LTT) and (3) Widely Tunable Transponders (WTT). Fixed tunable transponders transmit or receive at fixed wavelengths which cannot be changed dynamically whereas tunable transponders can be tuned to different wavelengths. Widely tunable transponders have the ability to tune to the entire range of C-band wavelengths ($\sim$1530 to $\sim$1565 nm) and sometimes even to the L-band ($\sim$1570 to $\sim$1610 nm) whereas limited or narrowly tunable transponders can only tune to a certain wavelength range within the entire wavelength spectrum. The number of wavelengths a narrowly tunable transponder can tune to can vary, e.g., 4 or 8 wavelengths in a 32-wavelength system. Transponders are expensive components [8] and carriers are likely to employ a pay-as-you-grow strategy in deploying them. This means that initial transponder deployments may be small in number and limited in tunability. In order to achieve full reconfigurability, the transponders at the colorless ports of a ROADM should be tunable. Tunable transponders can reduce the inventory costs significantly since one transponder can be used for more than one wavelength. In [9] it is shown that LTTs result in more inventory savings than WTTs. LTTs are currently available in the market from several equipment providers. For example, Finisar have transceivers using chirp-managed laser technology called CML transceivers (model no. DM80-01-3/4, DM200-01-3/4) which can tune to 2, 4 or 8 wavelengths within the C-band or the L-band [10]. Customers can order such transceivers that are tunable to their desired wavebands. Moreover, limited tunable

transponders have a lower cost than widely tunable transponders.

There are two models considering the use of transponders within a reconfigurable node. In the first model, there are dedicated transponders for each link's corresponding add/drop ports. This model is called Share-Per-Link (SPL) and it is illustrated in Fig. 1.4 (a). On the other hand, Share-Per-Node (SPN) model allows sharing of transponders within a node among all of the links connected to it. Every add/drop port of any outgoing/incoming link is connected to an optical switch as seen in Fig. 1.4 (b) and the optical switch can connect any of these ports to any of the transponders.

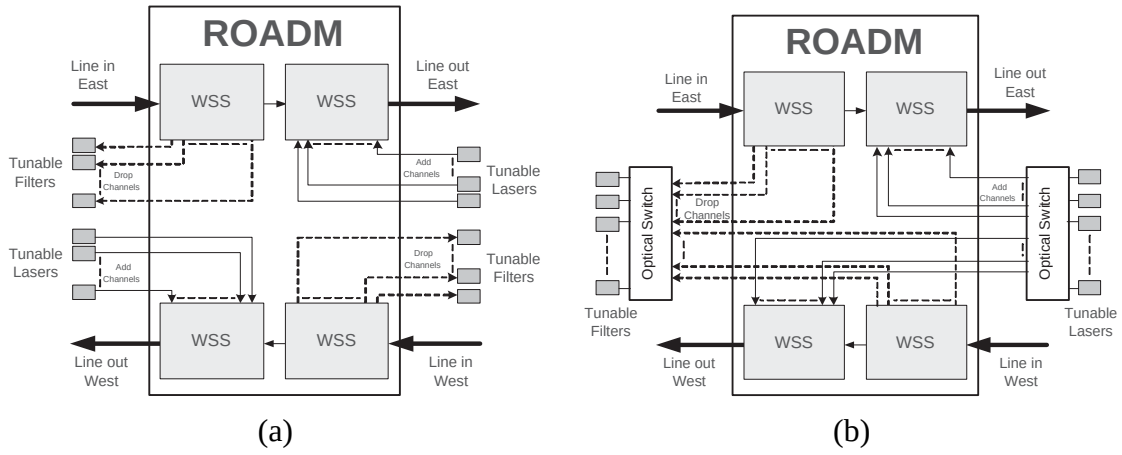

Figure 1.4: SPL and SPN transponder models.

1.2 Wavelength Conversion

The lightpaths considered have to be wavelength-continuous end-to-end along a route with the *wavelength continuity constraint*. We can relax this constraint, if we allow wavelength conversions along the route. Wavelength conversions can be done in an all-optical way or by using a technique called O-E-O conversion. O-E-O conversion is done by dropping a wavelength at a ROADM and after conversion to electric signal by a transponder, the ROADM adds the signal on another wavelength using another transponder. Wavelength conversion is studied extensively in the literature considering full, limited and fixed wavelength conversion [8]. In full wavelength conversion, a node is capable of changing an incoming wavelength to any outgoing wavelength.

1.3 Waveband Switching

The rapid increase in data demand calls for increasingly higher number of wavelengths in an optical fiber, requiring a higher switching complexity of optical cross-connects. The idea of waveband switching is introduced to reduce the size of the optical cross-connects by grouping the wavelengths into a waveband. Wavebands are routed and switched together as a band occupying only one port in all-optical cross-connects along the path. Multi-granular optical cross connects (MG-OXC) have the ability to switch at fiber, waveband and wavelength levels [11]. Several multi-granular architectures are also proposed in [12], [13], [14], [15]. It is shown that by efficient waveband grouping algorithms the switching complexity can be reduced significantly [16, 17, 18].

Waveband switching strategies can be categorized into two: 1) End-to-End grouping, 2) Intermediate grouping. The former one allows grouping of lightpaths into wavebands only if they have the same terminal nodes while the later allows grouping of several lightpaths in an intermediate node.

Waveband sizes can also be uniform and non-uniform. In the uniform case, every waveband contains the same number of wavelengths, whereas wavebands may have different sizes in non-uniform waveband switching. Non-uniform wavebands are considered in [18], [19] where optimal ways of partitioning the wavelength set into wavebands are shown for various network and traffic models.

1.4 Motivation

1.4.1 Performance of Limited Reconfigurable Networks

In order to quantitatively illustrate the benefits of reconfigurability considering different levels of reconfiguration in an optical network, we develop an analytical model in Chapter 2 and conduct simulations to obtain the blocking performance. We consider a dynamic traffic model where lightpath establishment and teardown requests arrive according to a stochastic process. If an arriving lightpath request cannot be established by the reconfigurable network (without changing the already established lightpaths), then it is blocked.

The blocking metric used together with such a stochastic model is widely used in the literature in the context of optical networks. We consider a fully reconfigurable ROADM (i.e., WSS ROADM) with limited tunable transponders at the colorless ports. ROADMs with colored ports can also be adapted into our model by considering only fixed tunable transponders at the add/drop ports.[2] Limited reconfigurability in such a network is the result of limited tunability of transponders. The actual constraint on wavelengths which can be received/transmitted by a node comes from the limited tunable transponders. At each port there is a limited tunable transponder that can add/drop only a certain set of wavelengths. These wavelengths actually determine if a lightpath can be originated or terminated at that node. We call the constraint brought by tunable transponders on the add/drop capability of a reconfigurable node as *wavelength termination constraint*. Key parameters directly affecting blocking are the number of transponders (ports) that a ROADM has and the wavelength range over which narrowly tunable transponders are tunable. Our analytical model is based on these parameters as well as the number of wavelengths in the system and traffic loads on each route.

1.4.2 Transponder Wavelength/Waveband Assignment

Noting that we can only set up a lightpath between the nodes each having a transponder tunable to the same wavelength, we focus on how to choose these wavebands/wavelengths for the transponders at each node to improve the blocking. Having observed in Chapter 2 that blocking directly depends on the strategy of how we choose these wavebands, in Chapter 3 we show several waveband/wavelength assignment strategies based on heuristics for uniform and non-uniform traffic models. The main idea for improving blocking is that at the end nodes of a lightpath, transponders should have as many wavebands in common as possible and at the same time the availability of the wavelengths of common wavebands should also be improved on the links along that path. We include optimal formulations of wavelength assignment for the transponders to reduce the blocking for other traffic models.

[2] FOADMs and limited ROADMs can also be modeled by using appropriate limited tunable transponders.

1.4.3 Alternate Multihop Routing

The effects of wavelength conversion (all optical or O-E-O) on network performance are studied extensively in the literature. However, none of these studies looked at the performance of the network when O-E-O conversions are enabled by limited tunable transponders in the network. The challenge in O-E-O conversion with LTTs is that O-E-O conversion cannot be done from every wavelength to every other wavelength at a node but it can only done from a wavelength that one LTT is tunable to to another wavelength that another LTT can tune to. The routing decision in this case should be based on these constraints brought by LTTs. We develop several algorithms to find the best route for the incoming lightpath requests in Chapter 4.

1.4.4 Waveband Switching

The last part of the dissertation focuses on reducing the switching costs in a network by using waveband switching. Generally each ROADM has one switching element per wavelength. If some lightpaths are grouped and switched together using one switching port at a ROADM, then fewer switching elements may be sufficient. Using waveband switching, we can achieve a reduction in switching complexity of ROADMs and hence reduction in costs. We propose a ROADM architecture that does waveband switching by using non-uniform wavebands and the size of these wavebands can be dynamically adjusted. In Chapter 5, we define an optimization problem with the objective of minimizing the total number of wavebands (i.e., switching elements) used at all ROADMs in the network.

Chapter 2

Performance of Limited Reconfigurable Optical Networks

Reconfigurable optical networks allow remote adjustment lightpaths by a central software control. New lightpath requests are established in the network by remotely configuring the ROADMs without rearranging the existing lightpaths. We analyze in this chapter how much reconfigurability is necessary in optical networks and whether limited reconfigurability can be as good as full. A fully reconfigurable ROADM (e.g. WSS ROADM) together with widely tunable transponders at its ports constitutes a fully reconfigurable node. However, if we use limited tunable transponders, the node becomes limited reconfigurable in the sense that not every wavelength can be added/dropped at every port. We develop an analytical model taking into account the number and tuning range of limited tunable transponders at each node. Two models of transponder usage in a node, Share-Per-Link (SPL) and Share-Per-Node (SPN) are considered separately in the following sections. A new ROADM architecture with limited reconfigurability is also introduced in Sec. 2.2.

2.1 Previous Work

There is very little previous work in the literature analyzing the performance of reconfigurable optical networks considering ROADMs and tunable transponders. In [20], the authors quantified the relationship between the number of fully reconfigurable OADMs that can be replaced by limited ROADMs (that can add/drop wavelengths only over a limited range) and the tuning range for static all-to-all traffic. In [21] authors consider the tuning process of ROADMs with the constraint that it does not interfere with working wavelengths and provides heuristics to avoid such interference. In [22], blocking performance of WDM

networks with limited tunable transponders is investigated. It is shown by simulation results that a network with limited number of transponders with limited tunability at each node can perform close to the case with full number of widely tunable transponders. The same authors developed an analytical model in [23] considering widely tunable transponders at the add/drop ports and showed that a limited number of add/drop ports is sufficient. In [24], for fully reconfigurable networks with limited ports and non-reconfigurable networks, an analytical model is developed for blocking only for ring topology.

On the other hand, wavelength blocking performance has been studied widely in the literature (e.g., [25, 26, 27, 28, 29, 30]). All of these papers consider *wavelength continuity constraint* which requires a lightpath to be routed using the same wavelength end-to-end when wavelength converters are not present.

2.2 Network and Traffic Model

There are N nodes in the network which are numbered $1, 2, \ldots, N$, and L bi-directional links interconnecting them (i.e., each link has two fibers in opposite directions). Each fiber carries W wavelengths. D_n denotes the number of links that a node is connected to or the degree of node n, $1 \leq n \leq N$. For any node, we denote the number of transponders per degree by T. Therefore, there are T transponders dedicated for each link connected to a node in the SPL Model. There are totally $T_n = D_n \cdot T$ transponders shared within a node n in the SPN model. By this way, the total number of transponders at a node is equal in both SPL and SPN and this enables us to make a fair comparison while presenting numerical results. We have $T \leq W$ for both models, since there is no advantage offered by having more transponders than wavelengths. Transponders at each port are limited tunable transponders. Each transponder is tunable to a contiguous set of wavelengths (waveband) of the same size. We call the size of this set as *tuning range* and its value is denoted by Θ. The extreme cases are obtained with $\Theta = 1$ and $\Theta = W$ corresponding to fixed transponders and widely tunable transponders, respectively. The number of non-overlapping wavebands in our system is $K = W/\Theta$. We assume K to be an integer.

The ports with limited tunable transponders do not require a fully reconfigurable ROADM

(i.e., those ports need not be totally colorless). It is sufficient for such ports to be connected only to the wavelength switches that are within the tuning range of those transponders. Therefore, a ROADM with less switching complexity is sufficient which further reduces the cost. We propose the following WSS architecture in Fig. 2.1. The switching complexity is calculated in terms of the number of switching ports of optical switches inside the WSS ROADM. The ROADM can drop wavelengths 1 to Θ to the first port, wavelengths $\Theta+1$ to 2Θ to the second port, and so on. We call this architecture as *Limited WSS ROADM*. Note that if $T\Theta \leq W$, then some of the wavelengths cannot be added or dropped and become bypass wavelengths only. Note that in Fig. 2.1 , we have $T\Theta = W$. In our network, each node is assumed to be equipped with such a limited reconfigurable ROADM.

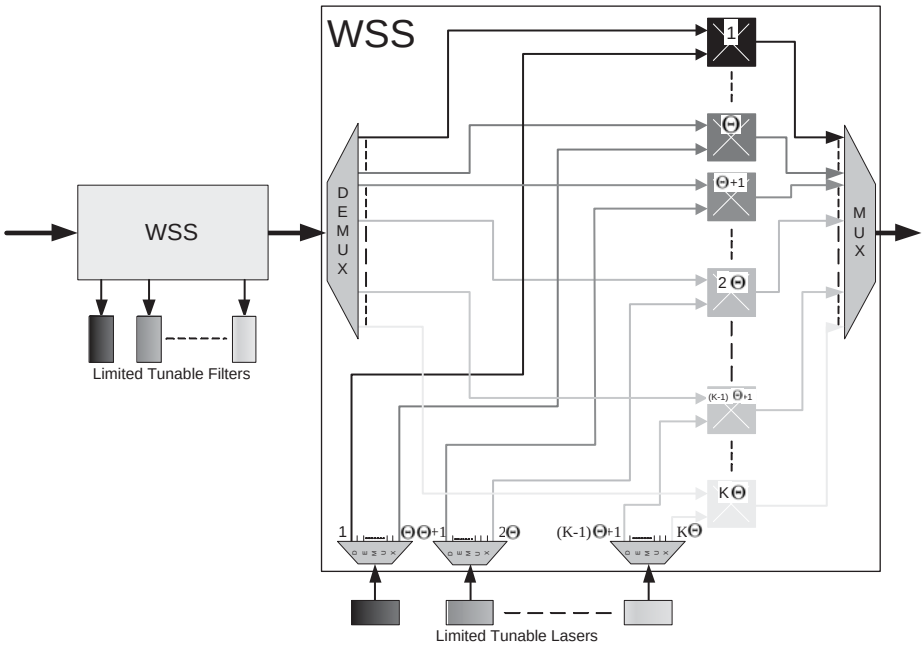

Figure 2.1: A Limited Reconfigurable WSS ROADM.

We calculate the switching complexity of ROADM as the number of switching ports. The switching complexity of the fully reconfigurable WSS ROADM considering only the drop module is $(T+2)W$. Under the random waveband assignment in Section 2.2.2, the switching complexity of a limited WSS ROADM is $3\Theta T$ for $T \leq K$ and $2W + \Theta T$ for $T > K$.

Fixed routes are calculated for every node-pair according to minimum hop routing. The set of routes is denoted by $\mathcal{R}$. Lightpath requests arrive according to a Poisson process at

each route. We assume the same call arrival rate ρ on all routes. This is just for simplicity, and any traffic pattern can be used in our model. Without loss of generality, call durations are exponentially distributed with unit mean. Thus, the Erlang load on each route is ρ.

2.2.1 Lightpath Establishment

When a lightpath request arrives, the set of wavelengths which are available end-to-end and to which a transponder on both ends can tune is found. A wavelength is chosen randomly from this set and the call is established on that wavelength. In this random selection scheme, each wavelength in the set is weighted by the number of available transponders tunable to it at the source node. Other selection strategies can also be applied but our goal is to understand the impact of reconfigurability rather than to examine differences due to wavelength selection policies. Weighting is applied for performance reasons and also to simplify the analytical model. If the wavelength set is empty, the call is blocked and lost.

2.2.2 Transponder Waveband Assignment

In this section, we explain how we choose the wavebands of limited tunable transponders at each node. We adopt a random strategy for this purpose, by which we want to have as many different wavebands as possible at a node. For the SPL model, we do the assignment for every T transponders for each link a node is connected to. There are $\lfloor T/K \rfloor$ transponders assigned to each waveband, and the remaining $b = T \mod K$ transponders are assigned wavebands randomly out of K wavebands without assigning the same wavebands twice. In particular, for the case of fixed transponders, the wavelengths of the T transponders are randomly selected out of the W wavelengths. For $T \leq K$, this scheme becomes completely random assignment.

For the SPN model, the total transponders (T_n) of a node n is chosen in the same fashion explained above. Our analytical model is developed based on this random assignment strategy. However, we examine another assignment strategy in Section 2.4.1 and develop an approximate analytical model for that strategy as well.

2.3 Analytical Model

We derive the blocking probability for a route $R \in \mathcal{R}$ initially for the SPL model. The network blocking is computed as the average of the blocking probabilities over all routes. In Section 2.3.7, we develop a similar analytical model for the SPN model. We start with some assumptions and definitions.

2.3.1 Assumptions and Definitions

Let $R = (l_1, l_2, \ldots, l_H)$ where l_1 is the first link on R, l_2 the second link, etc. Let s and d be the source and destination of route R. Let (s, l_1) denote the source node and the first link of route R, respectively. Throughout this section, random variables are represented using upper-case letters, and their sample values are represented by the same letter in lower-case. We categorize the wavelengths in l_1 into two as following:

1. *Free wavelength*: A wavelength which is not occupied on l_1. We denote the number of such wavelengths as W_f.

2. *Transmittable wavelength*: A free wavelength on l_1 to which an available transponder on s is tunable. The number of transmittable wavelengths is W_t.

The calls using l_1 is also categorized into two:

1. *Originating calls*: Calls starting at s and going onto l_1. Let C_o be the number of *originating calls*.

2. *Passing calls*: Calls going onto l_1 but not originating at s. Let C_p be the number of *passing calls*.

The two kinds of calls are illustrated in Fig. 2.2. In the SPL model, an originating call on l_1 occupies one of the transponders dedicated for the pair (s, l_1). Each of the passing calls and originating calls uses one of the wavelengths in l_1.

Our derivation of blocking probability for R consists of three parts. We first derive the joint distribution of W_t and W_f. The second part utilizes the path model developed in [27]

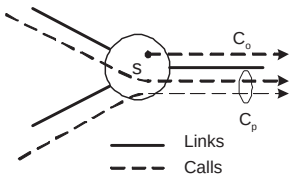

Figure 2.2: Illustration of *originating calls* and *passing calls.*

incorporating link-load correlation effects. Let $(l_1, l_2, \ldots, l_j) \ : \ j \leq H$ be a route segment of R, and redefine the transmittable wavelengths for the segment as the wavelengths available on all links $l_1, l_2, \ldots, l_j$ and to which an available transponder on (s, l_1) can tune. Similarly, redefine free wavelengths as the wavelengths that are not occupied on the last link l_j of the route segment. Then, the path model in [27] can be used to compute the joint distribution of the transmittable and free wavelengths for $j = 2, 3, \ldots, H$, in an iterative manner. In the third part, we find the blocking probability by computing the probability that none of the available transponders on (d, l_H) can tune to any of the transmittable wavelengths. We explain the details below.

2.3.2 The Distribution of W_t

We find the probability that there are w_t transmittable wavelengths on (s, l_1) given that there are c_o and c_p originating calls and passing calls, respectively. Call this probability $P_1(w_t|c_o, c_p)$, and define $a = \lfloor T/K \rfloor$. We know that $b = T \mod K$ wavebands have $a+1$ transponders and the rest have a transponders. We randomly distribute c_o originating calls onto transponders first. Note that, a waveband will be unavailable for transmission, if all of its transponders are occupied. We need to take into account the number of unavailable wavebands as a result of this distribution. Let α_1 and α_2 be the number of wavebands whose $a + 1$ and a transponders, respectively, are fully occupied by some of the c_o calls. We find the number of ways of having exactly α_1 and α_2 unavailable wavebands, which is denoted by $N_2(\alpha_1, \alpha_2|c_o)$. α_1 and α_2 unavailable wavebands are randomly assigned out of b and $K - b$ wavebands respectively. Moreover, none of the remaining wavebands should be fully occupied by the remaining originating calls. Distributing the remaining $c_o'' = c_o - \alpha_1(a + 1) - \alpha_2 a$ calls to the remaining wavebands in such a way constitutes a

balls and urns problem. Consider a set of urns that are arranged as s_1 columns of $a+1$ urns each and s_2 columns of a urns each, for a total of $\eta = (a+1)s_1 + as_2$ urns. Let $\zeta(r, s_1, s_2, a)$ be the number of ways of not filling any column of urns fully when r balls are thrown at random into the urns (no more than one ball per urn). Then,

$$\zeta\left(r, s_1, s_2, a\right) = \begin{cases} 0 & \text{if } r > as_1 + (a-1)s_2 \\ \binom{\eta}{r} & \text{if } r < a \\ \binom{\eta}{r} - \sum_{i=0}^{\mathrm{up}_i} \sum_{j=\mathrm{low}_j}^{\mathrm{up}_j} \binom{s_1}{i}\binom{s_2}{j} \cdot & \\ \zeta(r-(a+1)i-aj, s_1-i, s_2-j, a) & \text{otherwise,} \end{cases} \tag{2.1}$$

where $\mathrm{up}_i = \min\left(s_1, \lfloor \frac{r}{a+1} \rfloor\right)$ and $\mathrm{up}_j = \min\left(s_2, \left\lfloor \frac{r-i(a+1)}{a} \right\rfloor\right)$ and low_j is 1 if i is 0, and 0 otherwise.

Using (2.1), we calculate

$$N_2(\alpha_1, \alpha_2 | c_o) = \binom{b}{\alpha_1}\binom{K-b}{\alpha_2}\zeta\left(c_o'', \alpha_1', \alpha_2', a\right). \tag{2.2}$$

where $\alpha_1' = b - \alpha_1$, and $\alpha_2' = K - b - \alpha_2$.

After the assignment of c_o calls (each also uses a wavelength), c_p calls will be distributed randomly to any of the remaining available wavelengths. Note that some wavelengths in a waveband can still be assigned to a passing call, even if that waveband is unavailable for transmission. Passing calls do not require a transponder but they just use a wavelength. Since we have $T_s \leq W$ for SPL, it can be easily shown that $a+1 \leq \Theta$, which means α_1 wavebands will still have $\Theta - (a+1)$ wavelengths which can be used by a passing call. Similarly, α_2 wavebands have $\Theta - a$ remaining wavelengths for passing calls. Let us denote the passing calls in unavailable and available wavebands by c_p' and $c_p'' = c_p - c_p'$, respectively. Assuming random wavelength assignment, the number of ways this occurs is given by

$$N_3(c_p' | \alpha_1, \alpha_2) = \binom{\alpha_1(\Theta-(a+1)) + \alpha_2(\Theta-a)}{c_p'}\binom{(K-\alpha_1-\alpha_2)\Theta - c_o''}{c_p''}. \tag{2.3}$$

The number of transmittable wavelengths can be calculated using the values of α_1, α_2, c_p'',c_o'' as $w_t = (K-\alpha_1-\alpha_2)\Theta - c_p'' - c_o''$. We illustrate this calculation with an example

in Fig. 2.3 with the parameters $T = 10, \Theta = 4, W = 16$. We have $K = W/\Theta = 4$, $a = \lfloor T/K \rfloor = 2$, and $b = T \mod K = 2$. Therefore, there are $a + 1 = 3$ transponders for $b = 2$ wavebands, and $2(= a)$ transponders for the other $2(= K - b)$ wavebands. The wavebands are shown as the large rectangles and wavelengths as small rectangles. In the first waveband, 3 originating calls occupy 3 transponders and wavelengths. There is one available wavelength, however it is not transmittable since all 3 transponders in that waveband are occupied. The second and third wavebands are available for transmission since they have an available transponder. One passing call and one originating call occupy two wavelengths in the second waveband, so it has two transmittable wavelengths. In the third waveband, only one wavelength is transmittable. The last waveband is also unavailable for transmission. Therefore, we have $w_t = 3$ transmittable wavelengths in this example. Note that if the passing call in the last waveband was in the second or third waveband instead, then the number of transmittable wavelengths would be one fewer.

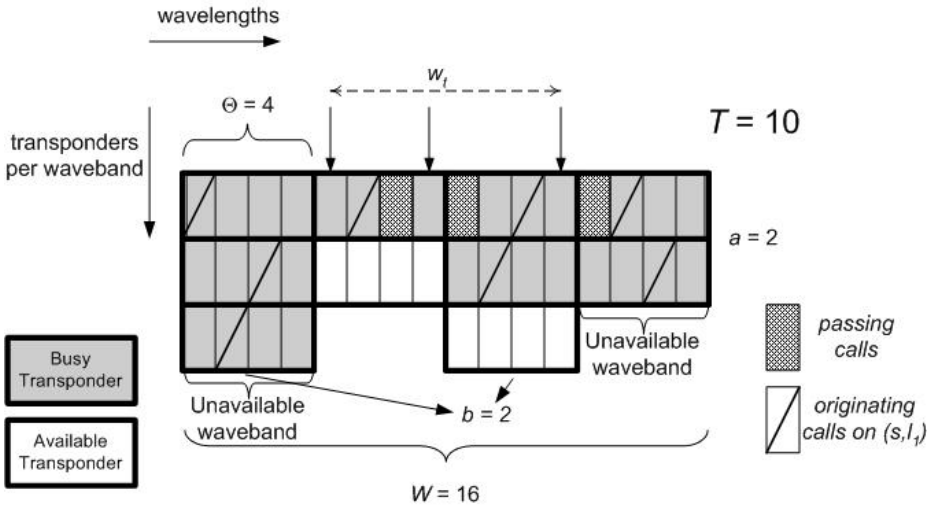

Figure 2.3: An example to illustrate how transmittable wavelengths are determined.

The final expression for the total number of ways of having w_t is calculated as follows:

$$N_4(w_t|c_o, c_p) = \sum_{\{\alpha_1,\alpha_2,c'_p:(K-\alpha_1-\alpha_2)\Theta-c''_p-c''_o=w_t\}} N_2(\alpha_1, \alpha_2|c_o) N_3(c'_p|\alpha_1, \alpha_2), \tag{2.4}$$

for $w_t = 0, 1, \ldots, \min(T\Theta, W)$.

Continuing the analysis, we now consider the overall number of ways of assigning c_o and c_p calls. Each of the c_o and c_p calls is on a different wavelength, and each of the c_o

calls takes up a transponder on (s, l_1). Because of random wavelength/band assignment to transponders and random wavelength assignment to calls, the total number of distinct ways in which transponders are assigned to the c_o calls and the $W - c_o$ wavelengths to the c_p calls is

$$N_1(c_o, c_p) = \binom{K}{b}\binom{T}{c_o}\binom{W - c_o}{c_p}. \tag{2.5}$$

The probability that there are w_t transmittable wavelengths given c_o originating and c_p passing calls is given by

$$P_1(w_t|c_o, c_p) = \frac{\binom{K}{b} N_4(w_t|c_o, c_p)}{N_1(c_o, c_p)} = \frac{N_4(w_t|c_o, c_p)}{\binom{T}{c_o}\binom{W-c_o}{c_p}}. \tag{2.6}$$

The multiplication by $\binom{K}{b}$ in the numerator of (2.6) is to account for the random choice of the wavebands which have an extra transponder.

Special Cases:

1. When $\Theta = 1$, we have $\alpha_1 = c_o$ and $\alpha_2 = W - T$, and $\zeta(.) = 1$.

   Using these values, (2.6) simplifies to:

   $$P_1(w_t|c_o, c_p) = \frac{\binom{W-T}{w_t+c_o+c_p-T}\binom{T-c_o}{w_t}}{\binom{W-c_o}{c_p}}. \tag{2.7}$$

   This can be shown to be the same as the expression for fixed transponders in [31].

2. When $\Theta = W$ as in widely tunable transponders, (2.6) reduces to: For $c_o = T$, $P_1(w_t = 0|c_o, c_p) = 1$ and 0 otherwise, and for $c_o < T$, $P_1(w_t = W - c_o - c_p|c_o, c_p) = 1$ and 0 otherwise.

2.3.3 The Joint Distribution of C_o and C_p

In this section we calculate the joint distribution of the passing calls and the originating calls on the first link l_1. Due to the assumption that calls arrive at each route according to a Poisson process, we can model passing calls and originating calls as a 2-dimensional Markov chain. The state space for this model is shown in Fig. 2.4. ρ_o and ρ_p are the Erlang loads of originating and passing calls, respectively, on l_1 of route R. These can be easily obtained because the routing is fixed and the loads on routes are given.

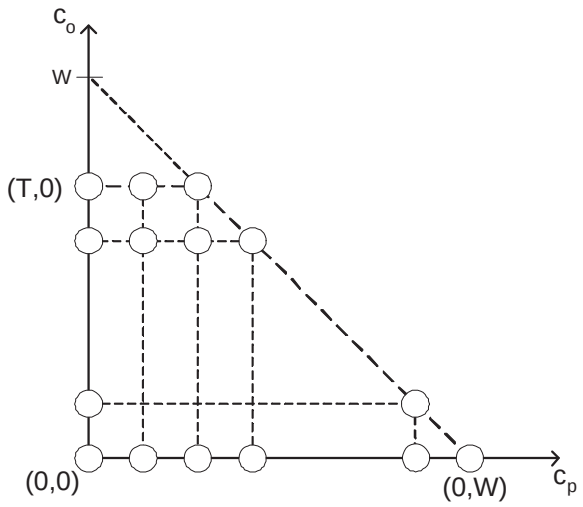

Figure 2.4: State space for the 2-Dim Markov chain of C_o and C_p.

This distribution is calculated as follows.

$$P_2(c_o, c_p) = \frac{(\rho_o^{c_o}\rho_p^{c_p})/(c_o!c_p!)}{\Delta} \tag{2.8}$$

where the normalization factor Δ is obtained by

$$\Delta = \sum_{c_p=0}^{\min(W,T_p^{\max})} \sum_{c_o=0}^{\min(W-c_p,T)} (\rho_o^{c_o}\rho_p^{c_p})/(c_o!c_p!). \tag{2.9}$$

$T_p^{\max}$ in (2.9) is an upper limit on the number of passing calls. This upper limit is determined by the total number of transmitters of distinct node-link pairs (s', l_1') from which a route $R' \in \mathcal{R}$ originates, and R' passes through link l_1 in SPL. If there are e such pairs, then $T_p^{\max} = eT$.

2.3.4 The Joint Distribution of W_t and W_f

Using P_1 and P_2, the joint distribution of W_t and W_f can be calculated by the following equation:

$$P_3(w_t, w_f) = \sum_{c_o=0}^{T} P_1(w_t|c_o, c_p)P_2(c_o, c_p), \tag{2.10}$$

where $c_p = W - c_o - w_f$.

2.3.5 Extension to Last Link of Route

Using $P_3(w_t, w_f)$ from the previous section, our goal is to obtain the the joint probability of transmittable wavelengths over the entire route R and free wavelengths on the last link l_H. Calculating the distribution of the number of transmittable wavelengths and free wavelengths for every route segment (denoted by $P_3^{(i)}(w_t, w_f)$) iteratively, we finally obtain $P_3^{(H)}(w_t, w_f)$ on l_H. The iterative method in [27] assumes the wavelength usages on adjacent links are correlated, and the correlation is captured by using the two-link model. This model considers the adjacent link pair (l_i, l_{i+1}) on R and splits the calls using one or both of the links into three parts: (a) C_l is the number of leaving calls, i.e., calls that use l_i and leave the route R at the intermediate node, (b) C_c is the number of continuing calls from l_i to l_{i+1}, and (c) C_n is the number of joining calls, i.e., calls that join route R at the intermediate node and use only l_{i+1}. The Erlang loads for these types of calls can also be readily obtained. Then, the joint distribution of (C_l, C_c, C_n) is obtained in [27] using a 3-D Markov chain approximation. Call this distribution $P_4(C_l, C_c, C_n)$. The additional constraint on (C_l, C_c, C_n) is that their numbers are not only less than or equal to W but also they are limited by the number of transponders at the source nodes of the routes contributing to such calls. Given $P_3^{(i)}(w_t, w_f)$, [27] uses $P_4(.)$ to obtain $P_3^{(i+1)}(w_t, w_f)$.

2.3.6 End-to-End Blocking Probability

Our end-to-end blocking probability calculation is based on the number of free receivers of the (d, l_H) pair, denoted by R_f. Before we find the distribution of R_f, we define *terminating calls* as the calls that go through the link l_H and terminate at the node d. Let C_t be the number of terminating calls and ρ_t be the load of such calls. The definition of the passing calls (C_p) is slightly modified to be the calls passing through l_H but not terminating at the node d and ρ_p is the load. Now we can calculate $P_2(c_t, c_p)$ with those load values and obtain the distribution of R_f conditioned on W_f on (d, l_H) with the following equation

$$P_5(r_f|w_f) = \frac{P_2(T - r_f, W - T + r_f - w_f)}{\sum_{c_p=\max(W-T-w_f,0)}^{W-w_f} P_2(W - c_p - w_f, c_p)}. \tag{2.11}$$

In (2.11), since we have r_f free transponders, then we should have $c_t = T - r_f$ terminating calls, and the value of c_p is calculated as $W - w_f - c_t$.

The probability that there is at least one transmittable wavelength end-to-end can be calculated using the distribution in (2.7) with the given values of r_f and w_t as follows.

$$P_6(.|w_t, r_f) = 1 - P_1(0 \mid T - r_f, W - T + r_f - w_t). \tag{2.12}$$

It involves finding the probability that there is no receivable wavelength (defined similar to transmittable wavelength) and then taking the complement. In this calculation, we include $w_f - w_t$ free wavelengths in the total value of c_p since they also reduce the number of wavelengths on the last link, just like passing calls. Then the non-blocking probability for route R is given by

$$B'_R = \sum_{w_f=1}^{W} \sum_{w_t=1}^{w_f} \sum_{r_f=1}^{T} P_3^{(H)}(w_t, w_f) P_5(r_f|w_f) P_6(.|w_t, r_f),$$

and the blocking probability is $B_R = 1 - B'_R$.

2.3.7 Blocking Analysis for the SPN Model

In this section, we apply the above analysis for the Share-Per-Node Model. We first define *total originating calls* as all the calls starting at s and going onto any of the links connected to s. Note that *originating calls* is a subset of the *total originating calls*. C_s denotes the number of *total originating calls* from s. The difference in analysis for SPN is that each of the *total originating calls* occupies one of the transponders which is in the common pool of transponders of s. There are $T_s = TD_s$ transponders at node s. Therefore, the analysis for the number of ways of having exactly α_1, α_2 unavailable wavebands now depends on the value of c_s. We have $N_2(\alpha_1, \alpha_2|c_s)$ in which $a = \lfloor T_s/K \rfloor$and $b = T_s \mod K$.

At this point, we now consider the assignment of c_o calls out of c_s calls. We distinguish between the c_o calls in the unavailable and available wavebands as c'_o and $c''_o = c_o - c'_o$, respectively. The number of ways of having c'_o is given by

$$N_5(c'_o|\alpha_1, \alpha_2) = \binom{\alpha_1(a+1) + \alpha_2 a}{c'_o} \binom{c_s - \alpha_1(a+1) - \alpha_2 a}{c''_o}. \tag{2.13}$$

Note that (2.13) is valid only for the case $T_s \leq W$. If we consider the wavebands having more than Θ total originating calls, then we can only assign at most Θ originating calls to those wavebands. This can only occur for the case $\lceil T_s/K \rceil > \Theta$ which corresponds to $T_s > W$. However, we approximate this case with (2.13).

For the assignment of c_p calls, we have

$$N_3(c_p'|\alpha_1, \alpha_2, c_o') = \binom{(\alpha_1+\alpha_2)\Theta - c_o'}{c_p'} \binom{(K-\alpha_1-\alpha_2)\Theta - c_o''}{c_p''}. \tag{2.14}$$

Then the number of ways of having w_t transmittable wavelengths is given by

$$N_4(w_t|c_o, c_p, c_s) = \sum_{\{\alpha_1,\alpha_2,c_o',c_p':(K-\alpha_1-\alpha_2)\Theta - c_p'' - c_o'' = w_t\}} N_2(\alpha_1, \alpha_2|c_s) N_5(c_o'|\alpha_1, \alpha_2) N_3(c_p'|\alpha_1, \alpha_2, c_o') \tag{2.15}$$

for $w_t = 0, 1, \ldots, \min(T_s\Theta, W)$.

We illustrate this calculation again with a similar example in Fig. 2.5. We have a 2-degree node with $T = 5$ and the total number of transponders is $T_s = 10$. All the parameters are the same as in the previous example for SPL model. We have $c_o = 4$, $c_p = 4$ and $c_s = 8$. c_o calls are distributed among the c_s calls. We assigned some of the c_s calls on the same wavelength since they could be on different links (we can at most make double assignment since the degree of the node is 2). The first waveband is unavailable, since all 3 transponders are occupied by some of the c_s calls. The last waveband also has all two of its transponders occupied. The second waveband is available for transmission since only one of its transponders is occupied. There is one passing call on this waveband. Note that the total originating call does not use a wavelength of the second waveband on this link. Therefore, the number of transmittable wavelengths is 3. The third waveband has one if its transponders free, so it is also available. One passing call and one originating call occupy wavelengths so the number of transmittable wavelengths is 2. We have a total of 5 transmittable wavelengths in this example.

Going back to the analysis, the total number of distinct ways of assigning c_s, c_o and c_p calls (again omitting the restrictions on the assignment of c_o calls) is given by

$$N_1(c_o, c_p, c_s) = \binom{K}{b} \binom{T_s}{c_s} \binom{c_s}{c_o} \binom{W - c_o}{c_p}. \tag{2.16}$$

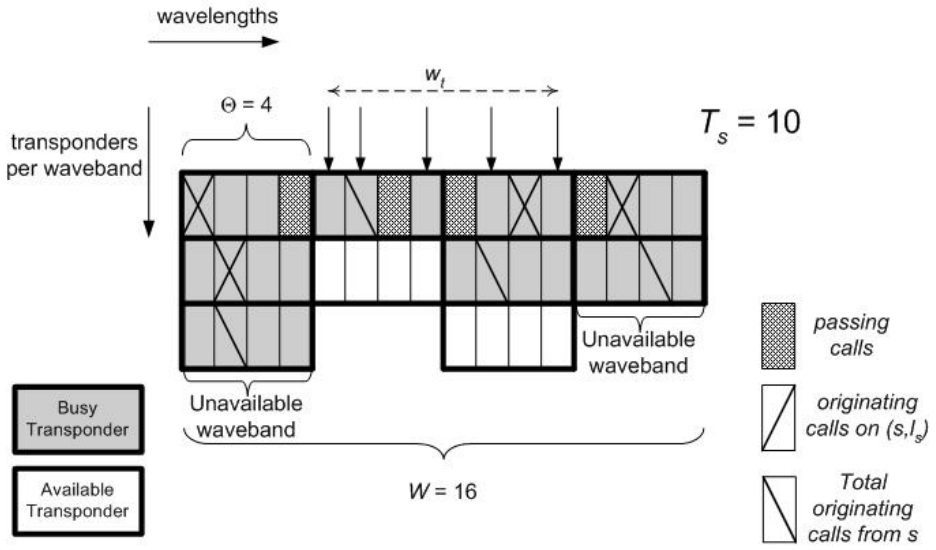

Figure 2.5: An example to illustrate how transmittable wavelengths are determined.

The probability that there are w_t transmittable wavelengths given c_o, c_p, and c_s is obtained from (2.16) and (2.15) (again including the $\binom{K}{b}$ term) as

$$P_1(w_t|c_o, c_p, c_s) = \frac{N_4(w_t|c_o, c_p, c_s)}{\binom{T_s}{c_s}\binom{c_s}{c_o}\binom{W-c_o}{c_p}}. \tag{2.17}$$

For the case $T_s > W$, our approximation in (2.13) and (2.16) does not give accurate results, so we calculate P_1 by the following equation:

$$P_1(w_t|c_o, c_p, c_s) = \frac{N_4(w_t|c_o, c_p, c_s)}{\sum_{w_t=0}^{\min(W,T_s\Theta)} N_4(w_t|c_o, c_p, c_s)}. \tag{2.18}$$

We can obtain special cases of $P_1(.)$:

1. When $\Theta = 1$: (case $T_s \leq W$)

$$P_1(w_t|c_o, c_p, c_s) = \frac{\binom{W+c_s-T_s-c_o}{w_t+c_s+c_p-T_s}\binom{T_s-c_s}{w_t}}{\binom{W-c_o}{c_p}}. \tag{2.19}$$

   For $T_s \geq W$, no simpler solution can be obtained.

2. When $\Theta = W$: For $c_s = T_s$, $P_1(w_t = 0|c_o, c_p, c_s) = 1$ and 0 otherwise, and for $c_s < T_s$, $P_1(w_t = W - c_o - c_p|c_o, c_p, c_s) = 1$ and 0 otherwise.

2.3.7.1 The Joint Distribution of C_o, C_p and C_s

Similarly, we can model C_o, C_p and C_s as a 3-dimensional Markovian model. We define ρ_s as the load for the total originating calls. Let $\mathcal{L}_s$ denote the set of links connected to s including l_1 and let $\rho_{o,i}$ be the loads of originating calls from s on each link $l_i \in \mathcal{L}_s$. Note that $\rho_s = \sum_{l_i \in \mathcal{L}_s} \rho_{o,i}$. The joint distribution is obtained as

$$P_2(c_o, c_p, c_s) = \frac{(\rho_o^{c_o} \rho_p^{c_p} \rho_s^{c_s})/(c_o! c_p! c_s!)}{\Delta}. \tag{2.20}$$

where the normalization factor Δ is obtained by

$$\Delta = \sum_{c_p=0}^{\min(W, T_p^{\max})} \sum_{c_o=0}^{\min(W-c_p, T_s)} \sum_{c_s=c_o}^{\min(T_s, D_s W - c_p)} \frac{\rho_o^{c_o} \rho_p^{c_p} \rho_s^{c_s}}{c_o! c_p! c_s!}. \tag{2.21}$$

In (2.21), $T_p^{\max}$ is determined by the total number of transmitters of distinct nodes s' originating a route. If the set of such nodes is $\mathcal{N}_s$, then $T_p^{\max} = \sum_{s' \in \mathcal{N}_s} D_{s'} T$.

For SPN model, the Markovian model developed is valid only for the case $T_s \leq W$. When $T_s > W$, this model assumes on the other links of s the number of originating calls to be higher than W for some specific values of c_o. For instance, consider the case when $W = 16$, $T = 10$, $d_s = 2$. We have $T_s = 20$. If $c_o = 2$, $c_s = 20$, it means that the number of originating calls on the other link of s is $c_s - c_o = 18$, which is not a possible case because there are only 16 wavelengths per link. However, for $T_s > W$ we are still going to use it as an approximate model. An exact multi-dimensional Markovian model can be developed having two dimensions for originating calls and passing calls per link of a node, however the model would become very complex and we do not pursue it here.

2.3.7.2 The Joint Distribution of W_t and W_f

This distribution is obtained as

$$P_3(w_t, w_f) = \sum_{c_o=0}^{\min(T_s, W)} \sum_{c_s=c_o}^{T_s} P_1(w_t | c_o, c_p, c_s) P_2(c_o, c_p, c_s). \tag{2.22}$$

2.3.7.3 End-to-End Blocking Probability

On the receiver side, we define the calls terminating at the destination node d using any of the links connected to d as *total terminating calls*. Let C_d denoted the number of *total terminating calls* on d. Denote by ρ_t, ρ_p and ρ_d the loads corresponding to terminating calls, passing calls and total terminating calls, respectively. The total number of transponders of the destination node is $T_d = D_d T$. We need the following distributions:

The Distribution of the Number of Free Receivers We can calculate the distribution of the number of free receivers R_f on d and C_p on (d, l_h) by utilizing the distribution in (2.20). P_2 distribution for (d, l_h) also gives the joint distribution of C_t, C_p and C_d on (d, l_h) with load values of ρ_t, ρ_p and ρ_d respectively. Thus,

$$P_5(r_f, c_p | w_f) = \frac{P_2(W - w_f - c_p, c_p, T_d - r_f)}{\sum_{c'_p=0}^{W-w_f} \sum_{c'_s=W-w_f-c'_p}^{\min(T_d, WD_d - c'_p - w_f)} P_2(W - c'_p - w_f, c_p, c'_s)}.$$

Probability of Non-blocking Given W_t, W_f, R_f and C_p We use the distribution in (2.17) using T_d for the number of transponders with the values of *terminating calls, passing calls* on (d, l_h), and *total terminating calls* on d to find the probability of blocking. The corresponding values of c_t and c_d are obtained from w_t, w_f on l_h and r_f on d. Blocking occurs when there is no receivable wavelength on (d, l_h).

$$P_6(\cdot | w_t, w_f, r_f, c_p) = 1 - P_1(0 \mid c_t, W - c_t - w_t, T_d - r_f),$$

where $c_t = W - w_f - c_p$.

Then the non-blocking probability for route R is given by

$$B'_R = \sum_{w_f=1}^{W} \sum_{w_t=1}^{w_f} \sum_{r_f=1}^{T_d} \sum_{c_p=\max(0, W-w_f-T_d+r_f)}^{W-w_f} P_3^{(H)}(w_t, w_f) P_5(r_f, c_p | w_f) P_6(\cdot | w_t, w_f, r_f, c_p),$$

The blocking probability is given by $B_R = 1 - B'_R$.

2.3.8 Model Complexity

In the SPL model, the complexities of the functions N_1, N_2, N_3, N_4, and ζ are $O(TW)$, $O(TW^2)$, $O(W^3)$, $O(TW^5)$, and $O(TW^2)$, respectively. The complexity of P_1 is $O(T^2W)$. The complexity of P_2 for each (s, l_1) pair is $O(TW)$ and for the whole network it is $O(NDTW)$ where D is the maximum degree of all nodes. P_3, P_5, and B'_R have the complexity of $O(TW^2)$ for a route. The complexity of the path model regardless of SPL and SPN models is $O(HW^5)$ for a route of hop-length H. Therefore, in the SPL model, the overall complexity of calculating blocking probability is $O(|\mathcal{R}|\, H_m W^5)$ where $|\mathcal{R}|$ is the size of the set $\mathcal{R}$ and H_m is the maximum hop-length of all routes. The complexity is for one iteration, and we use a reduced load approximation in the next section that requires the blocking probability to be computed for a few iterations before it converges.

In the SPN model, the complexities of the functions N_1, N_2, N_3, N_4, N_5, and ζ are $O(DTW^2)$, $O(DTW^2)$, $O(DW^4)$, $O(DTW^7)$, $O(DW^3)$, and $O(DTW^2)$, respectively. The complexity of P_1 is $O(DTW^3)$. P_2 has the complexity $O(DTW^2)$ for a node and $O(NDTW^2)$ for the whole network. P_3, P_5, and B'_R have the complexity of $O(DTW^3)$, $O(DT^2W^3)$, and $O(TW^3)$, respectively, for each route. Therefore, in the SPN model, the overall complexity of calculating blocking is $O(DTW^7)$.

2.3.9 Reduced Load Approximation

In all of our calculations of the loads in our model, we have used the offered loads on the routes. However the actual load on it is only a portion of the offered load, since some of the calls are blocked due to non-existence of a transmittable wavelength end-to-end. When we use the offered load in the analytical model calculations, the model overestimates the blocking probability due to this effect. Especially in the case of high blocking, the calculated blocking values deviate more from the actual ones. This effect can be overcome by using the well-known reduced-load approximation. First, we calculate the initial blocking probability $B_R^{(0)}$ for route R with the offered load value ρ. Then for every iteration $i = 1, 2, \ldots$ we calculate the new blocking value $B_R^{(i)}$ with the adjusted value of the load $\rho^{(i)} = \rho(1 - B_R^{(i-1)})$. The blocking value converges after a few iterations.

2.4 C-fixed Random Assignment

Our analytical model assumed random assignment of wavebands to transponders as described in Section 2.2.2. With small number of transponders, we have nodes having transponders with wavebands mostly different from the wavebands at the other nodes as a result of this random strategy. Therefore, transponder blocking becomes the main type of blocking in such cases. For instance, the set of transponder wavebands at a source node s of a route R may have no common wavelength with the set of transponder wavebands at the destination node d. If this happens, then every call on R will be blocked. Therefore, the aim of an assignment strategy should be to increase the probability of transponders at different nodes having wavebands in common. Here, we propose an algorithm for this purpose.

Let us define C ($0 \leq C \leq T$) as the number of transponders assigned to the same C distinct wavebands at every node-link pair (n, l_j) in SPL. Similarly for the SPN model, we assign the same C ($0 \leq C \leq TD_{min}$) distinct wavebands to transponders at every node n. Here $D_{min} = \min_{n \in 1,2,\ldots,N} D_n$. For $T \leq K$, the remaining $T - C$ or $T_n - C$ (for SPL and SPN, respectively) transponder wavebands are chosen randomly out of $K - C$ wavebands. For $T > K$, the value of C affects the assignment only if $C > \lfloor T/K \rfloor K$. Then, $T - C$ transponder wavebands are chosen randomly out of $K - T \mod K$ wavebands for the SPL model. The same condition applies for SPN.

Note that if $C = T < K$, then we essentially have a $T \cdot \Theta(< W)$-wavelength system (or if $C = T_n < K$ we have a $T_n \cdot \Theta(< W)$-wavelength system for SPN).

2.4.1 Analytical Model for C-fixed Random Assignment

We modify our earlier analytical model in a simple way to find the blocking probability under C-fixed Random assignment. We first compute $P^{(H)}_{3,\text{fix}}(W_t, W_f)$ for the range of C *fixed* wavebands and $P^{(H)}_{3,\text{ran}}(W_t, W_f)$ for the *randomly* assigned wavebands separately by assuming that $\rho_{\text{fix}} = \rho C/T$ and $\rho_{\text{ran}} = \rho - \rho_{\text{fix}}$ are loads for calls within the two sets of wavebands. Also, the number of wavelengths and transponders used in computing the two probabilities are assumed to be $W_{\text{fix}} = C\Theta$ and $T_{\text{fix}} = C$, and $W_{\text{ran}} = W - C\Theta$ and $T_{\text{ran}} = T - C$, respectively.

In this case, the non-blocking probability expressions for the two ranges are exactly the same (but with different values for the loads, number of transponders, and wavelengths, as explained above). The only difference between the two ranges is that the wavebands of the transponders in the fixed range cover the entire band of wavelengths of size $C\Theta$ in the fixed range, whereas they may not in the random range. These two situations are already accounted for in our analysis for the random assignment. Thus,

$$B'_{\text{fix}} = \sum_{w_f=1}^{W_{\text{fix}}} \sum_{w_t=1}^{w_f} \sum_{r_f=1}^{T_{\text{fix}}} P^{(H)}_{3,\text{fix}}(w_t, w_f) P_5(r_f|w_f) P_6(w_t, r_f),$$

and

$$B'_{\text{ran}} = \sum_{w_f=1}^{W_{\text{ran}}} \sum_{w_t=1}^{w_f} \sum_{r_f=1}^{T_{\text{ran}}} P^{(H)}_{3,\text{ran}}(w_t, w_f) P_5(r_f|w_f) P_6(w_t, r_f).$$

The blocking probability $B = (1 - B'_{\text{fix}})(1 - B'_{\text{ran}})$.

Special Case $\Theta = 1$: The non-blocking probability calculation for the fixed range becomes simpler since it is guaranteed to have a free receiver for any of the transmittable wavelengths along the route due to the fixed assignment. Thus, the non-blocking probability within this wavelength range is

$$B'_{\text{fix}} = \sum_{w_f=1}^{W} \sum_{w_t=1}^{w_f} P^{(H)}_{3,\text{fix}}(w_t, w_f).$$

For SPN, we assume that the degrees of all nodes are the same, for simplicity of explanation. The loads for the two ranges on a route R depends on the total number of transponders (T_n) at the nodes. They are calculated as $\rho_{\text{fix}} = \rho C/T_n$ and $\rho_{\text{ran}} = \rho - \rho_{\text{fix}}$. Different from SPL, we have $T_{\text{ran}} = T_n - C$. We have the following expressions for blocking

$$B'_{\text{fix}} = \sum_{w_f=1}^{W_{\text{fix}}} \sum_{w_t=1}^{w_f} \sum_{r_f=1}^{T_{\text{fix}}} \sum_{c_p=\max(0, W_{\text{fix}}-w_f-T_{\text{fix}}+r_f)}^{W_{\text{fix}}-w_f} P^{(H)}_{3,\text{fix}}(w_t, w_f) P_5(r_f, c_p|w_f) P_6(\cdot|w_t, w_f, r_f, c_p),$$

and

$$B'_{\text{ran}} = \sum_{w_f=1}^{W_{\text{ran}}} \sum_{w_t=1}^{w_f} \sum_{r_f=1}^{T_{\text{ran}}} \sum_{c_p=\max(0, W_{\text{ran}}-w_f-T_{\text{ran}}+r_f)}^{W_{\text{ran}}-w_f} P^{(H)}_{3,\text{ran}}(w_t, w_f) P_5(r_f, c_p|w_f) P_6(\cdot|w_t, w_f, r_f, c_p).$$

2.5 Numerical Results

We apply the blocking analysis for SPL and SPN models and compare it with the actual values obtained from the simulations for two network topologies – 14-node NSFNet topology and a 20-node ring. We assumed a 32-wavelength system ($W = 32$) in our results. We ran simulations using 10^6 call arrivals per trial and 10 trials for each data point. These trials are for averaging out the effect of random waveband assignment used in each trial. The load value we use in our results is the load per route (ρ) as defined in previous sections. All confidence intervals shown are 95% intervals.

We first plot the blocking probability B vs. the load ρ for the ring network with $T = 8$ and $\Theta = 4$ in Fig. 2.6 (a) for SPL and SPN models. We have the same comparison in Fig. 2.6 (b) for NSFNet with $T = 12$. We observe a good match between analytical model and simulation results in both topologies, with results being less accurate for the ring. This reduced accuracy in rings is due to the well-known high load correlation between links [27]. Note that our model only includes correlation between adjacent links. The effect of the increasing load is obvious in all curves. We observe that blocking is lower in SPN than SPL, as expected, in both graphs. Sharing of the transponders within a node offers a significant improvement in blocking. We note that the difference between SPL and SPN is higher at lower loads.

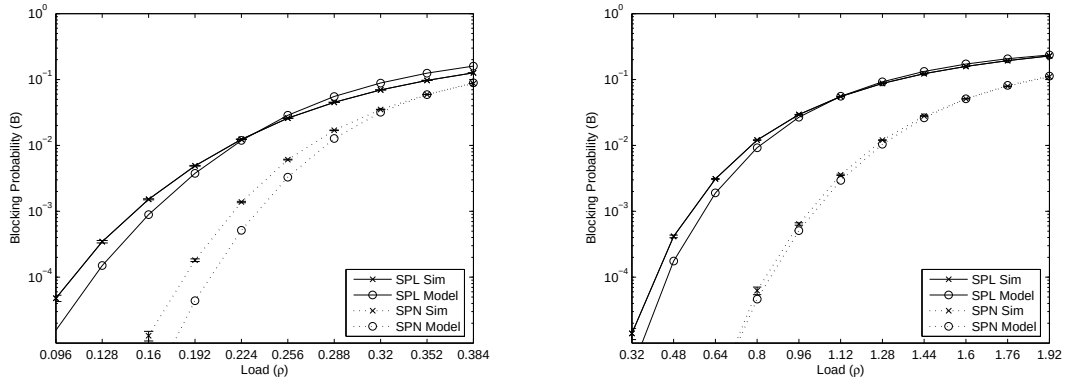

(a) (b)

Figure 2.6: Blocking probability vs. load with $\Theta = 4$ in (a) ring for $T = 8$, and (b) NSFNet for $T = 12$.

We plot B vs. Θ in Fig. 2.7 (a) for various values of T for the ring network. For the value

of $T = 8$, we don't show the model results in order to be able to distinguish between curves. In all of the curves, there is a significant drop in B until the point where $\Theta = 8$, and no further improvement is achieved for larger values of Θ. Limited tunable transponders with a tuning range value of 8 gives the same performance as the widely tunable transponders in the ring network. We also observe a significant difference between SPL and SPN for $T = 8$ at all values of Θ. However, for $T = 12$, the gap between SPL and SPN has diminished and especially for $\Theta \geq 8$ the two models almost give the same results. This is due to the fact that when $T = 12$ there are sufficiently many transponders so that the blocking caused by unavailable transponders (i.e., we call this transponder blocking) is no longer dominant. However, blocking is mainly due to unavailability of wavelengths along the route (i.e., path blocking). Especially with large values of Θ, transponder blocking becomes less and less dominant. We conclude that for such cases SPN model does not offer a big advantage over SPL.

We plot B vs. Θ for for various values of T for the NSFNet in Fig. 2.7 (b). For all of the curves, a significant drop is observed until the value $\Theta = 4$ and after that the blocking is almost exactly the same. In this case, there is also a significant amount of difference between SPL and SPN. For these parameters, in the observed load range, transponder blocking is always dominant in NSFNet. Both results for the ring network and NSFNet show that limited tunability is as good as full tunability. Moreover, some tunability in the network gives much better performance than no tunability.

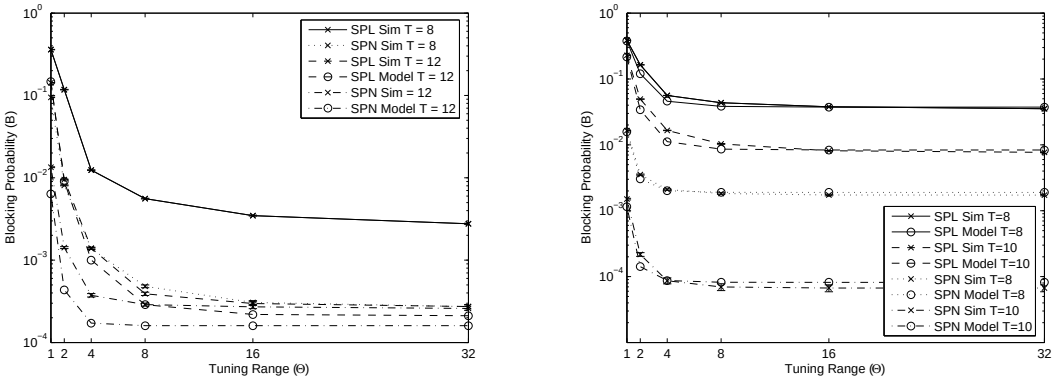

(a) (b)

Figure 2.7: Blocking probability vs. tuning range in (a) ring for $\rho = 0.2240$, and (b) NSFNet for $\rho = 0.64$.

We plot B vs. Θ for SPL model and various values of ρ for the ring in Fig. 2.8 (a). As in previous figures, we observe a significant drop until the value of $\Theta = 8$ for every load value. We note that the difference between the points $\Theta = 0$ and $\Theta = 8$ for the $\rho = 0.192$ curve is more than 3 orders of magnitude. We omit the curves for SPN model here but the results are similar. We show B vs. Θ for both SPL and SPN models with various values of ρ for the NSFNEt in Fig. 2.8(b). Again, for all of the curves, the blocking settles down a value after $\Theta = 4$. We observe the significant difference between the curves of SPL and SPN and note that the gap between them is larger with the lower load value of $\rho = 0.48$.

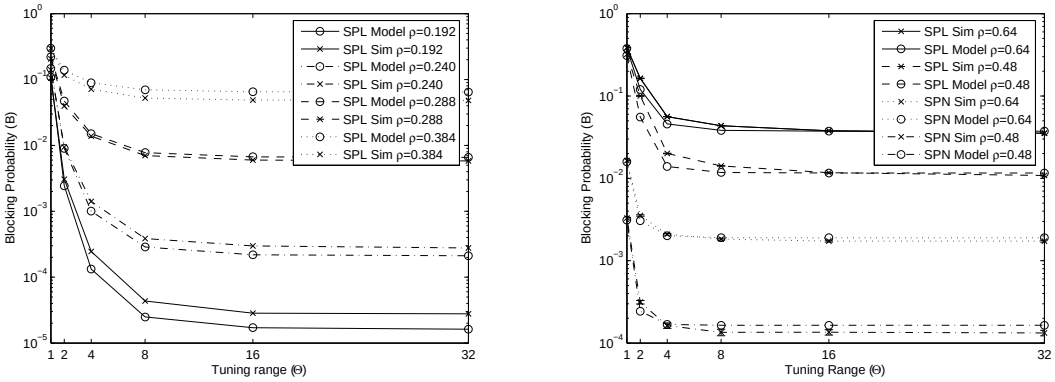

(a) (b)

Figure 2.8: Blocking probability vs. tuning range in (a) ring for $T = 12$, and (b) NSFNet for $T = 8$.

In Fig. 2.9, we plot B vs. T for various values of Θ in the ring network. Fig. 2.9 (a) shows the results for SPL model. The decrease in blocking is more steady for the values of $\Theta = 1$ and $\Theta = 2$. For $\Theta = 2$, the blocking probability settles down after the point $T = 16$. At this point transponder wavebands cover the entire wavelength range ($T\Theta = 32$) and beyond that point path blocking becomes more dominant. Similar behavior is observed for $\Theta = 4$ for which the slope of the curve first slows down after the point $T = 8$ where $T\Theta = 32$, and it settles down at the same level after $T = 16$ where $T\Theta = 64$ is a multiple of 32. For the curve of $\Theta = 8$, blocking settles down after $T = 12$ where $T\Theta = 96$. In Fig. 2.9 (b) we show the same set of curves for the SPN model which have a similar behavior as the SPL model. We observe that the model approximates the blocking less accurately in the SPN case. This is because the SPN model includes one additional

variable *total originating calls*. Because of the extra dimension in the Markovian model for this variable, the Markovian model approximation becomes less accurate.

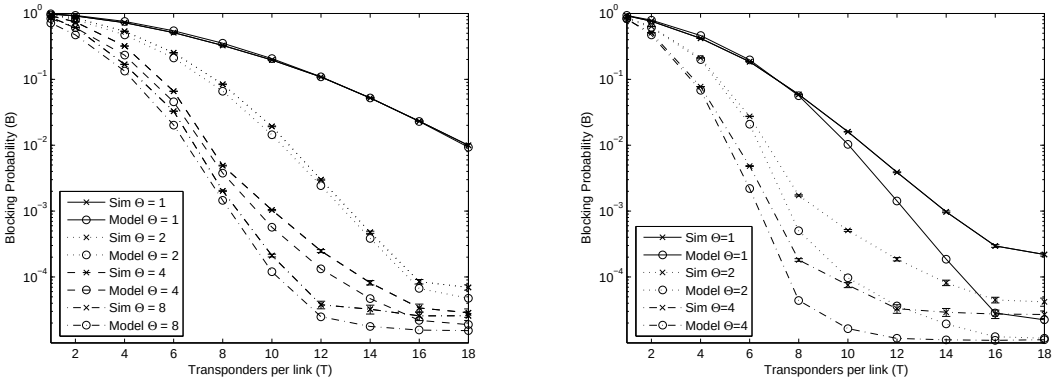

(a) (b)

Figure 2.9: Blocking probability vs. T in ring with load $\rho = 0.192$ (a) for SPL, and (b) for SPN.

In Fig. 2.10 we plot B vs. T for various values of Θ in NSFNet for both SPL and SPN. In all cases, there is a steady and sharp decrease in blocking as T increases. The number of transponders is very important in determining the blocking performance of the network. Even with large values of T, additional transponders still improve the performance. For both sets of curves ($\Theta = 1$ and $\Theta = 4$), the difference between SPL and SPN becomes larger as T increases. This is again due to transponder blocking being always dominant for NSFNet for the load range considered.

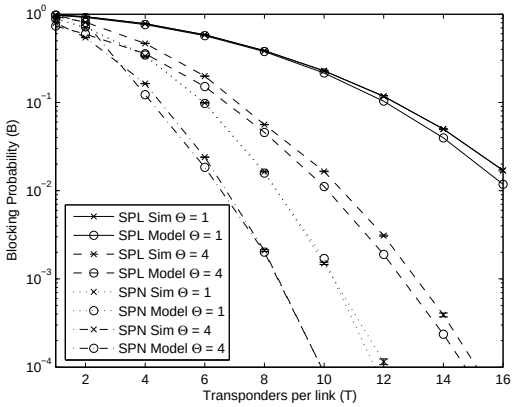

Figure 2.10: Blocking probability vs. T in NSFNet with load $\rho = 0.64$.

We now analyze the effect of transponder waveband assignment in blocking. We first

plot the results of C-fixed random assignment in a ring network for SPL model in Fig. 2.11. With $T = 6$ in in Fig. 2.11 (a), we observe a steady decrease in blocking with increasing C with a load value of $\rho = 0.0256$. Best blocking is achieved with $C = T = 6$ when we have totally fixed assignment of wavebands at every node. The difference between the two end points is significant (e.g., more than two orders of magnitude). We also observe that our approximate model for the C-fixed assignment is very accurate at the end points ($C = 0$ and $C = 8$), and in the mid-points the approximation is still reasonable while following the same trend with the actual curves. With a higher load value of $\rho = 0.096$, we no longer have the decrease in blocking with higher C values. On the contrary, there is initially a slight increase in blocking and with $C = 8$, a slight decrease in the end. The model approximates even the slight changes very accurately. We conclude that in a lightly loaded system such as $\rho = 0.0256$ in our case, to have the same wavebands for the transponders at every node gives much better blocking than totally random assignment. However, as we increase the load, blocking starts to dominate due to limited number of wavelengths utilized. Therefore, having fixed wavebands does not offer any advantage. In Fig. 2.11 (b), we show a case with higher T and Θ, $T = 12$ and $\Theta = 2$. The general trend of the curves is a steady increase in C. A little drop in blocking is observed at the point $C = 12$ for two lower load values, but it does not drop below the value of $C = 0$. With large values of T and Θ, transponders are very likely to have the same wavebands at different nodes with random assignment. As a result, transponder blocking is already low, and with higher C values we increase the load on the fixed wavebands in the network which results in higher path blocking.

In Fig. 2.12, we show similar results for SPN model in a ring with $T = 5$, $\Theta = 2$ and various values of load. For $\rho = 0.072$, blocking decreases with larger C, which is not the case for $\rho = 0.16$. The difference between the blocking values of $C = 0$ and $C = 10$ is smaller than in SPL in this case; however the same amount of difference can be obtained with lower values of T in SPN.

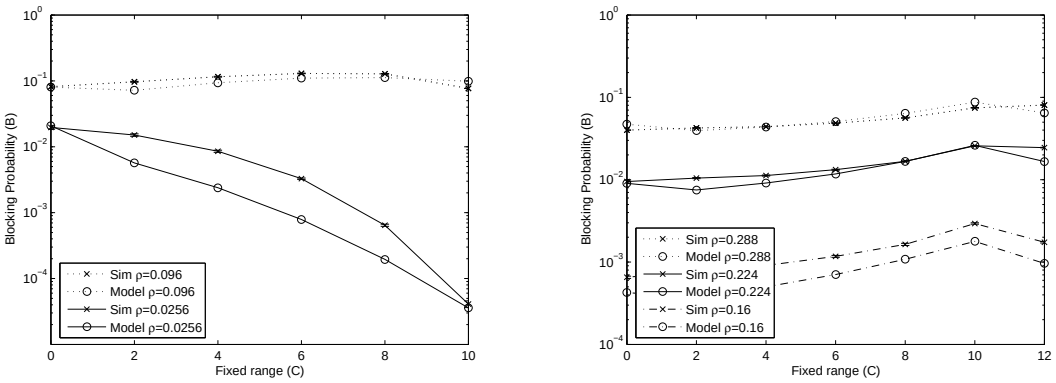

(a) (b)

Figure 2.11: Blocking probability vs. C in ring for SPL with (a) $T = 10$ and $\Theta = 1$, and (b) $T = 12$ and $\Theta = 2$.

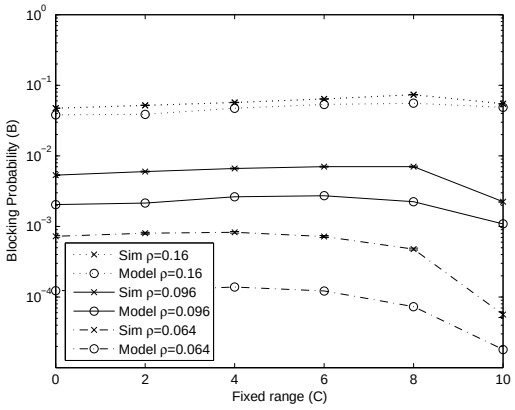

Figure 2.12: Blocking probability vs. C in ring for SPN with $T = 5$ and $\Theta = 2$.

2.6 Summary

In this chapter, the blocking performance of reconfigurable optical networks is investigated. The use of limited tunable transponders in conjunction with fully reconfigurable ROADMs is evaluated. We defined a constraint on lightpath establishment called *wavelength termination constraint* which depends on the number of transponders at the nodes and transponders' tunable ranges (wavebands). Based on this constraint, an analytical model is developed for two transponder sharing models, namely Share-Per-Link and Share-Per-Node. Both analytical and simulation results are provided to compare SPL and SPN models and also to see the effects of load, number of transponders and tuning range on blocking. It

is shown that limited tunable transponders are sufficient to achieve the same blocking performance as widely tunable transponders, and that limited tunability does provide large improvements over no tunability. SPN model is always advantageous over SPL, however in certain cases the performance gap between them closes (e.g., dominating path blocking). A heuristic algorithm for transponder waveband assignment is also introduced. The analytical model is modified to analyze the performance of the heuristic. In certain conditions, the blocking is significantly improved by the heuristic which shows that waveband assignment has a significant effect on blocking.

Chapter 3

Transponder Wavelength/Waveband Assignment

Transponders are employed in optical nodes wherever it is necessary to add/drop a lightpath and convert it to the electronic domain. Most of the work in the literature taking into account the effect of transponders in blocking consider WTTs being used at the switching ports. When WTTs are deployed in the network, only the number of transponders is a factor effecting the blocking rather than the tunability capabilities of the transponders as in the case of LTTs. With WTTs, there is no problem concerning the selection of the wavebands to which transponders can tune. However, for LTTs it is shown that the selection of wavebands to transponders is an important problem in Chapter 2 and it can affect the blocking significantly.

With the *wavelength termination constraint*, in order for a lightpath to be established, there have to be available transponders on both ends that can tune to an available wavelength along the path. This constraint is more restrictive with LTTs and Fixed Transponders (FTs) since they can only tune over a waveband or to a fixed wavelength, respectively. Considering this constraint, it may not be possible to establish a lightpath even if there is an end-to-end continuous wavelength and there are some available transponders at both terminal nodes. Therefore, selection of wavebands of LTTs or the fixed wavelengths of FTs is very important and assignment policies other from random may improve blocking.

Depending on the transponder sharing model used in each node (SPL or SPN), the waveband assignment problem applies either to the transponders of node-link pairs or to the transponders of a whole node, for SPL and SPN respectively. We will distinguish between these models in our algorithms whenever necessary. The network model is the same as that introduced in Chapter 2. In the case of non-uniform traffic, the arrival rate on

a route is the base load ρ multiplied by a scaling factor s_r where $1 \leq r \leq R$. Since the call durations are exponentially distributed with unit mean, the Erlang load on a route r is ρs_r.

The rest of the chapter is organized as follows. In Section 3.1 we review two assignment schemes from the previous chapter and present several Integer Linear Program (ILP) formulations and heuristics to accomplish transponder waveband assignment for several traffic models. We do a performance comparison of algorithms in Section 3.2, and the chapter is concluded in Section 3.3.

3.1 Transponder Waveband Assignment

In this section, we propose several transponder wavelength/waveband assignment algorithms. Initially, we introduce two general algorithms for wavelength/waveband assignment that can be applied to any traffic model. Moreover, we later propose traffic specific algorithms that can improve the performance more than those general algorithms. The first two algorithms can be applied to both SPL and SPN models. However, we assume only the SPL model to do the assignment for all node-link pairs (n, l) in the network in the cases of non-uniform traffic and arbitrary traffic matrix in Sections 3.1.3 and 3.1.4, respectively.

We classify the blocking in a network into two categories: 1) Path blocking and 2) Transponder blocking. Path blocking happens when there is no available wavelength along the entire path of the connection. High correlated networks have more path blocking since many routes share many common links. Transponder blocking happens in the case that there are available wavelengths end-to-end however there is no transponder that can transmit/receive at any of those wavelengths at either end.

We define two objectives for the transponder assignment problem. The first objective is to assign as many common wavelengths as possible to transponders of source and destination node-link pairs of a route. The second objective is to assign as many different wavelengths as possible from each other to the terminal node-link pairs of routes that are sharing common link(s). The first objective serves to minimize the transponder blocking whereas the second objective serves to minimize the path blocking.

Here we consider two simple scenarios and show the best transponder assignment for

those cases. However, in an actual network it is hard to find such a simple case, hence it is harder to obtain the optimal assignment. The first scenario is when there is a single path (denoted by R_1) in our network with the source and destination node link pairs denoted by $(s_1, l_{s,1})$ and $(d_1, l_{d,1})$, respectively. Then the best assignment is to assign exactly the same set of wavebands for both $(s, l_{s,1})$ and $(d, l_{d,1})$. By doing so, we completely eliminate transponder blocking and the only reason of blocking for that path would be path blocking.

Now, we consider a second scenario when there is another path (R_2) in the network sharing a common link with R_1. The terminal node-link pairs of R_2 are denoted by $(s_2, l_{s,2})$ and $(d_2, l_{d,2})$, respectively. The optimal assignment for such a case is when $(s_1, l_{s,1})$, $(d_1, l_{d,1})$ are assigned the same set of wavebands, while both $(s_2, l_{s,2})$ and $(d_2, l_{d,2})$ are assigned to another set which consists of as many different wavebands as possible from $(s_1, l_{s,1})$, $(d_1, l_{d,1})$. In this case, transponder blocking is again eliminated. Moreover, since the transponders of the two routes with common link(s) are assigned wavebands as differently as possible, we also minimize the path blocking. In the example shown in Fig. 3.1 with 5 transponders per node-link pair and eight possible wavebands, the terminal node-link pairs of R_1 are assigned wavebands 1 to 5 and terminal node-link pairs of R_2 are assigned wavebands 4 to 8. Therefore, there is a minimum overlap of 1 between the wavebands of routes R_1 and R_2.

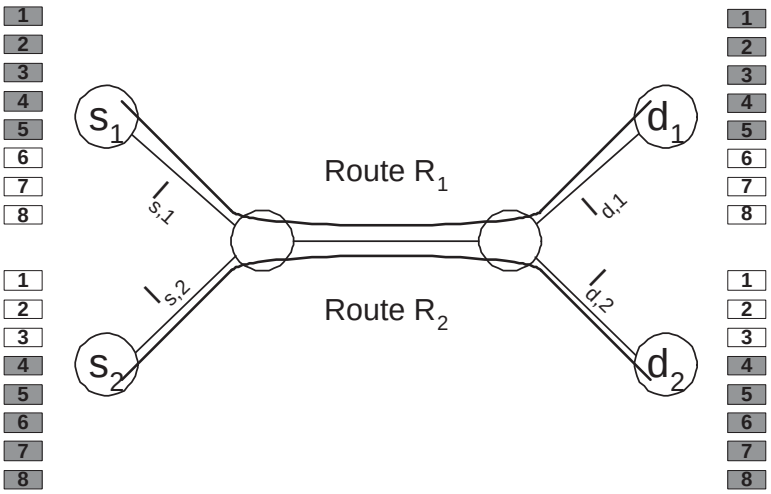

Figure 3.1: Transponder waveband assignment example.

3.1.1 Random Assignment

Every transponder of (n, l) is assigned in a random fashion with the following restrictions for the SPL model. In the case $T < K$, transponders are randomly assigned to one of the K wavebands with none of them being assigned to the same waveband. For $T \geq K$, each of the K wavebands have $\lfloor T/K \rfloor$ transponders assigned. The remaining $b = T \mod K$ transponders are assigned randomly as in the first case. Same strategy applies for SPN model at each node n with T_n transponders.

In the case of small number of transponders per node-link pair or node, the probability of a mismatch between wavebands of transponders of different nodes is very high. For $T > K/2$, we are guaranteed to have at least $T - \lfloor K/2 \rfloor$ common wavebands overall nodes. The probability of having more common wavebands increases with T. However, for $T \leq K/2$ there is a possibility of not having any waveband in common between two nodes, and as T decreases this probability increases.

3.1.2 C-fixed Random Assignment

Recall that we introduced C-fixed assignment in Section. 2.4. This assignment aims to improve the high mismatch between the node-link pairs or nodes which happens in the case of random assignment. It assigns the same C wavebands to C transponders at every node-link pair and chooses the rest randomly out of the remaining wavebands. This method aims to eliminate the mismatch between the wavebands of transponders at different nodes which results in high transponder blocking for small values of T. Same strategy applies for SPN model at each node n with T_n transponders. Note that with $C = 0$, we have a totally random assignment. It is advantageous for all-to-all traffic that every node or node-link pair have some number of wavebands in common. By this way, we guarantee that every source destination pair have at least a certain number of common wavebands. Therefore, a possibility of a poor mismatch (or no mismatch at all) for any route is eliminated.

This assignment scheme targets to minimize transponder blocking, however it concentrates the load on a smaller number of wavelengths.

Note that with $C = T$, the network utilizes only $\Theta = C$ wavelengths. This results

in increased traffic load on the limited number of wavelengths (if $\Theta C < W$) used in the network. This results in more blocking occurring due to the unavailability of wavelengths rather than transponders.

3.1.3 Wavelength Assignment under Non-Uniform Traffic

The traffic is all-to-all, but the load on some of the routes have a higher load than the others by a certain scale factor. We want to assign the same set of wavebands for the terminal node-link pairs of a route, and these wavebands should be chosen such that the load on the wavelengths of the shared links with other routes is minimized (i.e., these routes are assigned to wavebands as different as possible from each other) as illustrated by the simple scenarios at the beginning of this section. We also consider the routes sharing the same node-link pairs. In those cases, the terminal node-link pairs of such routes are all assigned to the same waveband set. We require all of the node-link pairs in the network to have a certain number of common transponder wavebands to maintain a reasonable blocking for each route since the traffic is all-to-all. We give priority to the groups of routes with the same higher scaling factor since those routes will contribute to the blocking more than the others.

We first introduce algorithms (ILP and heuristic (MOWA)) designed specifically for uniform traffic. We later go on to introduce another heuristic approach to apply to the highly loaded routes which works best for the highly loaded routes not sharing any common link. We denote load scaling factors of the routes as s_r where $1 \leq r \leq R$.

3.1.3.1 ILP Algorithm

We first group the routes with the same scaling factor and sort the groups in descending order with respect to their loads. We start doing the assignment for the group with the highest load. The same procedure is applied to the consecutive groups. If a route within the next group has already been assigned as part of a previous group (note that the route may have a smaller load but still may be connected to one of the higher load routes), then the new assignment is ignored.

Wavebands are numbered as $1, \ldots, B$. We make all of the (n, l) pairs in the network to have the same C wavebands and we run the ILP algorithm for the remaining $B - C$ wavebands and $T - C$ transponders. This is done to achieve an acceptable blocking value between every pair of nodes, since we have an all-to-all traffic.

Consider that there are G groups with different load scale factors. We denote those groups as Σ_g and their size σ_g where $1 \leq g \leq G$. If the route r is sharing terminal node-link pairs with other routes in the same group, we denote the set of all those routes including r by Ψ_r^g (the connectivity set of r in Σ_g). We calculate the connectivity sets within each group.

The ILP parameters are given as

Γ_g :	Set of routes in group Σ_g
X_r^l :	1 if link l is present on Route r, 0 otherwise
$Y_{i,j}$:	1 if routes i and j are in the same group and have a common terminal, 0 otherwise

ILP Variables: We first have the main variable for the assignment of transponders to wavebands in each node-link pair present in the traffic matrix.

A_r^b: 1 if a transponder in the terminal node-link pairs of route r is assigned to the waveband b, and 0 otherwise where $C + 1 \leq b \leq B$.

Other variables are used as metrics to calculate the load on the wavelengths on each link as a result of the wavelength assignment. O_l^b is the load on the waveband b on link l.

$$O_l^b = \sum_{l,b,r} (A_r^b * s_r) X_r^l.$$

We denote by $O_{\max}^l$ the maximum load on any wavelength on the link l.

$$O_{\max}^l \geq O_l^b \; \forall \; l, b.$$

The first constraint below ensures that there are a total of T transponders assigned to any route:

$$\sum_{b} A_r^b = T \; \forall \; r.$$

The second constraint ensures that routes are assigned the same wavebands if they share a terminal node-link pair:

$$\text{if } Y_{i,j} = 1 \text{ then } A_i^b = A_j^b \; \forall i, j, r$$

There are two possible objectives. The first objective is to minimize the maximum load on any link and wavelength in the network:

$$\min \; \max_{l,b} O_l^b.$$

The second objective is to minimize the sum of the maximum loads on every link.

$$\min \sum_{l} O_{\max}^l$$

3.1.3.2 Minimize Overlap of Wavebands Algorithm (MOWA)

The algorithm does the assignment for each group starting first with the one having the highest scaling factor. We first sort the routes within a group in descending order with respect to their hop-lengths and do the assignment for each route one-by-one. We again assign the first C wavebands to every (n, l) pair and the heuristic takes care of the selection of $T - C$ wavebands out of $B - C$ for each route. We calculate the connectivity sets within each group and all (n, l) pairs within the same connectivity set are assigned the same wavebands.

We use the variable O_l^b but this time it stores the current load value on the wavebands of the links during the assignment algorithm. The selection of the wavebands for a route is done by calculating the metric shown below and the first $T - C$ wavebands with the lowest values of the metric are chosen to be assigned to the transponders. The metric used is calculated based on O_l^b.

We also denote the links on route r with hop-length of h_r by l_r^i where $1 \leq i \leq h_r$. The metrics are then defined as follows.

$$\Upsilon_b^1 = \sum_{r \in \Psi} \sum_{i=1}^{h_r} O_{l_r^i}^b. \tag{3.1}$$

After each assignment of wavebands to a route, the load values affected by the assignment (O_l^b) are updated. During this update process, O_l^b's for the links along the route are incremented by scaling factor of that route. The outline of the algorithm is shown in Alg. 3.1.

input : Set of routes $(\mathcal{R})$ and their loads

output: Wavelength Assignment for every node-link pair

1 *Initialization:* Sort $\mathcal{R}$ in descending order w.r.t. their load;
2 Create the groups Σ_g where $1 \leq g \leq G$;
3 Sort each Σ_g in descending order w.r.t. their hop-lengths;
4 Calculate the connectivity set of each route (Ψ_r) within Σ_g;
5 Assign wavebands 1 to C to the first C transponders for every (n, l) pair in the network;
6 **for** $g \leftarrow 1$ **to** G **do**
7 **for** $r \leftarrow 1$ **to** σ_g **do**
8 **if** $Assigned_r = 0$ **then**
9 Calculate the load on the wavebands $C + 1$ to B by using the metric;
10 Sort the wavebands in an ascending order w.r.t. the metric Υ_b^m. The sorted wavebands are $b^1, b^2, \ldots, b^{B-C}$;
11 Assign the waveband $b^{t \mod B-C}$ to transponder t $(1 \leq t \leq T - C)$ of terminal (n, l) pairs of the routes in Ψ_r;
12 *//Update the load on wavebands*;
13 **for** $rr \in \Psi_r$ **do**
14 **for** $i \leftarrow 1$ **to** h_{rr} **do**
15 **for** $j \leftarrow 1$ **to** $T - C$ **do**
16 $O_{l_{rr}^i}^{b^j} = O_{l_{rr}^i}^{b^j} + s_r$;
17 $Assigned_{rr} = 1$;

Algorithm 3.1: Pseudocode for Minimize Overlap of Wavebands Algorithm (MOWA).

3.1.3.3 Consecutive Offset Waveband Assignment (COWA) Algorithm

For a non-uniform traffic scenario, the main purpose is to reduce the blocking on highly loaded routes since they contribute to the overall blocking more than the others. We want the end node-link pairs of highly loaded routes to have as many common wavebands as possible whereas the other node-link pairs can be assigned to other wavebands to reduce the load on the wavelengths used by the highly loaded paths. We still require all of them to share a few wavebands in order not to have very high blocking for some routes. We also note that for longer routes (i.e., higher hop-length), it is harder to find end-to-end available wavelengths along the route. Hence, the average number of end-to-end available wavelengths on the path is smaller with longer routes. This reduces the probability of finding an available transponder on one of those wavelengths also. Accordingly, we conclude that transponder blocking is higher on the routes with higher number of hops than the ones with lower number of hops.

In this algorithm, transponders of a node-link pair (n, l) are assigned wavebands that are contiguous, and we specify such an assignment by its first waveband $w_{first}(n, l)$. As explained in the above paragraph we want to give the highly loaded and longer routes the priority during waveband assignment. We initially sort $\mathcal{R}$ in descending order w.r.t. their loads and we sort the routes with the same load in descending order w.r.t. their hop-count. Assume the routes in sorted order are $(r_1, r_2, \ldots, r_R)$, and $(h_1, h_2, \ldots, h_R)$ are the hop-lengths.

We start iterating over the routes one-by-one starting with the first route. Assume r_i in iteration i $(1 \leq i \leq R)$ consists of the nodes $(n_1, n_2, \ldots, n_{h+1})$ and the links $(l_1, l_2, \ldots, l_h)$. The source and destination pairs (n_1, l_1) and (n_{h+1}, l_h), respectively are assigned the same wavebands such that $w_{first}(n_1, l_1) = w_{first}(n_{h+1}, l_h) = p_{off}$ (in the case that none of the end node-link pairs are previously assigned). p_{off} makes sure that the routes with different loads are not assigned to the same wavebands. It is initially 1 but it is incremented every time we iterate into a route with lower load. If one of the end pairs is already assigned, then the other end pair has the same w_{first} as the first one.

For the node-link pairs along a route, we want the intermediate nodes assigned to dif-

ferent wavebands in order to reduce the path blocking. The offset of wavebands depends on how many hops they are away from one end. For a node k ($k = 2, \ldots, h$) along the route, the pairs (n_k, l_{k-1}) that communicate with the source node n_1, are assigned more wavebands in common with (n_1, l_1) for larger k. The pairs (n_k, l_k) that communicate with the destination node n_{h+1} have more wavebands in common with (n_{h+1}, l_h) for smaller k. The amount of overlap between the intermediate and the end node-link pairs depends on two parameters: D and S. D is the minimum offset in the wavelength spectrum from one of the end pairs, and S is a multiplicative factor depending on the hop distance of the intermediate pair. If not already assigned, $w_{first}(n_k, l_k) = (h_k - k)S + D + (h_{max} - h_k) + 1$ and $w_{first}(n_k, l_{k+1}) = (k-2)S + D + (h_{max} - h_k) + 1$ where h_{max} is the maximum hop length. Note that if the consecutive waveband number exceeds B, then the assignment wraps around to $w_{first}(n_k, l_k)$. We show an example in Fig. 3.2 for a route with hop length 5 with parameters values $D = 2$, $S = 1$, $p_{off} = 1$. After each iteration, the number of already assigned node-link pairs on each route is calculated and the routes having the same load and hop-length are sorted with respect to this number in ascending order. This is done to give priority to the routes with more pairs to be assigned. We present this algorithm in Alg. 3.2.

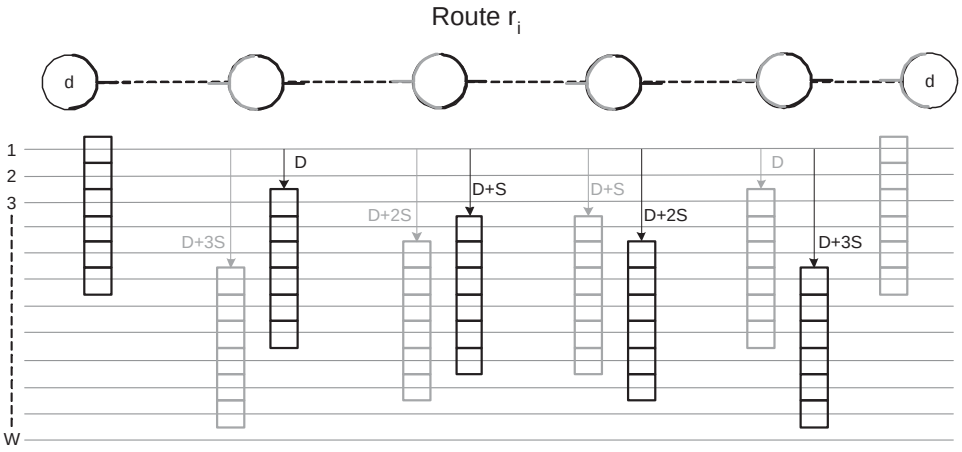

Figure 3.2: COWA example with $T = 6$ ($D = 2$, $S = 1$, $p_{off} = 1$).

input : Set of routes $(\mathcal{R})$ and their loads

output: Wavelength Assignment for every node-link pair

Initialization: $p_{offset} = 1$ and $w_{first}(i,j) = 0 \; \forall i = 1, \ldots, N \; j = 1, \ldots, L$;

Sort $\mathcal{R}$ in descending order w.r.t. their loads;

Sort routes with the same load in descending order w.r.t. their hop-count. $(r_1, r_2, \ldots, r_R)$ are the routes in sorted order, $(h_1, h_2, \ldots, h_R)$ are the hop-lengths, $h_{max} = \max_{1 \leq i \leq R} h_i$;

for $r \leftarrow 1$ **to** R **do**

  if $\rho_r < \rho_{r-1}$ **then**

    $p_{offset} = p_{offset} + 1$

  if $w_{first}(n_1, l_1) > 0$ *and* $w_{first}(n_{h+1}, l_h) = 0$ **then**

    $w_{first}(n_{h+1}, l_h) = w_{first}(n_1, l_1)$

  else if $w_{first}(n_{h+1}, l_h) > 0$ *and* $w_{first}(n_1, l_1) = 0$ **then**

    $w_{first}(n_1, l_1) = w_{first}(n_{h+1}, l_h)$

  for $k \leftarrow 2$ **to** h_k **do**

    if $w_{first}(n_k, l_k)$ = *0* **then**

      $w_{first}(n_k, l_k) = (h_k - k)S + D + (h_{max} - h_k) + 1$

    if $w_{first}(n_k, l_{k+1})$ = *0* **then**

      $w_{first}(n_k, l_{k+1}) = (k-2)S + D + (h_{max} - h_k) + 1$

  Sort routes with the same load and hop length w.r.t. least number of assigned (n, l) pairs;

Algorithm 3.2: Pseudocode for Consecutive Offset Waveband Assignment (COWA) Algorithm.

3.1.4 Assignment for an Arbitrary Traffic Matrix

Given a network, we assume that there is dynamic traffic between certain nodes only (not all-to-all) denoted by a traffic matrix $\mathcal{T}$. Given $\mathcal{T}$, we want to find an assignment for the node-link pairs involved in the specific traffic pattern (if not all). Our strategy is to assign the same set of wavebands for the terminal node-link pairs of a route, and these wavebands should be chosen such that the load on the wavelengths of the shared links with other

routes is minimized (i.e., these routes are assigned to wavebands as differently as possible from each other). Similar to the non-uniform traffic case, for the routes sharing the same node-link pairs, their terminal node-link pairs are all assigned to the same waveband set.

For this traffic type, we modify the previous formulation of the ILP algorithm and also provide a similar heuristic to MOWA. We start with the ILP algorithm.

3.1.4.1 ILP Algorithm for Arbitrary Traffic Matrix

The ILP formulation is almost the same except for the fact that now we do not require all of the node-link pairs in the network to commonly have the same C wavebands since the traffic is not all-to-all. Considering $C = 0$, now the optimization algorithm chooses the wavebands of the transponders out of B possible wavebands.

The new input to the ILP algorithm which is the arbitrary traffic matrix is defined below while the rest of the input parameters are the same as in the previous section.

$$\mathcal{R}: \quad \text{Set of routes specified by the traffic matrix } \mathcal{T}$$

ILP Variables: O_l^b denotes the load on the waveband b on link l as a result of waveband assignment but now defined by the following formula:

$$O_l^b = \sum_{l,b,r} A_r^b X_r^l.$$

Note that since the traffic load on each route within the traffic matrix $\mathcal{T}$ is the same, there is no scaling factor in the above formula. The rest of the constraints and the two objectives are the same as in the case of non-uniform traffic.

3.1.4.2 MOWA for Arbitrary Traffic Matrix

We first sort the routes in descending order with respect to their hop-lengths and do the assignment for each route one-by-one. O_l^b similarly stores the current value of load on the wavebands of the links during the assignment algorithm. The selection of the wavebands for a route is done by calculating the same metric in (3.1) and the first T wavebands with the lowest values of the metric are chosen to be assigned to the transponders. This algorithm

can be summarized as Alg. 3.3. We again calculate the connectivity set Ψ_r of each route r and every terminal pair of the routes in Ψ_r is assigned the same wavebands.

input : Set of routes $(\mathcal{R})$

output: Wavelength Assignment for the terminal node-link pairs of the routes in $\mathcal{R}$

```
1  Initialization: Sort R in descending order w.r.t. their hop-lengths;
2  Calculate the connectivity set of each route (Ψ_r);
3  for r ← 1 to R do
4      if Assigned_r = 0 then
5          Calculate the load on wavebands by using one of the metrics;
6          Sort the wavebands in an ascending order w.r.t the metric ϒ_b;
7          Assign the first T wavebands in the sorted order to terminal (n, l) pairs of
           the routes in Ψ_r;
8          for rr ← 1 to |Ψ_r| do
9              Assigned_rr = 1;
10             for i ← 1 to h_rr do
11                 for b ← 1 to B do
12                     O^b_{l^i_rr} = O^b_{l^i_rr} + 1;
```

Algorithm 3.3: Pseudocode of MOWA algorithm for arbitrary traffic matrix.

3.1.4.3 COWA for Arbitrary Traffic Matrix

COWA algorithm can also be applied to arbitrary traffic. In this case, all of the routes have the same load; therefore a route does not have any priority over other routes because of the load factor. Since the sorting w.r.t. loads is not required, the routes in the traffic matrix are treated in decreasing order of their hop-lengths. Therefore, the assignment for the route with largest number of hops is done first.

3.1.5 Waveband Assignment to Support Maximal Traffic Set in a Fiber

In this section, we examine the problem of calculating the minimum range of transponders at a node to support a maximal traffic set on the spectrum. Considering W wavelengths in the spectrum and nodes having T transponders each ($T < W$), we want to find the minimum range of these transponders to support the maximal traffic set in the spectrum. By maximal traffic set, we mean that the transponders can support any of the $\binom{W}{T}$ possible traffic patterns. Transponder i is denoted by t_i and let w_i^s, w_i^e denote the smallest and largest numbered wavelengths it is tunable to, respectively ($i = 1, \ldots, T$). The minimum value of the tuning range can be found in a straightforward manner to be $\Theta_{min} = W - T + 1$. We explain how to obtain this minimum value as follows. If we consider the traffic pattern in which the first T wavelengths are busy, then we should make at least one transponder tunable to each of the first T wavelengths. We can make t_1 tunable to wavelength 1, t_2 tunable to wavelength 2, and hence have $w_i^s = i$ for $i = 1, \ldots, T$. Now, if we consider the other end of the spectrum and take the traffic pattern of the last T wavelengths being busy. For the last T wavelengths ($W - T + 1, W - T + 2, \ldots, W$), each requires at least one transponder tunable to each wavelength. In order to have the minimum ranges for each transponder, we can make t_1 tunable to wavelength $W - T + 1$, t_2 to $W - T + 2$ and hence have $w_i^e = W - T + i$. Therefore, the tuning range of a transponder t_i is $\Theta_i = w_i^e - w_i^s + 1 = W - T + 1$. The reduction in tuning range compared to widely tunable transponders is then $T - 1$. Note that in the extreme cases, the minimum ranges are $\Theta_{min} = 1$ and $\Theta_{min} = W$ for $T = 1$ and $T = W$, respectively.

3.2 Numerical Results

3.2.1 Uniform Traffic Results

We ran simulations for 20-node ring and NSFNET topologies (see [32]) for $W = 32$ with 10^6 call arrivals per trial and 10 trials (to average over the random waveband assignments). Overall blocking probability is calculated by taking the average of route blocking probability over every route $r \in \mathcal{R}$. ρ is the load per route. Fixed routes among every pair of nodes

are calculated using a minimum hop routing strategy.

In order to compare random and C-fixed assignment of transponders, we plot B vs. C for various loads and ring in Fig. 3.3 with $\Theta = 2$. In Fig. 3.3 (a), with lower loads, the blocking probability decreases rapidly with increasing C for SPL. In fact, the lowest blocking is obtained with $C = T = 6$ which is only a 12-wavelength system. (For SPN we obtained a similar behavior for $T = 4$, $\Theta = 2$) In Fig. 3.3 (b) we plot for $T = 12$, $\Theta = 2$ and observe that blocking probability is higher with larger C values than $C = 0$. Random assignment performs better with larger values of T.

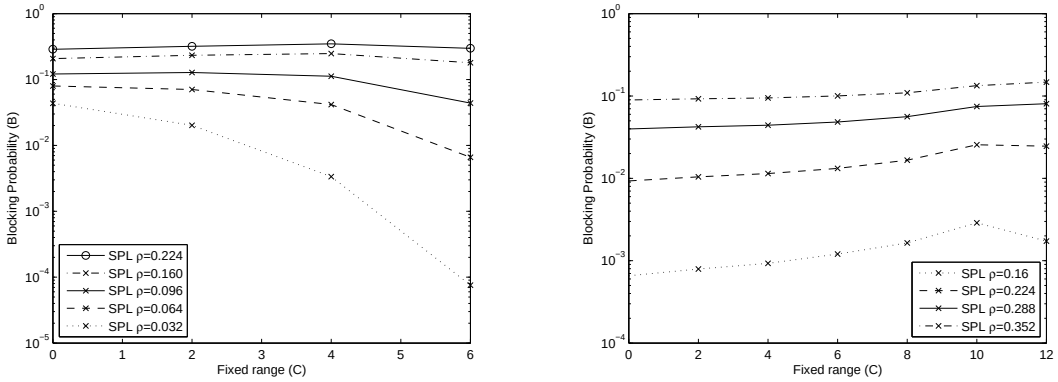

(a) (b)

Figure 3.3: Blocking probability vs. fixed range C in SPL with $\Theta = 2$ in ring for (a) $T = 6$, and (b) $T = 12$.

In Fig. 3.4, we plot B vs. C for various loads in the ring network for SPN model. In Fig. 3.4 (a), we observe a significant decrease in blocking with increasing C as in the case of SPL model with $\Theta = 2$ but now for a smaller value of $T = 4$. However, for $C = 6$ we see that the drop in blocking with higher C is relatively much smaller in Fig. 3.4 (b).

3.2.2 Non-Uniform Traffic Results

For non-uniform traffic, we ran simulations for 10-node ring and NSFNET topologies (see [32]) again for $W = 32$ with 10^6 call arrivals per trial and 10 trials for each data point in order to average out the effect of randomness in each trial. For specifying a non-uniform traffic, here ρ denotes the load on a route per wavelength with a scale factor of 1. ILP programs are solved using the C-plex solver [33]. We observed that for most cases

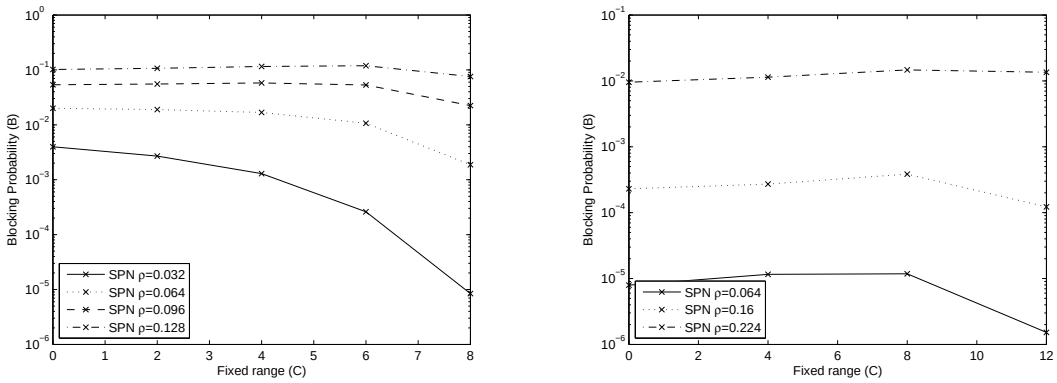

(a) (b)

Figure 3.4: Blocking probability vs. fixed range C in SPN with $\Theta = 2$ in ring for (a) $T = 4$, and (b) $T = 6$.

$S = 1$ performs better than other S values. We present our results here with $S = 1$.

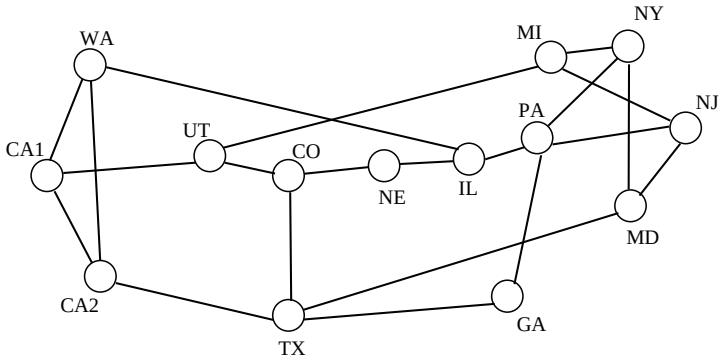

Figure 3.5: 14-node NSFNet topology.

We first plot blocking vs. load for the NSFNET topology. We use the labeling of the nodes of the NSFNet as shown in Fig. 3.5. The traffic used for Fig. 3.6 (a) has nodes CA1, CA2, MI, and NY originating the high load paths. CA1-UT-MI-NY, CA2-TX-MD-NY, CA2-CA1-UT-MI have a load scale factor of 20, while CA1-UT-MI has 10, MI-NY and CA1-CA2 have 5. The rest of the routes have a load scale factor of 1. We see the results of our new algorithm with this traffic compared with C-fixed assignment for $C = 0$ and $C = 16$. $C = 16$ performs much better than $C = 0$ for lower load values but as the load increases the gap between the two closes completely. We see that our algorithm performs better than C-fixed with $C = 16$, and also $D = 5$ is slightly better than $D = 3$. We show the curves with only a few D values here but we will analyze the effect of D below. For

$\rho < 0.128$, $D = 3$ is better than $D = 5$ and they are both closer to $C = 16$.

In Fig. 3.6 (b), we consider a case with 5 nodes originating high load paths. Routes between CA1-NY, CA2-NY, TX-IL (3 hops) have scale factor of 20, routes between CA1-IL, CA1-TX, CA2-IL, TX-NY, IL-NY (2 hops) have scale factor of 10 and CA1-CA2, CA2-TX have 5. A similar behavior is observed for the curves; $D = 5$ gives the lowest blocking for load values above 0.128. Below that point $D = 3$ is slightly better. They are both below the blocking values of C-fixed with $C = 16$ for all load values.

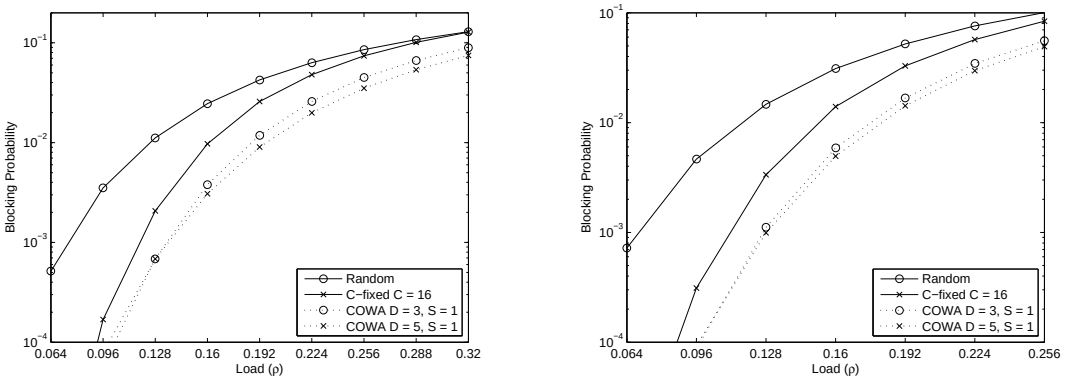

Figure 3.6: Blocking probability vs. load for $T = 16$ in NSFNet with (a) 6 high load paths, and (b) 10 high load paths.

We now plot blocking vs. load for the 10-node ring topology. Assume nodes in the ring are numbered from 0 to $N - 1$. The traffic used for Fig. 3.7 (a) have one high load path with a scale factor of 10 between nodes 0 and 5. We see in Fig. 3.7 (a) that the proposed algorithm gives better blocking in ring for the observed load range. With higher loads, $D = 4$ gives the best blocking and there is a significant difference from C-fixed with $C = 14$. The traffic in Fig. 3.7 (b) has an additional high load path of scale factor 10 between nodes 0 and 6 which does not overlap with the first high load route. In Fig. 3.7 (b) the curves are obtained with $T = 16$. We observe a significant amount of improvement in blocking compared to C-fixed with $T = 16$ and as the load increases the difference gets bigger. The best blocking is achieved with $D = 5$. With lower loads, all of the curves with different D values have very close blocking values.

In Fig. 3.8 (a), we plot the blocking vs. D with several T values for the non-uniform

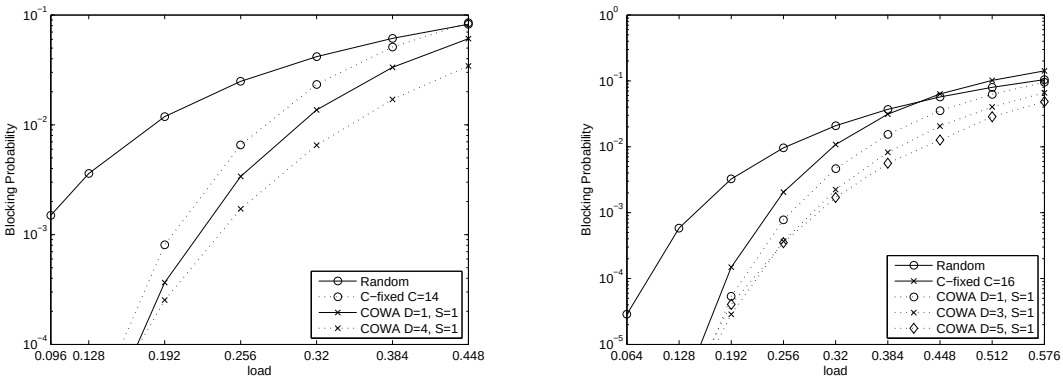

(a) (b)

Figure 3.7: Blocking probability vs. load for 10-node ring with (a) 1 high load path for $T = 14$, and (b) 2 high load paths for $T = 16$.

traffic pattern of 10 high load paths in NSFNet. Dotted lines show the blocking level of the C-fixed algorithm with $C = T$. We observe that the best blocking is achieved for medium values of D. The values are $D = 5$ for $T = 16$ and $T = 18$, $D = 4$ for $T = 12$, and $D = 3$ for $T = 8$. With lower T values, we need more overlap (i.e., lower D) between any intermediate node and end nodes. Note that for $T = 18$ with $D = 5$ the blocking value is lower by more than a factor of 4 than C-fixed with $C = 18$. We observe that the maximum difference between our algorithm and C-fixed with $C = T$ increases with higher T values. In Fig. 3.8 (b), we make the same comparison for different ρ values. The points where best blocking is achieved are $D = 3$ for $\rho = 0.064$, $D = 4$ for $\rho = 0.128$, and $D = 5$ for $\rho = 0.192$. The algorithm achieves best blocking with less overlap for higher loads in which it reduces the load on the wavelengths used by the high-load routes. For $\rho = 0.064$, $D > 5$ results in higher blocking than C-fixed with $C = 12$.

We now compare the various algorithms for non-uniform traffic with different non-uniform traffic patterns. For the NSFNet, there are 21 highly loaded routes with a scaling factor 20. These routes are between the source-destination pairs: (CA1-TX), (CA1-NE), (CA1-NJ), (CA2-UT), (CA2-PA), (CA2-NY), (WA,GA), (WA-MI), (WA-NY), (TX-UT), (TX-PA), (TX-NJ), (GA-MI), (UT-PA), (CO-IL), (CO-MI), (CO-MD), (NE-MD), (IL-MD), (PA-NJ), (MI-NJ). The ring has 14 highly loaded routes with a scaling factor of 20 between the following source destination pairs : (0,2), (0,5), (0,8), (1,3), (1,6), (1,9),

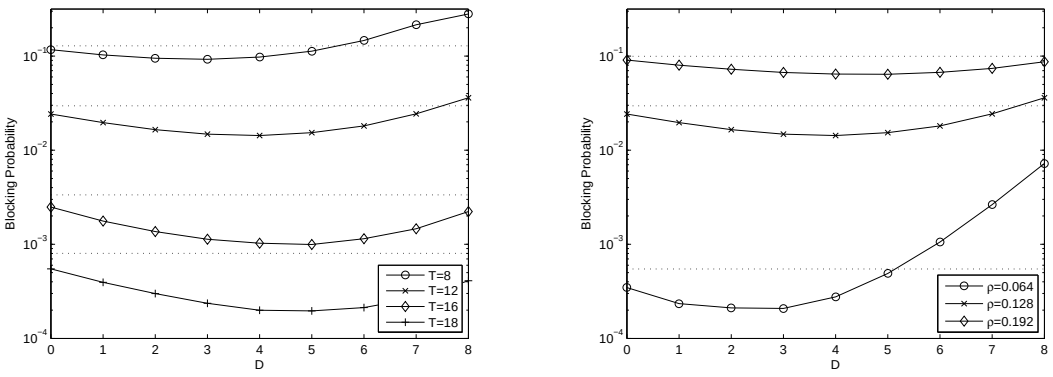

(a) (b)

Figure 3.8: Blocking probability vs. D with 10 high load path in NSFNet for different (a) T values with $\rho = 0.004$, and (b) ρ values with $T = 12$.

(2,4), (3,5), (3,8), (4,6), (4,9), (5,7), (6,8), (7,9). The ILP algorithms are terminated when the tree size reaches a certain limit.

We first plot the blocking probability vs. the load ρ for the NSFNet and ring network in Fig. 3.9 with $T = 16$ and $\Theta = 1$. We show the results of C-fixed algorithm with $C = 0$ which corresponds to totally random assignment, and with $C = 16$ which is totally fixed, and also the ILP with two different objectives, MOWA and COWA. We choose to show results for ILP and MOWA with $C = 10$ because the best performance is obtained with that value. For COWA, we use the parameters $D = 5$ and $S = 1$. We analyze the effect of C in a later graph. In Fig. 3.9 (a), we see C-fixed with $C = 16$ is better than random assignment and the difference is higher with lower loads. ILP with two different objectives and the MOWA all with $C = 12$ perform very similar to each other and also they are significantly better than both C-fixed algorithms. The COWA curve is in between C-fixed and MOWA curves. MOWA is slightly better than the ILPs and it gives 15 times lower blocking than C-fixed with $C = 16$ at $\rho = 0.064$. This is also 125 times better than the random assignment. In Fig. 3.9 (b), C-fixed with $C = 16$ is better than $C = 0$ for lower load values than $\rho = 0.064$ and vice versa for larger values. Both ILP algorithms and the heuristic with $C = 10$ is better than C-fixed algorithm. ILP with Objective 1 is slightly better than the others starting at $\rho = 0.064$ and the MOWA slightly better before that. We observe a 12 times better performance with ILP and MOWA with $C = 10$ than C-fixed with $C = 16$ at

$\rho = 0.048$. It is also 346 times better than random assignment. By observing both graphs, we see that in lightly loaded networks totally fixed assignment (C-fixed $C = 16$) performs much better than totally random. However, when the load increases, since with the fixed assignment only 16 wavelengths are utilized, path blocking starts to dominate. Therefore, fixed assignment may become even worse than totally random. We also see that with the ILP and heuristic algorithms the performance is improved significantly for a wider range of loads.

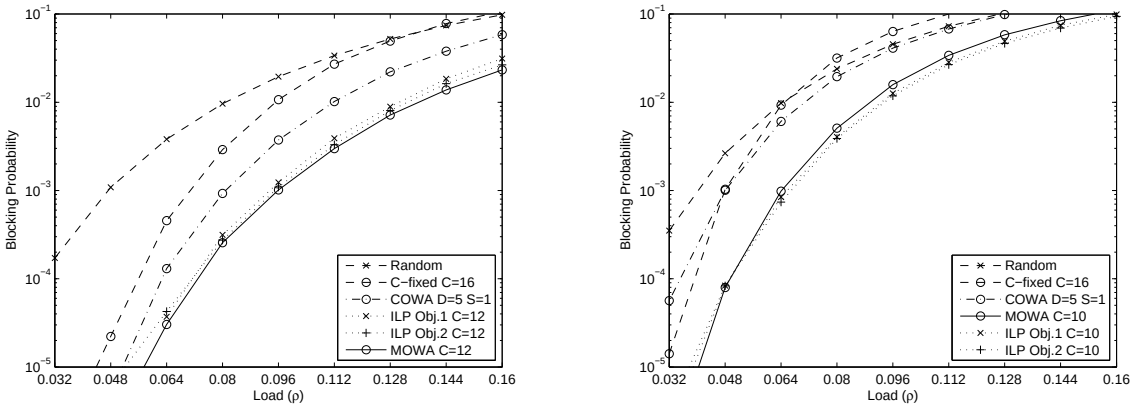

(a) (b)

Figure 3.9: Blocking probability vs. load with $\Theta = 1$ and $T = 16$ in (a) NSFNet, and (b) ring.

We now look at the performance when limited tunable transponders with $\Theta = 2$ are utilized by plotting the blocking probability vs. the load ρ for the NSFNet and ring network in Fig. 3.10 with $T = 2$. C-fixed with $C = 12$ offers an improvement over the random case with $C = 0$ as seen in Fig. 3.10 (a). The difference between these curves gets larger with smaller load. For loads higher than 0.096, MOWA and ILP give a little more improvement over C-fixed with $C = 12$. Similar results are obtained for the ring in Fig. 3.10 (b) where MOWA and ILP are better than C-fixed with $C = 12$ for $\rho \geq 0.064$. As seen from both graphs, the performance improvement by the proposed algorithms is not as high as in the case with fixed transponders. However, especially with lower loads, C-fixed with $C = T$ still improves it significantly and the other algorithms enhance the performance for higher load values.

We now investigate the effect of the parameter C in our algorithms by plotting blocking

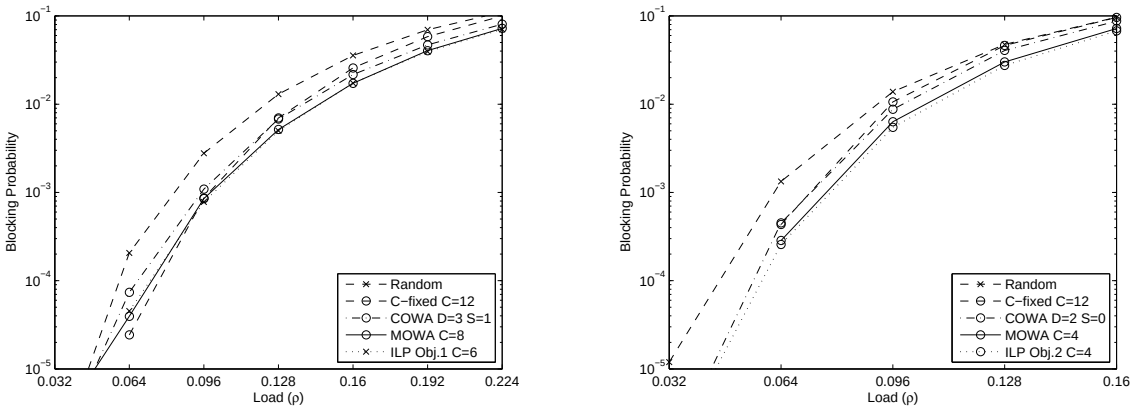

(a) (b)

Figure 3.10: Blocking probability vs. load with $\Theta = 2$ and $T = 12$ in (a) NSFNet, and (b) ring.

probability vs. C for both networks. In Fig. 3.11 (a), in the NSFNet with higher loads, C-fixed blocking increases slightly with increasing C but drops at the end with $C = T = 16$. However, with lower loads ($\rho = 0.064$) the blocking decreases with higher C, and the best blocking is obtained with $C = 16$. This confirms our observation that C-fixed improves blocking significantly with lightly loaded networks. We show the results of ILP with Objective 2 since they both perform very similarly. Every MOWA curve first decreases with increasing C, and then increases after some value of C. Hence, there is an optimum value of C that optimizes the performance. For example, for $\rho = 0.064$, $\rho = 0.096$ and $\rho = 0.128$, the best blocking is obtained with $C = 12$, $C = 10$, and $C = 10$, respectively, resulting in performance improvement factors of 15, 10 and 9, respectively (compared to the best C-fixed blocking ($C = 16$)). We observe that the best performance of the heuristic is obtained with lower values of C as the load increases. With high loads, the performance can be optimized by making each node have fewer common transponder wavebands with each other so that we do not apply too much load on certain wavebands. However, with lower loads we can make them share more wavebands without the concern of overloading certain wavebands and hence increasing the path blocking. For higher loads, since the load is concentrated on a smaller set of wavelengths as C increases, the path blocking becomes more dominant. Hence, we do not achieve any performance improvement.

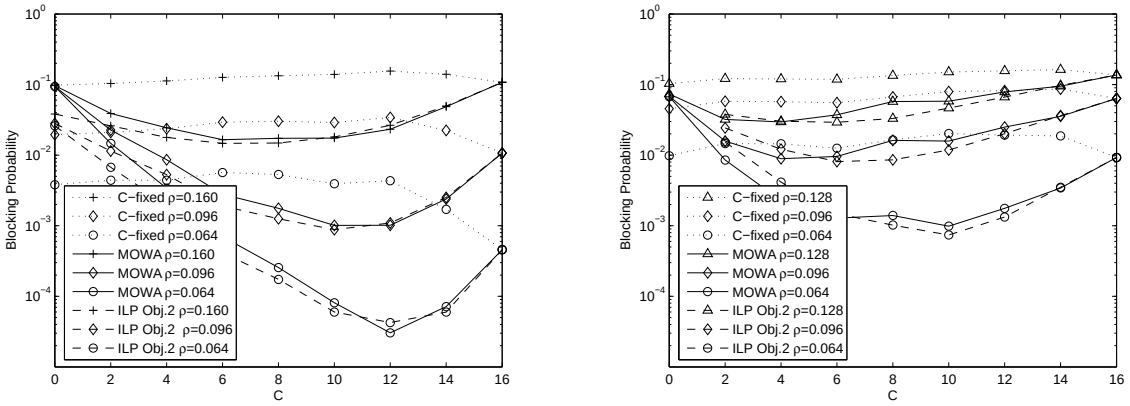

(a) (b)

Figure 3.11: Blocking probability vs. C with $\Theta = 1$ and $T = 16$ in (a) NSFNet, and (b) ring.

3.2.3 Arbitrary Traffic Matrix Results

In this section we consider 10-node ring network with the traffic matrix consisting of the shortest path routes between the following node pairs: $(0, 2)$, $(0, 5)$, $(0, 8)$, $(1, 3)$, $(1, 6)$, $(1, 9)$, $(2, 4)$, $(3, 5)$, $(3, 8)$, $(4, 6)$, $(4, 9)$, $(5, 7)$, $(6, 8)$, $(7, 9)$. For the NSFNet, the traffic matrix consists of 19 shortest paths between CA1-GA, CA1-PA, CA1-NY, CA2-UT, CA2-CO, CA2-NE, WA-CO, WA-MD, TX-IL, TX-MI, GA-UT, GA-MD, UT-PA, CO-IL, CO-PA, NE-MI, NE-NJ, IL-NY, PA-MI. There is dynamic traffic arriving only at those routes with load ρ.

We first plot blocking probability vs. load with fixed transponders for NSFNet and ring in Fig. 3.12. We see that C-fixed improves the results over random significantly with lower loads and COWA is slightly better than C-fixed starting with the load $\rho = 1.28$ in Fig. 3.12 (a). Both MOWA and ILP curves are much better than COWA (30 times lower at $\rho = 1.28$). The difference even increases with lower values. For the ring in Fig. 3.12 (b), C-fixed and COWA perform close to each other and their curves are much lower than random assignment for lower loads. ILP and MOWA are significantly better than C-fixed and COWA at all load values. The ILP curve is slightly lower than the MOWA curve. ILP is 1000 and 225 times better than COWA for $\rho = 0.64$ and $\rho = 0.96$, respectively. We conclude that ILP and MOWA improve the performance significantly compared to any

other algorithm and the improvement factor is large for even high load values.

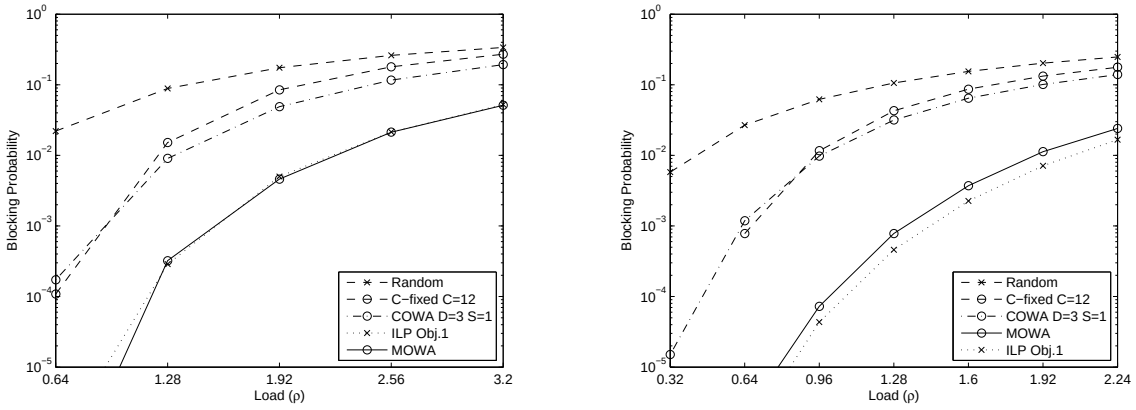

Figure 3.12: Blocking probability vs. load with $\Theta = 1$ and $T = 12$ in (a) NSFNet, and (b) ring.

We now plot blocking probability vs. load with $\Theta = 2$ for NSFNet and ring in Fig. 3.13. We see in Fig. 3.13 (a) that C-fixed offers a very big improvement over random and the performance of COWA and MOWA fall between these curves. However, ILP is slightly better than C-fixed. A similar observation can be made for the ring as seen in Fig. 3.13 (b), but in this case the difference between ILP and C-fixed is larger (results of ILP is less than half of C-fixed results). We see that with $\Theta = 2$, most of the improvement can be gained by using C-fixed; and ILP offers some improvement over C-fixed which is higher for the ring. Generally, we can say that the performance gap between the ILP curves and the other algorithms is higher in ring.

3.3 Summary

We studied the design of reconfigurable optical networks when fixed and tunable transponders are used. We studied the wavelength/waveband assignment problem which focuses on the *wavelength termination constraint* and proposed ILP and heuristic algorithms designed for non-uniform traffic. We compared these algorithms with the ones proposed in the previous chapter (random and C-fixed) and showed that these algorithms improve the blocking performance significantly. For uniform traffic and a lightly loaded network we showed that

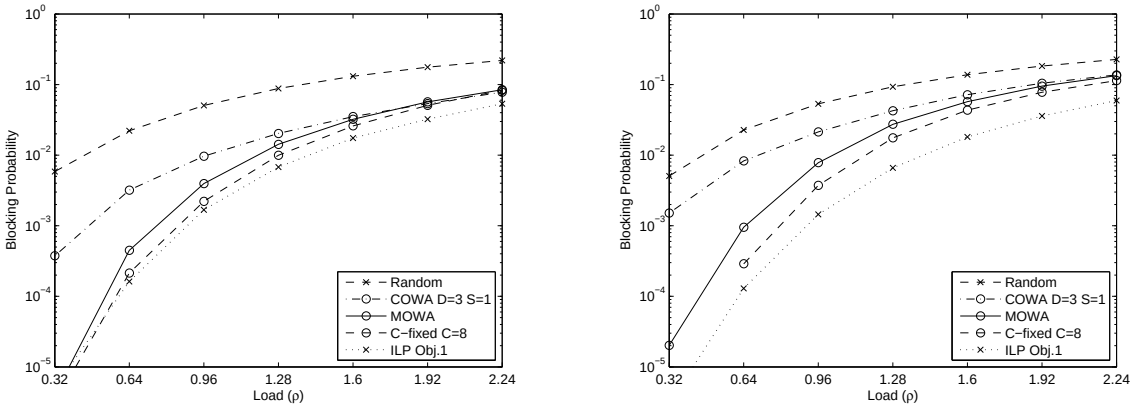

Figure 3.13: Blocking probability vs. load with $\Theta = 2$ and $T = 8$ in (a) NSFNet, and (b) ring.

the C-fixed algorithm works significantly better than random assignment. For non-uniform traffic, we showed that the proposed algorithms work better than C-fixed assignment even with high loads for non-uniform traffic patterns. The best performance improvement is achieved with fixed transponders (i.e., more than 2 orders of magnitude better performance than random assignment) for non-uniform traffic. We also applied similar algorithms to the case of an arbitrary traffic matrix and obtained similar performance improvements.

Chapter 4

Alternate Multihop Routing

Thus far, we did not consider O-E-O conversions or wavelength conversions at intermediate nodes. In this chapter, we consider wavelength conversions occurring at intermediate nodes by O-E-O. An intermediate node can drop a certain wavelength, and transmit on another wavelength. It does this by electronically connecting the drop port to the add port. We call this scheme *multihopping*. We note that at each intermediate node two transponders are required: one for drop and one for add. With wavelength conversions, the entire path does not have to be wavelength-continuous but instead each hop is wavelength-continuous individually. All-optical wavelength conversion is studied in [27] which proposes having wavelength conversion only in a subset of the nodes in the network. In [15], the authors consider wavelength conversion within a multi-granular optical crossconnect (MG-OXC) and a heuristic is proposed for dynamic traffic to reduce the blocking probability by efficiently routing and assigning wavelengths to new lightpath requests and grouping them into bands such that the number of used wavelength converters is reduced. Routing and wavelength assignment algorithms are proposed in [12] for the MG-OXC architecture with an objective of minimizing the number of ports needed by the MG-OXCs. In [34], the hybrid hierarchical switch consisting of an optical crossconnect for waveband routing and an O-E-O switch is introduced. O-E-O switch is used for wavelength routing and, similar to our case, for wavelength conversion. The authors evaluate the throughput performance and the cost depending on the size of the switch which takes into account the number of transponders in the O-E-O switch. An RWA algorithm is introduced in [35] to be used in the presence of sparse or/and full wavelength conversion that reduces the blocking compared to other RWA algorithms.

The effect of multihopping has not been investigated when LTTs are employed in the network. The number of transponders is one constraint on multihopping since allowing too

many hops will exhaust available transponders. On the other hand, with LTTs not every conversion from a wavelength to another is possible (there should be a LTT tunable to the dropped wavelength and also another LTT tunable to the added wavelength). Our goal is to find out how advantageous it is to use multihopping with LTTs. We develop a graph model based on the constraints of LTTs to calculate a route for a lightpath request. Our model not only finds a possible route with our without multihopping, but also chooses the best multihop route on which transponder resources are the least exhausted. We also note that the poor blocking performance due to the mismatch of wavebands of the transponders at different nodes can be eliminated by the use of multihopping. We illustrate this case with an example in Fig.4.1. We show by small rectangles the available transponders in the node and the numbers denote the wavelengths that they can receive/transmit. (The sizes of the wavebands of LTTs are 1 in this example, i.e., these are fixed transponders.) Here, all 4 wavelengths are available along a two-hop route. However, the source node can only transmit on the wavelengths 1 and 2 whereas the destination node can only receive at wavelengths 3 and 4. Even though there is an end-to-end wavelength-continuous path in this case, a lightpath cannot be established due to the wavelength termination constraint. If we allow multihopping, the intermediate node can drop the first wavelength and then add the fourth wavelength using all of its available transponders. Hence, a multihopped lightpath can be established by using wavelength 1 and 4 in the first and second links, respectively.

We also analyze the performance of multihopping together with various waveband assignment algorithms. We first describe the multihopping scheme that we use in the network. We then briefly review the waveband assignment algorithms that were introduced in Chapter 3 for uniform and non-uniform traffic, respectively. While making this comparison, we only consider fixed routing where all routes for source and destination pairs are initially computed according to minimum-hop routing. Multihopping is done on the fixed route by choosing the intermediate node(s) to do the drop/add.

The rest of the chapter is organized as follows. In Section 4.1, we describe the network model. In Section 4.2, the graph model for alternate multihop routing and fixed multihop routing is explained in detail. We provide simulation results to evaluate the performance

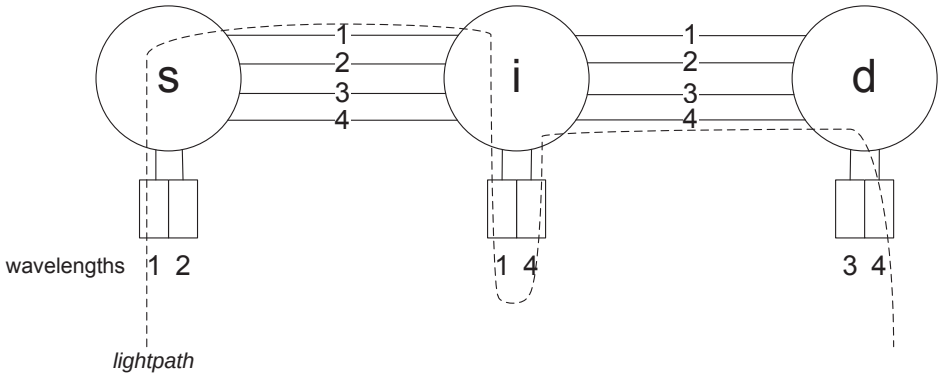

Figure 4.1: Example of multihopping.

of the new routing algorithm in Section 4.3 and also compare the effectiveness of multihopping and waveband assignment policies together. We conclude the chapter in Section 4.4.

4.1 Network Model

There are N nodes in the network numbered as $1, \ldots, N$, and L bidirectional links interconnecting them (i.e., each link has two fibers in opposite directions) numbered as $1, \ldots, L$. Each fiber carries W wavelengths numbered as $1, \ldots, W$. Each node is equipped with a fully reconfigurable multidegree ROADM with colorless ports. We adopt a Share-Per-Link model for the usage of transponders within a node. The number of transponders that a node has is T per link. Each LTT is assigned to a waveband of size Θ. There are B nonoverlapping wavebands where $B = W/\Theta$. We assume B to be an integer. D_n denotes the number of links that a node n is connected to, or the degree of node n. We denote the set of transponders for the incident link t of a node n by T_n^t where $t = 1, \ldots, D_n$. All lightpath requests are bidirectional and established on the same wavelength in both directions. Lightpath requests arrive in a Poisson fashion and they have exponential holding times. We show a 2-degree ROADM in Fig. 4.2 as an example. A lightpath can be dropped using the receiver of link 1 (T_n^1) and added using transmitter of the link 2 (T_n^2) for lightpath 1; or it

can be added/dropped by the transmitter/receiver of the link 1 (T_n^1), hence routed back on the same link as lightpath 2. We note that this requires the use of an O-E-O switch (not shown in the figure) that allows any receiver to be connected to any transmitter. Since we have bidirectional lightpaths, a transmitter/receiver pair together called as a transponder will be used for both add and drop. Wavebands of transponders at a node are assigned with the random algorithm described in Chapter 3.

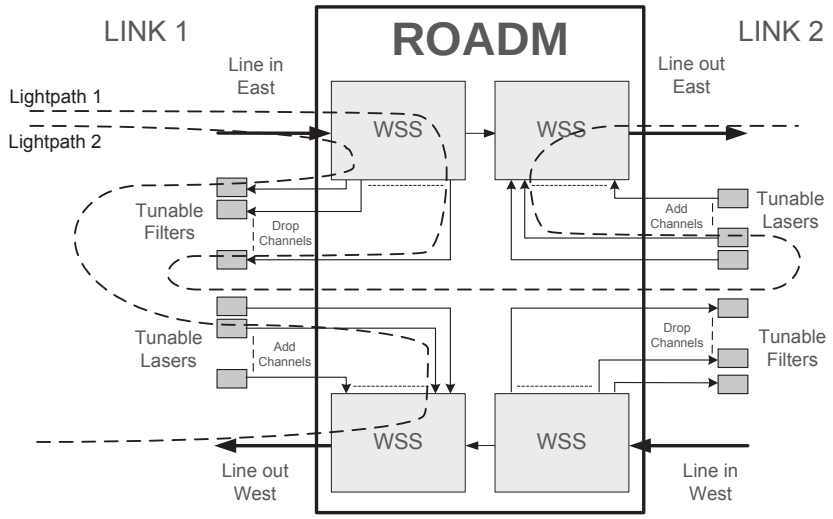

Figure 4.2: SPL Model.

4.2 Graph Model and RWA Algorithms

4.2.1 The Augmented Graph

We create an augmented graph consisting of W layers, one corresponding to each wavelength. A similar multi-layer graph is used in [36] but we need a more complex graph for the reasons explained in the following paragraphs. The number of nodes in the graph is $4LW$. The graph consists of directional links but the path calculated is established for a bi-directional lightpath. We call the directional links in the augmented graph as **connections** to distinguish them from the links in the actual network. We create the graph in three steps.

In the first step we create each wavelength layer of the graph. In the second step, we connect the auxiliary source and destination nodes to the graph. In the third step, we connect the different layers by creating the connections corresponding to possible wavelength conversions at an intermediate node by adding and dropping. After running the shortest path algorithm on the graph, we get the route as well as the wavelength. Transponder selection at the source and destination nodes or at any intermediate node where an add/drop occurs is done in a random fashion. We denote the cost of a directional connection from node i to node j in the augmented graph by $C(i, j)$. We now explain these steps in detail.

Step 1: We have two subnodes for a node n for each of its incident links. One of the subnodes is the ingress subnode to which a directional link enters, and the second one is the egress node from which an outgoing link starts. We denote ingress and egress subnodes of incident link t of node n at graph layer w by $S^w_{n,t,i}$ and $S^w_{n,t,e}$, respectively, where $1 \leq t \leq D_n$. We show the original network that we use as an example in Fig. 4.3 (a) and the subnodes corresponding to all 4 nodes in the original network are shown in Fig. 4.3 (b). n_1 and n_4 have 4 subnodes whereas n_2 and n_3 have 6 subnodes (2 subnodes per degree). Since we adopt the SPL model for transponders, having subnodes corresponding to each degree of a node is mandatory. Additionally, since there can only be one add/drop at a node, we implement an O-E-O conversion by a directional connection from an ingress subnode at one layer to an egress subnode at another layer of the graph. Egress subnodes are only connected to the other nodes in the network (i.e., not to any other subnode of its own node). Hence, if a path crosses an egress subnode, it is guaranteed that it leaves that node without resulting in multiple O-E-O conversions within the same node.

For a node n, every ingress subnode of one of its degrees is connected to every other egress subnode of the other degrees. Therefore, $C(S^w_{n,t_1,i}, S^w_{n,t_2,e}) = 0 \ \forall \ n, w;$ $1 \leq t_1, t_2 \leq D_n (t_1 \neq t_2)$. These connections correspond to bypass connections (i.e., no add/drop) at that intermediate node. Fig. 4.4 (a) shows the bypass connections for a 2-degree node and we can see the bypass connections in Fig. 4.3 (b) for the 3-degree nodes n_2 and n_3. A link l connecting nodes n and m in the physical network corresponds to a connection between the egress subnode of n to the ingress subnode of the node m and also

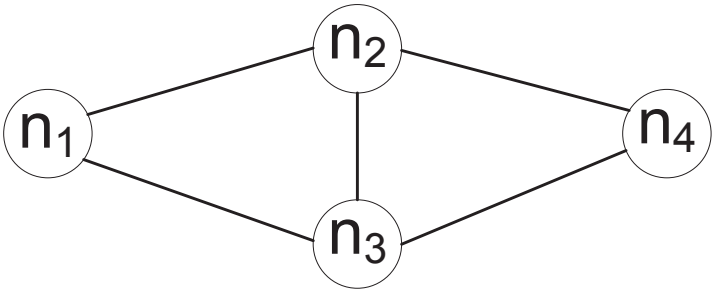

(a)

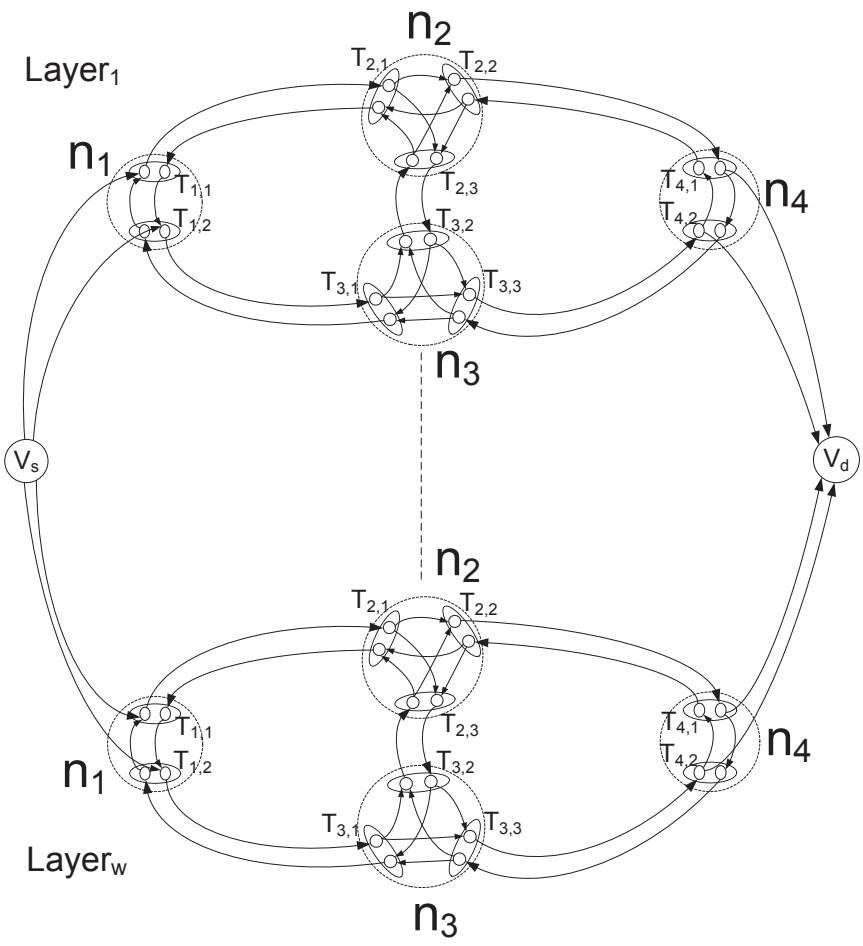

(b)

Figure 4.3: (a) Original network (b) Augmented multi-layer graph;

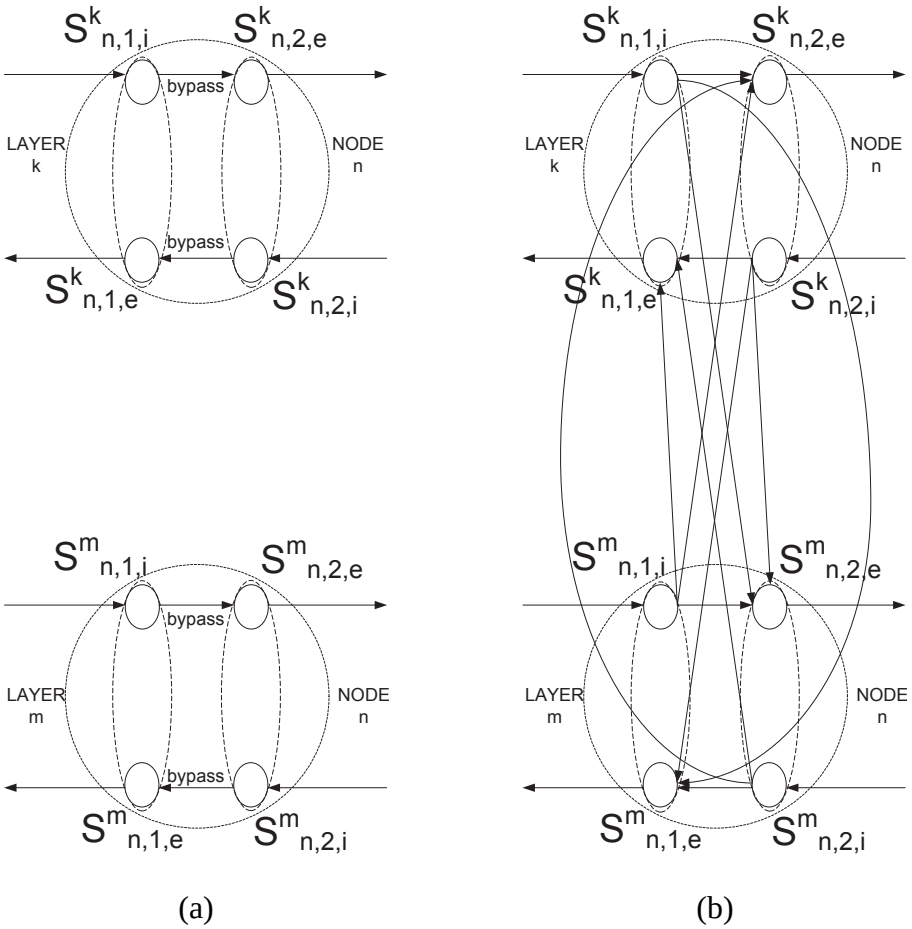

Figure 4.4: a 2-degree node in the augmented graph after establishing (a) bypass connections in Step 1, and (b) add/drop connections in Step 3.

between the egress subnode of m to the ingress subnode of the node n. For example, in Fig. 4.3 (b) we show the connections in opposite directions between the nodes n_1 and n_2. Such a connection within a layer exists only if that wavelength is available on that link. We do the cost assignment between the corresponding subnodes in the same layer w by the following formula.

$$C(S^w_{n,t_n,e}, S^w_{m,t_m,i}) = C(S^w_{m,t_m,e}, S^w_{n,t_n,i}) = \begin{cases} \frac{L-U(w)}{L}\sigma & \text{if } U(w) < L \\ \infty & \text{if } U(w) = L \end{cases} \quad \forall\, n, m(n \neq m), w. \tag{4.1}$$

where t_n and t_m are corresponding degrees of the nodes n and m to the actual link l, respectively; and σ is a scaling factor. $U(w)$ is the count of the overall usage of the

wavelength w in the network ($0 \leq U(w) \leq L$); this information is based on the network state. With this cost assignment the more utilized a wavelength in the network is, the lower will be its cost, hence more likely to be chosen on a route. This is chosen because the most used wavelength assignment has been shown to perform very well [37].

After the cost assignment for each link is done at every layer, the graph looks like in Fig. 4.3 (b).

Step 2: We add nodes V_s and V_d to specify which nodes are the source and destination of the arriving lightpath. V_s is connected to every egress subnode of the source node s, and every ingress subnode of destination node d is connected to V_d in every layer w. For example, V_s is connected to every egress node of n_1, and every ingress node of n_4 is connected to V_d in Fig. 4.3 (b) if a lightpath is requested between n_1 and n_4. The costs of these connections are

$$C(V_s, S^w_{s,t_s,e}) = \frac{1}{Z(s, t_s, w)} \tag{4.2}$$

and

$$C(S^w_{d,t_d,i}, V_d) = \frac{1}{Z(d, t_d, w)}, \tag{4.3}$$

where $1 \leq t_s \leq D_s$ and $1 \leq t_d \leq D_d$. $Z(n, t, w)$ is the number available transponders in the degree t_n of node n and that can tune to wavelength w.

Step 3: In the last step, connections are formed between different layers. As we have seen in the previous section, a conversion takes place in an intermediate node n and it can be either within the same degree or other degrees of the same node. There exists a connection from an ingress subnode of t_1 in layer w_1 to the egress subnode of t_2 in layer w_2 and from the ingress subnode of t_2 in layer w_2 to egress subnode of t_1 in layer w_1. These connections for a 2-degree node are illustrated in Fig. 4.4 (b). We assign costs as below.

$$C(S^{w_1}_{n,t_1,i}, S^{w_2}_{n,t_2,e}) = C(S^{w_2}_{n,t_2,i}, S^{w_1}_{n,t_1,e}) = \begin{cases} \frac{1}{\min(Z(n,t_1,w_1), Z(n,t_2,w_2))} & \text{if } t_1 \neq t_2 \\ \frac{1}{Y(n,t_1,w_1,w_2)} & \text{if } t_1 = t_2 \end{cases} \tag{4.4}$$
$$\forall\, n, w_1, w_2 (n \neq s, d)(w_1 \neq w_2),$$

where $Y(n, t_1, w_1, w_2)$ is the number of available transponder pairs, the first of which can tune to w_1 and the second to w_2, or vice versa. Functions Z and Y are chosen so that

multihopping is done at the nodes which have higher number of available transponders for the purpose of not exhausting transponders of a node.

4.2.2 RWA Algorithms

4.2.2.1 Alternate Multihop Routing Algorithm

The alternate multihop routing (AR-Multihop) algorithm is explained in Algorithm 4.1. We note that there are two connections in opposite directions in the augmented graph in one layer corresponding to one physical link in the network. Since we establish bidirectional calls, we prevent Dijkstra's algorithm from using both of these connections along a route at the same time by modifying the algorithm. Therefore, during a run of Dijkstra's algorithm, every time a subnode is reached via one such directional connection and it is included in the set for which shortest paths are already calculated, we make the connection in the opposite direction to have an infinite cost within the same layer w (i.e., if a subnode $S^w_{m,t_m,i}$ of node m is included in the set through a connection from another subnode ($S^w_{n,t_n,e}$) of node n, we set $C(S^w_{m,t_m,e}, S^w_{n,t_n,i}) = \infty$).

4.2.2.2 Fixed Multihop Routing Algorithm

In order to compare the performance of multihopping with fixed routing, we modify our algorithm as follows. All routes for source-destination pairs are initially computed according to minimum-hop routing. We create the augmented multilayer graph, however in this case each layer contains only the subnodes of physical nodes that are on the computed fixed route. For every lightpath request, this graph is created containing $4Wh$ nodes where h is the hop-length of the route. Costs of all the connections are calculated as in the previous case. Hence, this algorithm chooses the intermediate nodes that are best for multihopping on a fixed route. We name this algorithm as FR-Multihop. The augmented graph consists of W layers and each layer consists of nodes corresponding to a fixed route r connected with directional links. For each node along the path, we have two subnodes (ingress and egress) corresponding to two incident links of the node that is used on that route. Let H denote the hop-length of a route r. We denote the ingress and egress subnodes of the h^{th} node

input : Network graph and network state

output: Routing and wavelength assignment for the lightpath request between the source and destination nodes (s, d)

```
Generation of the augmented graph G
    Create every layer of graph;
    Connect nodes V_s and V_d to the subnodes of s and d in each layer;
    Connect layers to each other by connecting the same nodes in different layers;
Run the modified Dijkstra's Shortest Path Algorithm to find paths from node V_s to
every other node;
if a path is found between V_s and V_d then
    Trace the path from V_s to V_d;
    Establish the calls on each multihop on the calculated wavelengths;
    For the source and destination of each hop, choose the transponders
    randomly
else
    Block the call
```

Algorithm 4.1: Alternate multihop routing algorithm (AR-Multihop)

along the route in layer w by $S^w_{h,i}$ and $S^w_{h,e}$ where $2 \leq h \leq H$. The source and destination consists of only one node denoted as S^w_1 and S^w_{H+1}, respectively.

For each node along the route , the ingress subnode is connected to the egress subnode which establishes the bypass links (i.e., no add/drop). Therefore, $C(S^w_{h,i}, S^w_{h,e}) = 0, \;\; 2 \leq n \leq H, \forall w$. We see the bypass links in Fig. 4.5 (a). Consecutive nodes along the path in layer w are connected via a link, the cost of which is assigned by the following formula.

$$C(S^w_{h,e}, S^w_{h+1,i}) = \begin{cases} \frac{L-U(w)}{L}\sigma & \text{if } U(w) < L \\ \infty & \text{if } U(w) = L \end{cases} \qquad 1 \leq h \leq H, \forall w. \tag{4.5}$$

$U(w)$ is the overall usage of the wavelength w in the network ($0 \leq U(w) \leq L$). With this cost assignment more utilized wavelengths in the network have lower costs and they are more likely to be chosen on a route. In [37], it is shown that the most used wavelength

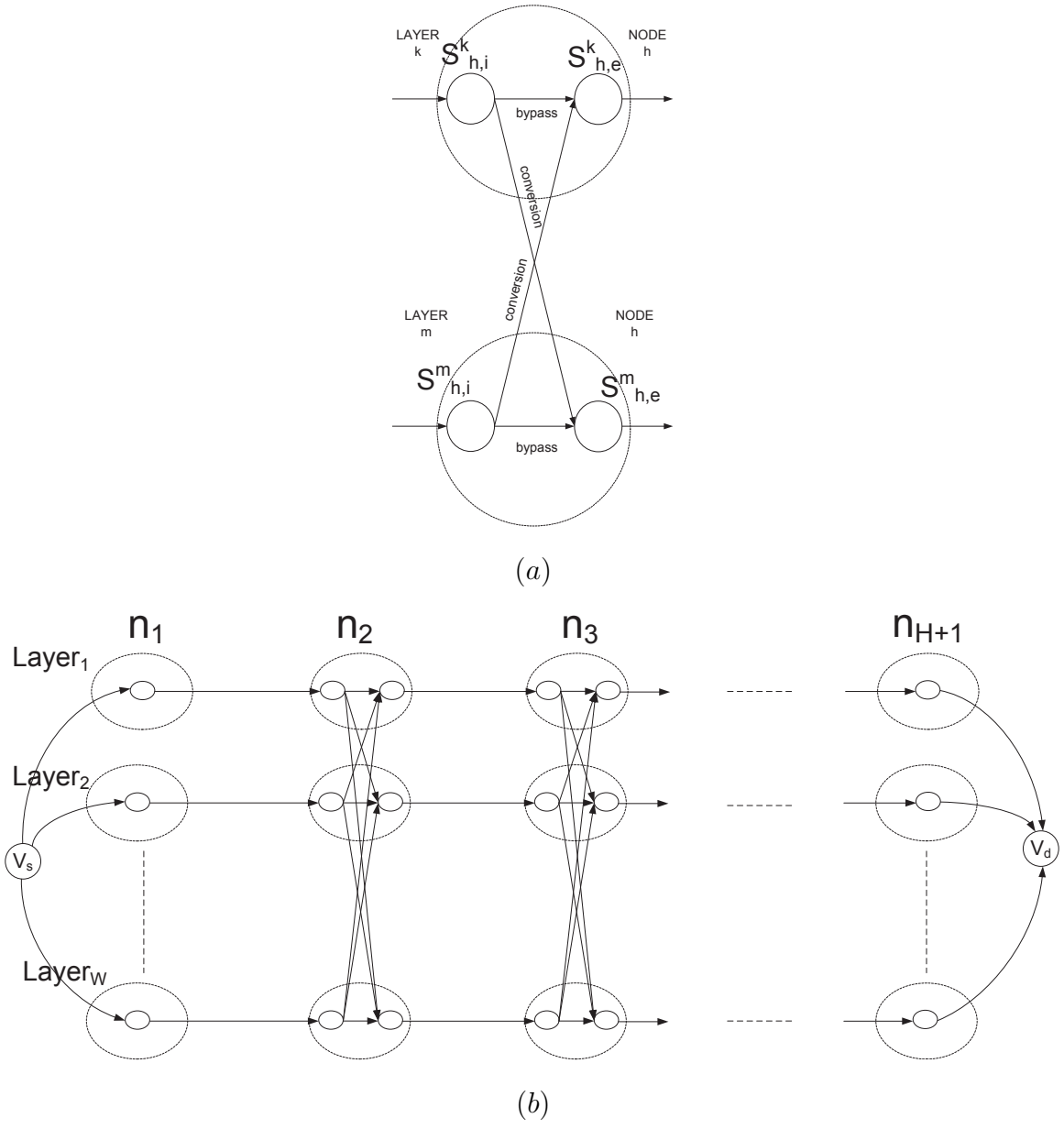

Figure 4.5: (a) Bypass and add/drop connections at a node between layers k and m (b) The augmented multilayer graph for a route with H hops.

assignment perform very well. σ is a scale factor. We create the links between different layers at a node along the path corresponding to a drop/add at that node. For the node n_h, the ingress subnode at one layer is connected to the egress subnode at another layer. In Fig. 4.5 (a), we see that the $S^k_{h,i}$ is connected to $S^m_{h,e}$ and $S^m_{h,i}$ to $S^k_{h,e}$. The costs of those links are assigned as below.

$$C(S^{w_k}_{h,i}, S^{w_m}_{h,e}) = \frac{1}{\min(Z(h,i,w_k), Z(h,e,w_k))}\ 1 \leq h \leq H, \forall\, w_k, w_m (k \neq m), \tag{4.6}$$

where $Z(n_h, i/e, w)$ is the number available transponders in the ingress/egress link of node n_h that can tune to wavelength w. The purpose of using function Z is to choose the nodes that have higher number of available transponders to do the drop/add. Therefore, the drop/add nodes are chosen fairly, not exhausting the transponders of a node. We also add the nodes V_s and V_d to the graph by connecting them to the source (n_1) and destination(n_{H+1}) nodes, respectively. Those links are assigned the costs $C(V_s, S^w_1) = \frac{1}{Z(n_1,e,w)}$ and $C(S^w_{H+1}, V_d) = \frac{1}{Z(n_{H+1},w)}$. The final graph looks like Fig. 4.5 (b) and it contains $2WH$ nodes.

Upon a lightpath request arrival, the augmented graph is created as explained in the previous paragraphs. We run the Dijkstra's shortest path algorithm on the augmented graph to find the shortest paths from node V_s to every other node. We follow the path calculated between V_s and V_d establishing the lightpath on each multihop on the chosen wavelength. For the source and destination of each hop, we choose the transponders randomly out of the available ones. We name this fixed routing multihopping algorithm as **FR-Multihop**.

4.2.2.3 Exhaustive Fixed Multihop Routing Algorithm

We want the multihop route on the fixed route to have minimum number of hops (drop/add(s)). We do this in an exhaustive way first starting by searching an end-to-end wavelength-continuous route. If such a route does not exist, we look for an intermediate node to do the drop/add starting with the next node along the fixed route (to establish a two-hop route). If a two-hop route cannot be found, then we look for a 3-hop route, and so on. We name this algorithm as **FR-Multihop-E** (We call the fixed routing algorithm without multihopping as **FR**). FR-Multihop-E is implemented in a recursive manner as shown in Algorithm. 4.2.

The function FindMultihopRoute(s, m) searches for a multihop route starting at the node s along R and consisting of m multihops after s. The function FindWavelength(n_1, n_2) finds if there is a transmittable wavelength– a wavelength that is available on the section of R between n_1 and n_2 and has available transponders that can tune to that wavelength on both n_1 and n_2.

input : The fixed route R with hop-length H and network state

output: Routing and wavelength assignment for the lightpath request on Route R

for $multihop \leftarrow 0$ **to** H **do**

  if `FindMultihopRoute`$(0, multihop)$ **then**

    Accept the call

  else

    Block the call

Algorithm 4.2: Exhaustive fixed multihop routing algorithm (FR-Multihop-E)

if $m > 0$ **then**

  for $h \leftarrow 1$ **to** $H - s - m$ **do**

    if `FindWavelength`$(s, s+h)$ *AND*

    `FindMultihopRoute`$(s+h, m-1)$ **then**

      Establish the lightpath on the section between nodes s and $s+h$ by randomly choosing transponders and wavelengths; Return SUCCESS

else if `FindWavelength`(s, H) **then**

  Establish the lightpath on the section between nodes s and H by randomly choosing transponders and wavelengths; Return SUCCESS

Return FAILURE

Function `FindMultihopRoute`(s, m)

In order to distill the benefits of multihopping alone (from the combination of multihopping and alternate routing), we compare the performance of our algorithm with an alternate routing algorithm without multihopping. We again modify our algorithm for this purpose by just skipping the third step of the graph generation procedure which creates the connections in the graph for multihopping. We call this algorithm AR. We also call the fixed routing without multihopping as FR.

4.3 Numerical Results

We ran simulations on the 10-node ring network and the well-known NSFNet using 100000 call arrivals (10000 arrivals at higher loads due to time constraints). In all of our simulations, we use $W = 16$. Overall blocking probability is calculated by taking the average of route blocking probability over every route (i.e., every source and destination pair). ρ is the load per route and per wavelength. Unless mentioned otherwise we use $\sigma = 0.2$ for the algorithms AR and AR-Multihop. The curves of FR-Multihop and FR-Multihop-E are very similar, so we only present FR-Multihop-E results in our graphs.

We first plot blocking vs. load for ring and NSFNet in Fig. 4.6 (a) and (b), respectively. In Fig. 4.6 (a), we see that FR gives the worst blocking and FR-Multihop-E improves the blocking compared to FR. Therefore, multihopping offers an advantage even for fixed routes. The blocking values of AR are lower than FR-Multihop-E, which shows that using alternate routes even without multihopping is more advantageous than having multihopping on a fixed route. AR-Multihop results in the lowest blocking values (significantly lower than AR) and the difference between the other curves is much larger with lower loads. For load $\rho = 0.03$, the ratio of the blocking values of FR and and AR-Multihop is 53. Therefore, the addition of multihopping in alternate routing improves the blocking significantly compared to only alternate routing. As the load increases, all of the curves merge to the same value. The same behavior is true for the NSFNet in Fig. 4.6 (b), AR-Multihop results in better blocking than the other algorithms. The curve of AR-Multihop increases in a linear fashion while the difference is larger with lower loads. However, the performance difference between AR and AR-Multihop is not significant in NSFNet compared to the ring. AR-Multihop and AR curves get closer after $\rho = 0.04$. We conclude that alternate routing offers advantage over all fixed routing methods with or without multihopping, but alternate multihop routing improves the blocking even further (except for higher loads after $\rho = 0.050$ for the NSFNet).

We now look into the performance of AR-Multihop when WTTs are utilized in the network (i.e., $\Theta = 16$). In Fig. 4.7 (a), we observe that AR and AR-Multihop curves are very close and they are both better than both of the FR algorithms. The gap between AR

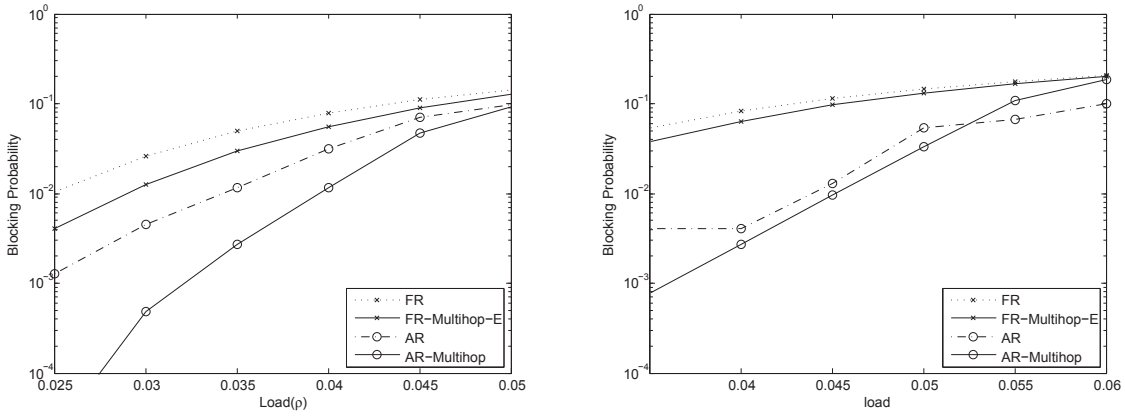

Figure 4.6: Blocking probability vs. load (ρ) for $T = 8$ and $\Theta = 2$ in (a) ring (b) NSFNet.

and FR curves is larger for lower loads. This is the same for NSFNet as seen in Fig. 4.7 (b) where we observe a larger gap between FR and AR curves. We conclude that when WTTs are used in the network multihopping with alternate routing is not as advantageous as when LTTs are used.

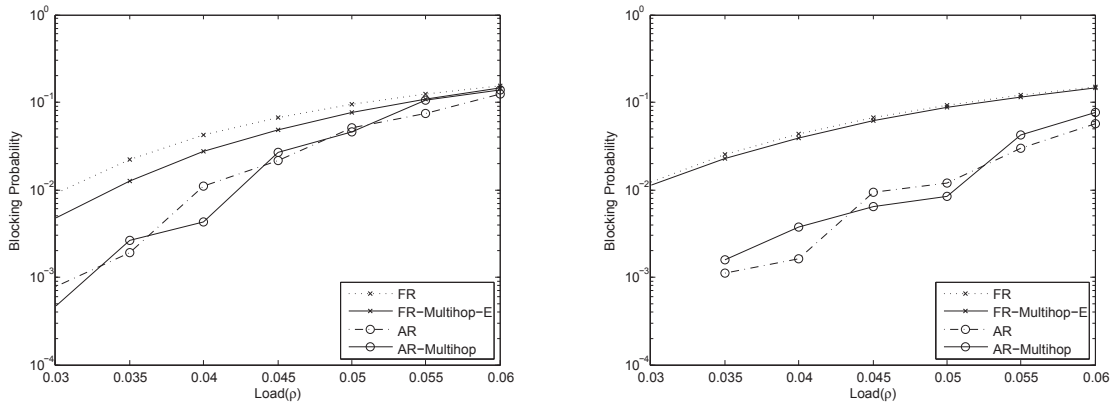

Figure 4.7: Blocking probability vs. load (ρ) for $T = 8$ and $\Theta = 16$ in (a) ring (b) NSFNet.

We compare the performance of the two FR algorithms and AR-Multihop in Fig. 4.8 by plotting blocking vs. number of transponders (T) for ring and NSFNet. We observe that the blocking for AR-Multihop decreases until $T = 8$ for the ring in Fig. 4.8 (a) for AR-Multihop with $\sigma = 0.2$ at a fast rate. After that point, it decreases slightly until $T = 16$

except a slight increase at $T = 14$. With a higher σ value of 1.0, AR-Multihop performance gets better for larger T values than 8 with the expense of higher blocking than with $\sigma = 0.2$ for $T \leq 8$. FR and FR-Multihop-E performance is continuously decreasing with T while the gap between the two curves is increasing. The difference between the curves of both FR algorithms and AR-Multihop becomes significantly high after $T = 6$. Therefore, the advantage of multihopping increases with higher T, and for lower T values multihopping exhausts the transponders in the network. In Fig. 4.8 (b), we see that AR-Multihop performs much better than both FR algorithms for NSFNet, especially for higher T values. After $T = 8$, blocking with AR-Multihop is at least 30 times lower than FR algorithms. FR and FR-Multihop-E curves are close until $T = 8$ but after that FR-Multihop-E starts performing better. We again conclude that multihopping offers the most advantage at higher T values when the transponder resources are more abundant.

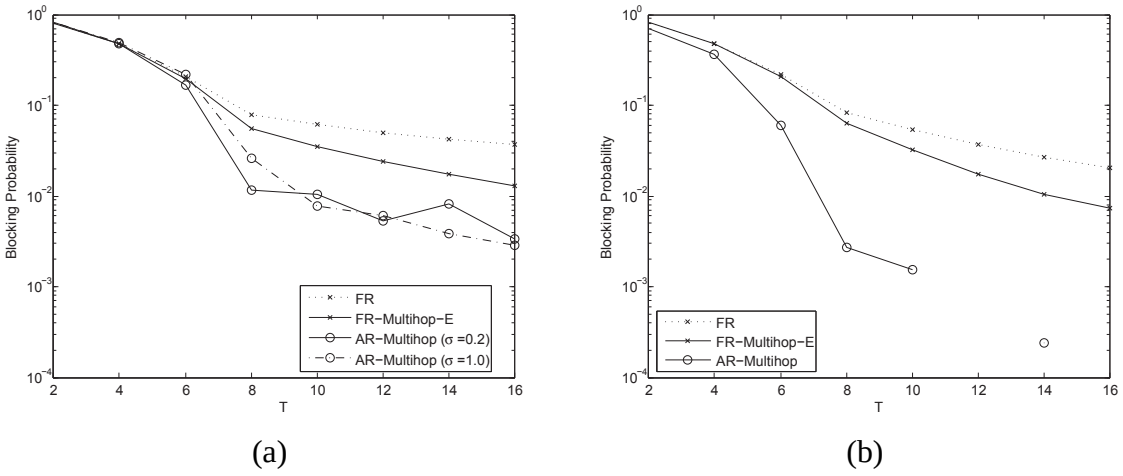

Figure 4.8: Blocking probability vs. number of transponders (T) for $\Theta = 2$ and $\rho = 0.04$ in (a) ring (b) NSFNet.

4.3.1 Comparison of Multihopping and Waveband Assignment

The wavelength/waveband assignment algorithms we take for comparison in this section are C-fixed random assignment and COWA from 3. During the comparison, we run each algorithm with multihopping and without multihopping for uniform and non-uniform traf-

fics. Whenever we mention the value of C, it corresponds to the C-fixed algorithm with that particular C value. $C = 0$ case corresponds to the random assignment.

We first show results with uniform traffic and $W = 16$ by plotting blocking vs. load in Fig. 4.9. For the ring in Fig. 4.9 (a) we see that FR-Multihop-E with $C = 8$ gives the best blocking for lower loads. For lower loads than $\rho = 0.32$, FR with $C = 8$ gets better than FR-Multihop-E with $C = 0$. This is when transponder waveband assignment is more effective than multihopping. Multihopping brings an improvement to blocking for lower loads close to an order of magnitude as observed between the curves of FR with $C = 0$ and $C = 8$. As the load increases the blocking values of all curves get closer to each other while FR-Multihop-E curves are slightly better than FR. In Fig. 4.9 (b), similar observations can be made for the NSFNet. In Fig. 4.10 (a) and (b), we plot curves with 3 different C values for $T = 4$ for ring and NSFNet, respectively. Higher C values always give better blocking than lower C values no matter if multihopping is used or not. The improvement brought by multihopping is smaller in this case and waveband assignment is more dominant. Additionally, the performance difference between FR and FR-Multihop-E is smaller with higher C. This is due to the fact that the waveband mismatch is already minimized and multihopping does not help as much to improve the mismatch.

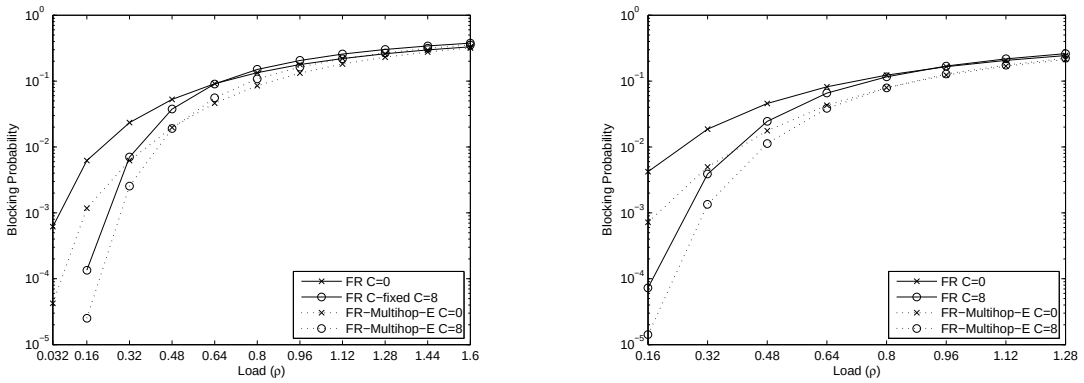

(a) (b)

Figure 4.9: Blocking probability vs. load (ρ) for $T = 8$ and $\Theta = 1$ in (a) ring (b) NSFNet.

We show blocking vs. load for non-uniform traffic with $W = 32$ in NSFNet for 4 and 5 highly loaded routes (see Section 3.2.2) in Fig. 4.11 (a) and (b), respectively. FR-

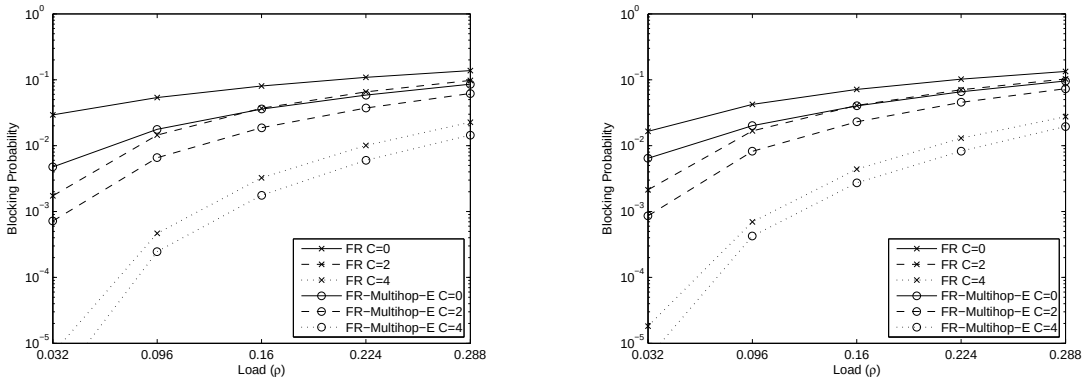

(a) (b)

Figure 4.10: Blocking probability vs. load (ρ) for $T = 4$ and $\Theta = 2$ in (a) ring (b) NSFNet.

Multihop-E used together with the COWA for non-uniform traffic with $D = 5$ and $S = 1$ gives the best blocking over all load values. For FR-Multihop-E, $C = 16$ is worse than $C = 0$. This can be again explained by multihopping not offering any advantage since the wavelengths of all nodes are the same and with $C = 16$ the network uses only 16 wavelengths resulting in path blocking being dominant. The difference between FR $C = 0$ and FR-Multihop-E $C = 0$ is significantly high (close to 2 orders of magnitude with lower loads). Multihopping is very advantageous in this case even without any scheme of transponder waveband assignment. The heuristic (FR-Multihop-E COWA $D = 5$, $S = 1$) only brings a small improvement over FR $C = 0$. In Fig. 4.11 (b) similarly FR-Multihop-E COWA $D = 5$, $S = 1$ gives the best blocking. There is also no difference between the FR-Multihop-E curves with $C = 0$ and $C = 16$. The performance difference with FR and FR-Multihop-E is again the largest with $C = 0$.

4.4 Summary

We studied the performance of multihopping with O-E-O conversions along the route of a lightpath considering the use of limited tunable transponders in the reconfigurable nodes. We developed an alternate multihop routing algorithm to select a multihop route based on the availability and tunabilities of limited tunable transponders while considering the

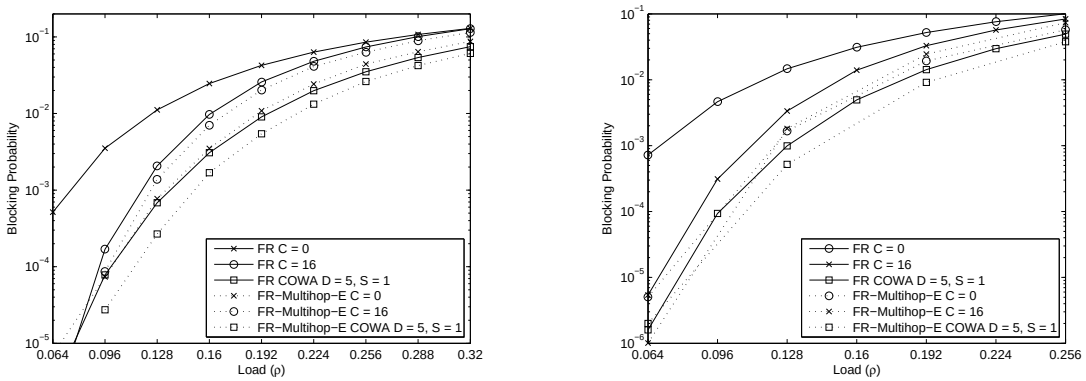

Figure 4.11: Blocking probability vs. load (ρ) with $T = 16$ and $\Theta = 1$ in NSFNet for (a) 4 (b) 5 high loaded paths.

wavelength usage as well. We compared the performance of the AR-Multihop algorithm with fixed routing algorithms (with or without multihopping) and also with alternate routing without multihopping. We showed that the AR-Multihop algorithm is superior to all in terms of blocking when limited tunable transponders are used and the performance gap is quite large with lower loads (e.g., 53 times better for $\rho = 0.03$ in the ring network). The results confirm that alternate routing results in a better performance than fixed routing methods with or without multihopping, but when it is used with multihopping the performance is further improved in the case of limited tunable transponders. We also showed that multihopping results in better blocking with higher number of transponders when O-E-O conversions do not exhaust the transponders in the network. We also evaluated the performance of exhaustive fixed multihop routing algorithms with several waveband assignment algorithms comparing with the case when no multihopping is allowed in limited reconfigurable networks. We showed that waveband assignment is generally more effective than multihopping in reducing blocking.

Chapter 5

Waveband Switching

The rapid increase in data demands is driving the need for higher number of wavelengths per fiber. Higher number of wavelengths also means higher switching complexity at optical nodes such as optical crossconnects (OXCs) and reconfigurable optical add/drop multiplexers (ROADMs). In a wavelength switched optical node, each wavelength is individually switched, requiring one switch per wavelength (or equivalently, one OXC port per wavelength). An example of a wavelength cross-connect for a ring network is shown in Fig. 5.1(a); all wavelengths from the network input are demultiplexed, and each wavelength is switched using a switching element shown in Fig. 5.1(b) [38]. The cost of such wavelength switching nodes can be very high considering the large number of wavelengths possible today [39, Ch. 2]. Waveband switching was introduced to reduce the size of optical switches by switching groups of wavelengths together using a single switch per group [11]. The wavelengths within a waveband are usually consecutive because of the way wavelengths are demultiplexed from a WDM signal, and sometimes because of how certain switches operate [40].

With this technique, the wavelength spectrum can be divided into wavebands and lightpaths that are in the same waveband can be switched together. Several multi-granular optical crossconnects with waveband switching capability were introduced in [12], [13]. With the constraint brought by waveband switching at optical nodes, one main objective was to group lightpaths into wavebands as much as possible to efficiently use the switching resources in the network. Several authors have looked into the problem of waveband grouping, and proposed algorithms to efficiently use the limited switching capability of the network [15, 16, 17].

Previous work considered two kinds of waveband switching: (a) uniform, and (b) non-uniform waveband switching. In uniform waveband switching, the waveband sizes at a

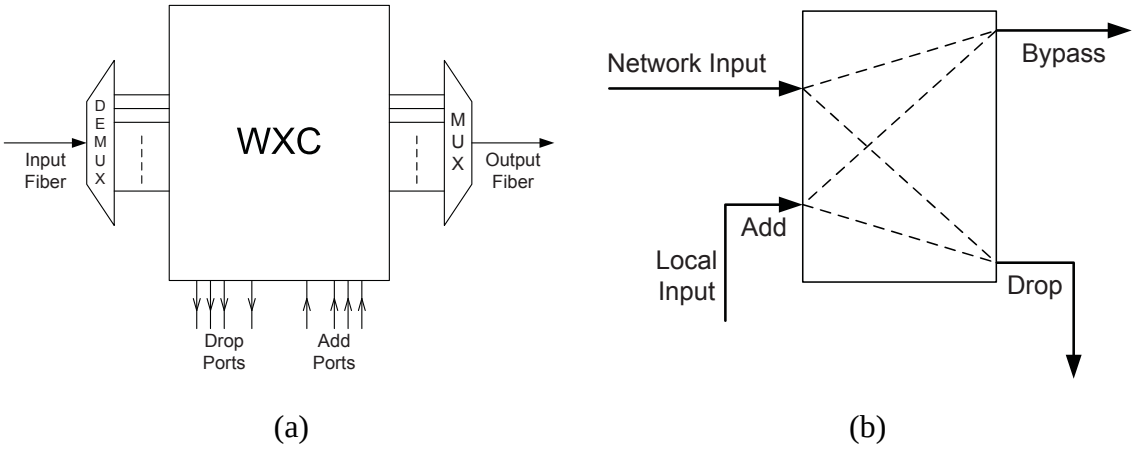

Figure 5.1: (a) A wavelength cross-connect (b) a wavelength switching element within the crossconnect for rings.

node are all equal and the same waveband sizes are used at every network node [15, 16, 41]. The case of different number of uniform wavebands at different nodes is considered in [42]. It was shown that having non-uniform waveband sizes is advantageous in minimizing switching requirements in [43, 18], where optimal ways of partitioning the wavelength set into wavebands are shown for various network topologies and traffic patterns.

In [18] and [43], the authors investigated non-uniform wavebands focusing on a single node. In [18], the optimal wavebands for a switch with a single input and multiple output fibers are obtained. A similar design is presented in [43] where they also included the case of a single switching node with multiple inputs and multiple outputs (i.e, a star network). Additionally, solutions for general network topologies are presented for permutation traffic in [43].

As we will show later, single-node solutions are incapable of handling even a simple set of connection requests in a *network*. In this chapter, we consider a waveband optimization problem defined for the entire network, and present a novel formulation of the problem. We then solve the problem for ring topologies for a specific deterministic traffic type. As it turns out, the waveband sizes are not only non-uniform at a node, but also vary between nodes – a scenario never considered before in the literature. We then evaluate the performance of the waveband design under stochastic dynamic traffic, and show that our design

can yield significant performance advantages over other designs.

Other related work has appeared in [44, 45]. Tuning bands of reconfigurable optical add/drop multiplexers (ROADMs) in ring networks were considered in [44]. However, that paper minimized the worst-case band size of contiguous wavelengths accessed by a transponder, and did not consider the optimization of switching costs. The blocking performance of ROADMs is evaluated in [45] where limited add/drop capability is brought by limited tunable transponders.

The rest of the chapter is organized as follows. In Section 5.1, we propose a ROADM architecture for rings that is capable of non-uniform waveband switching. In Section 5.2, we formulate an optimization problem for the number of wavebands in ring networks for deterministic traffic, and present a novel framework for solving the problem. We discuss the complexity of the problem, and present some heuristic solutions. In Section 5.3, we apply the formulation and heuristics to a specific traffic type, namely, all-to-all traffic, and present some numerical results to show the advantages of our approach. The performance of the waveband design under the oft-considered Poisson traffic is evaluated through simulations in Section 5.4. Conclusions and some directions for future work are given in Section 5.5.

5.1 Band Tunable OADM

The band tunable OADM architecture is based on a simple architecture proposed in [40], namely *Flexible Band Tunable Add/Drop Multiplexer*. While the architecture of [40] has only 3 wavebands, the general architecture we propose here can be built for any number of wavebands. It consists of an add and a drop module. We first show the drop module in Fig. 5.2 (a). Assuming that the wavelengths in the input fiber constitute 8 wavebands and each band is either a bypass band or an add/drop band (denoted by B and D, respectively), this architecture separates the input fiber into each individual waveband. It uses tunable edge filters (TEF) to divide an input optical signal into two bands. High λ and low λ TEFs serve as low pass and high pass optical filters, respectively. As a result of sequential filtering, the input signal is in the end separated into each individual optical band. Colorless de-multiplexers are used for each drop waveband to separate the bands into individual

wavelengths. The add module uses the same components fed in from the opposite direction as seen in Fig. 5.2 (b).

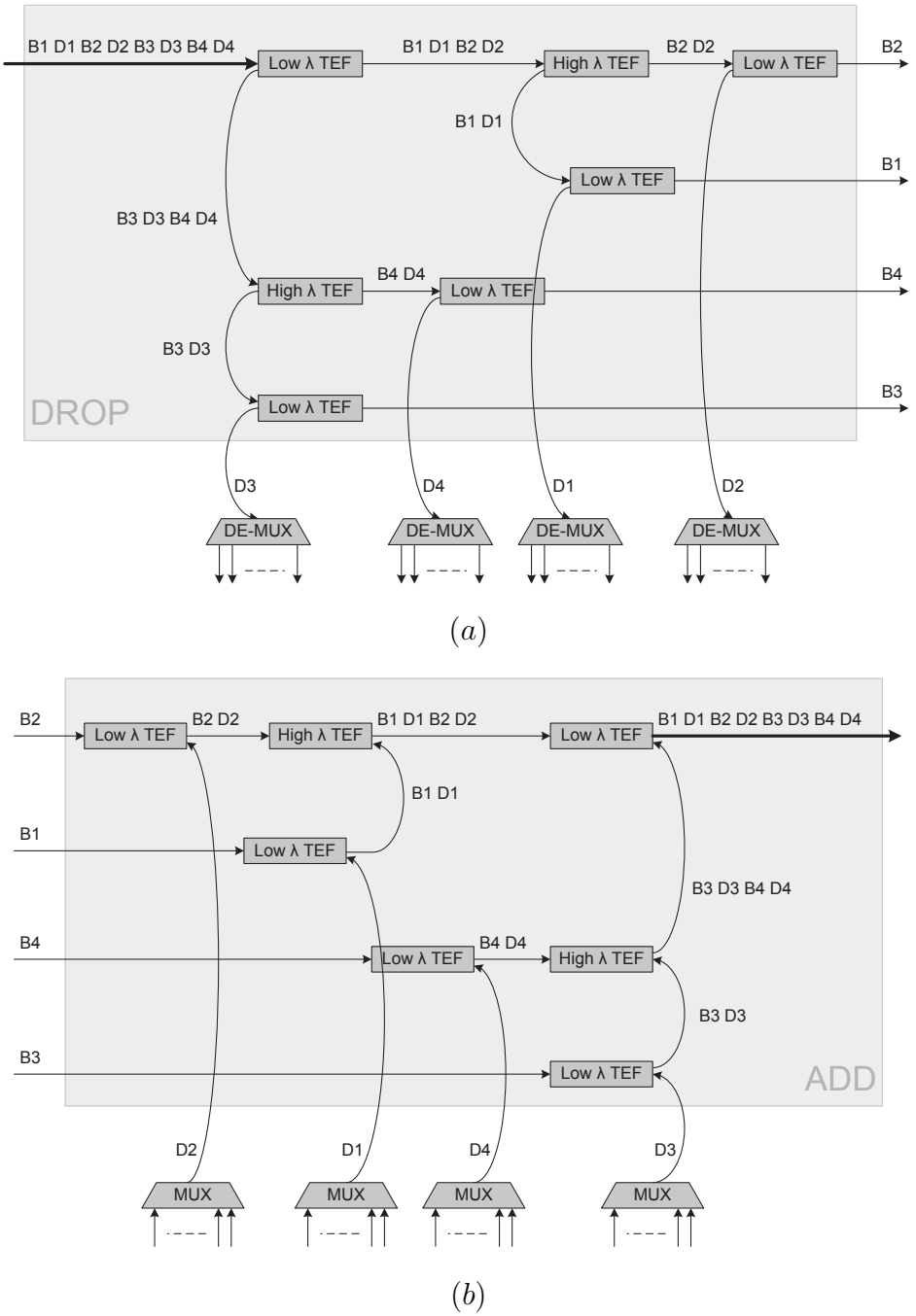

Figure 5.2: Band tunable OADM (a) drop module(b) add module.

By tuning the TEF, the sizes of the wavebands can be dynamically adjusted. Hence,

waveband sizes can be chosen as desired (i.e., non-uniformly) and also be changed over time. We note that this architecture requires the use of $2(B-1)$ TEF's in order to have B wavebands at the add and drop modules.

5.2 Banding in Ring Networks for Deterministic Traffic

We consider ring topologies – both uni-directional (with a single fiber per link, oriented in one direction) and bi-directional (with two fibers per link, oriented in opposite directions) – in this section. We define a *deterministic traffic* to be a specified set of lightpaths (LPs, or connections) that the network is required to support (i.e., the LPs can be provisioned) in the worst case. The actual LP traffic in the network may be random and/or dynamic; as long as the set of LPs at any time is a subset of the deterministic traffic, the network can support the LP set.[1] Let us suppose we are given such a deterministic traffic. In this section, we present a formulation for the problem of minimizing the number of wavebands in the network, discuss the complexity of the problem, and present solution approaches. We first show by example that single-node wavebanding solutions (as in [18]) do not work when the network is considered as a whole.

5.2.1 The Inadequacy of Single-Node Solutions

We briefly explain the single-node solution of [18] for reader convenience. Suppose a node has one input fiber and, say, F output fibers, and each fiber has W wavelengths. In order for the switch to support any breakdown of wavelengths from the input fiber to the output fiber, the authors developed an optimal algorithm that finds the non-uniform waveband sizes giving the minimum number of bands. The algorithm can be explained as follows: Initializing $W' = W$ at the beginning, calculate the size of the band at each step i by $b_i = \lceil W'/F \rceil$, and update W' as $W' = W' - b_i$. The algorithm stops when $W' = 0$. As an example, when $F = 2, W = 8$, the 8 wavelengths are grouped into 4 bands of size $4, 2, 1,$ and 1. The reader can easily verify that i wavelengths can be switched to the first output (and $W - i$ switched to the other output), for any value of i $(i = 0, 1, \ldots, 8)$

[1] If a LP request arrives that is not part of the deterministic LP set, then obviously it is blocked.

by combining the bands appropriately. For example, if 5 wavelengths are desired at the first output port, then the band of size 4 and one of the bands of size 1 can be assigned. Note that uniform banding would have required 8 bands of size 1 (which is the same as individual wavelength switching), and so non-uniform banding saves 4 switches in this case. A similar banding algorithm is given for a single switch (equivalent to a star network with a single source node) in the case of P-port traffic in [43]. The banding calculation becomes identical with [18] when $P = W$.

We now show that the same band sizes (calculated by the algorithm in [18] for a single node) cannot be used at every node to support all traffic for which there are sufficient number of wavelengths. Consider all-to-all traffic (one LP between every pair of nodes) in a 5-node bi-directional ring network. It has been shown that 3 wavelengths per fiber are necessary and sufficient to support this traffic (see [46], for example). Furthermore, LPs must be routed along the shorter direction, and all wavelengths are utilized on all links in this solution. Therefore, whenever a wavelength is dropped at a node to terminate a lightpath, the same wavelength must be added by the same node to originate another lightpath. Each wavelength or waveband at a node can be added/dropped (A/D) or bypassed (B). We need only consider one direction of the ring because the switches in the other direction are set correspondingly. The bands calculated by the algorithm of [18] with $W = 3, F = 2$ gives two wavebands of sizes 2 and 1. Since each node requires two A/D wavelengths to connect to the 4 other nodes, the waveband of size 2 should be A/D at each node. Out of the 3 wavelengths, the A/D band can be wavelengths $\{1, 2\}$, or wavelengths $\{2, 3\}$. Thus, the 3 wavelengths are arranged in 2 bands in one of the following two configurations at each node. (Note the two bands cannot both be A/D or both be B, because some LPs bypass and some LPs terminate at each node.)

Note that wavelength 2 is always in an A/D band as seen in Fig. 5.4(a). Now, since only one of the above two bandings is possible at any node, if wavelength 1 is in an A/D band, then wavelength 3 is in a B band, and vice versa. Of the 5 nodes in the network, let $k_1,\ k_1 = 0, 1, \ldots, 5$ nodes be of Type 1 and the other $k_3 = 5 - k_1$ be of Type 2. It is easy to see that $k_1 = 0, 1$ would not allow any LP to be provisioned on wavelength 1, while $k_1 = 2$ will let one LP to be provisioned, but leaves wavelength 1 un-utilized on the other

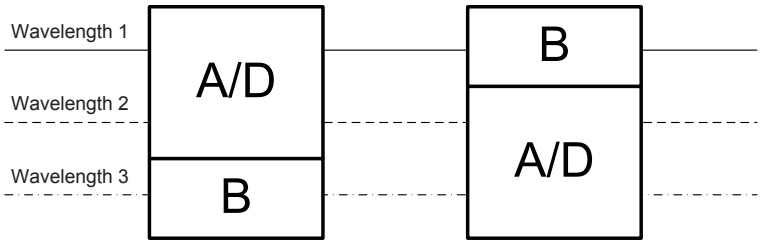

Figure 5.3: The two possible configurations of the two bands with $W = 3$ in a bi-directional ring. B means Bypass, A/D means Add/Drop. A node with the left configuration is called Type 1, and with the right configuration is called Type 2.

links, and is therefore not sufficient to support the given traffic. Now, when $k_1 = 3, 4, 5$, $k_3 = 2, 1, 0$, respectively, and wavelength 3 would have the same problem. Therefore, it is not possible to support all-to-all traffic using just the two bands. An example illustrating this impossibility is given in Fig. 5.4(a). It can be seen that two bands are sufficient if there are 4 nodes, but the addition of a fifth node requires one of the nodes to have 3 bands. A valid band assignment for all-to-all traffic is shown in Fig. 5.4(b).

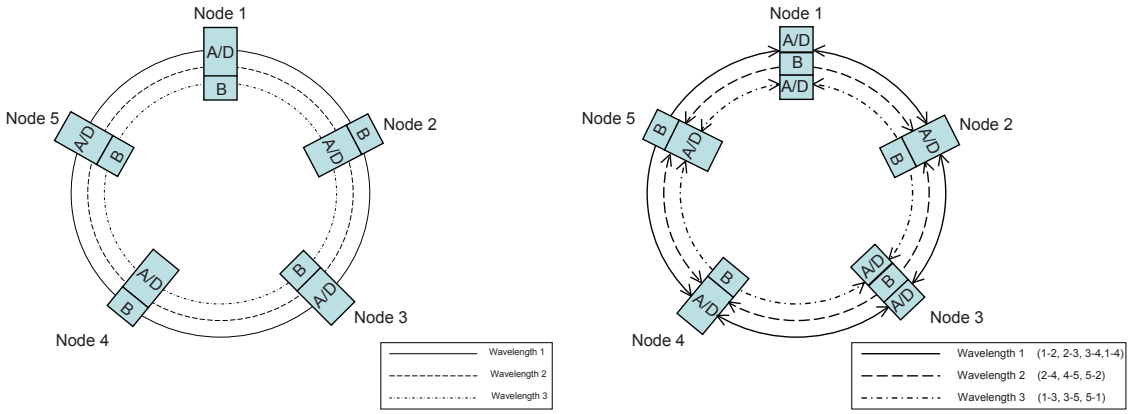

Figure 5.4: (a) Inadequacy of two bands for all-to-all traffic, and (b) a valid solution with 3 bands in a 5-node bi-directional ring. B: Bypass, A/D: Add/Drop

It can be shown that two bands are not sufficient for the case of uni-directional ring in a similar manner. Here, just a 3-node example suffices. Three wavelengths are required for a three node uni-directional ring as in Fig. 5.5. For all-to-all traffic, each node has an

LP to the other two nodes, requiring an A/D band of size 2. As in the bi-directional case, the second wavelength will always be in an A/D band. However, there should be only two nodes with A/D bands on each wavelength since one wavelength is used to connect each pair of nodes. A valid band assignment with one node having 3 bands is shown in Fig. 5.5.

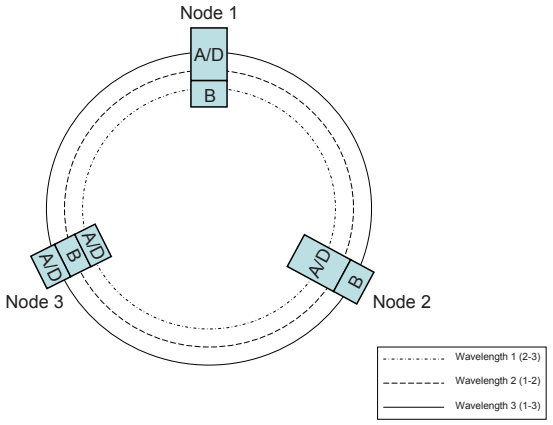

Figure 5.5: Illustration of banding in 3-node uni-directional ring, B:Bypass, A/D: Add/Drop

5.2.2 A Novel Framework for Band Optimization

Since we just showed that a single node cannot be considered in isolation and the network must be considered as a whole, we now proceed to formulate the band minimization problem in the following manner. Suppose the N nodes of a ring are numbered as $1, 2, \ldots, N$, and the W wavelengths numbered as $1, 2, \ldots, W$. Let β_n denote the number of wavebands at node n and $b_{n,i}$ denote the size of the i^{th} band at that node ($i = 1, \ldots, \beta_n$); so $\sum_{i=1}^{\beta_n} b_{n,i} = W \ \forall n$.

In a ring network, a wavelength is in either an A/D band or a B band. Let $\gamma_{w,n}$ be a binary variable representing which band wavelength w belongs to; if it's in a B band, $\gamma_{w,n} = 0$, and $\gamma_{w,n} = 1$ otherwise. Let Γ be the $W \times N$ binary matrix consisting of all the γ values. Given a deterministic traffic, a Routing and Wavelength Assignment (RWA) algorithm is used to provision the LPs; Γ is determined by the output of the RWA algorithm. Let r_w denote the row vector of Γ corresponding to wavelength w, and let c_n denote the column vector of Γ corresponding to node n.

While there is much literature on RWA algorithms, the goal is often to minimize the number of wavelengths required to support a given traffic. The output of the RWA algorithm has not been analyzed further from a banding point of view. For the results of a specific RWA algorithm that Γ represents, observe that runs of 1's or runs of 0's in a specific column, say c_n, represent opportunities for wavebanding at node n. Recall that a 0 represents B and 1 represents A/D, so a string of consecutive 0's (respectively, 1's) in a column means that all of those corresponding consecutive wavelengths are bypassed (respectively, added/dropped) at node n, and hence can be switched as a single band. From this point of view, the number of bands at node n can be obtained by simply counting the strings of consecutive 1's and 0's in column c_n. Let us denote the total number of bands in the ring network as B, i.e., $B = \sum_{n=1}^{N} \beta_n$. Here, we illustrate the calculation of bands using the example of Fig. 5.4(b). For the given RWA, Γ is obtained as:

$$\Gamma = \begin{pmatrix} 1 & 1 & 1 & 1 & 0 \\ 0 & 1 & 0 & 1 & 1 \\ 1 & 0 & 1 & 0 & 1 \end{pmatrix}. \tag{5.1}$$

The number of bands at each node with this configuration can be found as: $\beta_1 = 3, \beta_2 = 2, \beta_3 = 3, \beta_4 = 2, \beta_5 = 2$, and the total number of bands is $B = 12$. If banding were not done, then each of the 3 wavelengths would be switched independently at each node, leading to a total of 15 ports, so we get a saving of 3 ports, across the network. Can we do better? Suppose that the wavelength assignment is the same but the order of wavelengths is different. The following matrix shows Γ with the first and second rows (wavelengths) switched.

$$\Gamma' = \begin{pmatrix} 0 & 1 & 0 & 1 & 1 \\ 1 & 1 & 1 & 1 & 0 \\ 1 & 0 & 1 & 0 & 1 \end{pmatrix} \tag{5.2}$$

The number of bands now is $\beta_1 = 2, \beta_2 = 2, \beta_3 = 2, \beta_4 = 2, \beta_5 = 3$, giving $B = 11$. Thus, the number of bands can be optimized by reordering the wavelengths assigned to LPs by an RWA algorithm.

5.2.3 Problem Definition, Complexity, and Heuristics

The Band Minimization Problem can now be posed as the problem of reordering the rows of a given matrix Γ to obtain a new matrix Γ' so that the total number of consecutive runs of 1's and 0's in each column, summed over all columns is minimized.[2] It turns out that this problem is almost identical to a well-known problem in the low-power chip design community known as the *Data Ordering Problem*. The problem was first defined in [47] as follows: Given a binary matrix, a *transition* in a column vector is defined as the number of changes from 1 to 0 or vice versa. From this definition, the number of transitions in c_n is one less than the number of bands (β_n) at node n. Hence, the total number of transitions $\tau = B + N$. The number of transitions between two row vectors of wavelengths i and j is the Hamming distance between the binary vectors r_i and r_j. The Data Ordering Problem (DOP) is stated as: Find a permutation σ of the row vectors $r_1, r_2, \ldots, r_W$ of Γ such that the total number of transitions $\tau = \sum_{i=1}^{W-1} d(r_{\sigma(i)}, r_{\sigma(i+1)})$ is minimized. It is shown in [47] that the DOP is NP-complete.

We note that the matrix Γ may sometimes contain don't cares rather than just 1's and 0's. Such a situation will occur, for example, when not all wavelengths are occupied on all links for a given deterministic traffic, and so there are some band switches that don't have to be set to either B or A/D. Under this situation, a more complex problem called as *Band Minimization Problem with Don't Cares* arises. There are some results for the related Data Ordering Problem with Don't Cares in the literature [48], but we will defer further discussion on this problem to future work.

5.2.3.1 Characterization of the Problem

We show how the Data Ordering Problem is related to some other well-known problems here. These relationships may be exploited to obtain improved solutions to the DOP. Specifically, we show how we can transform this problem into a *Minimum Weight Hamiltonian Path Problem* (MWHPP). We can construct a graph $G = (V, E)$ consisting of W nodes,

[2] Other banding problems, for example, the minimization of the maximum number of bands over all nodes, are possible, but are not considered in this dissertation.

each corresponding to one row of Γ. Every node of this graph is connected to every other node with an edge having the weight as the Hamming distance between the corresponding rows. Hence, the edge (v_i, v_j) has the weight $d(r_i, r_j)$ for every i and j. Then the Hamiltonian path that visits every node in this graph with the minimum total weight gives the solution to the DOP. In other words, the Minimum Weight Hamiltonian Path gives the permutation of the rows of Γ for the minimum number of transitions. Different from the general version of the MWHPP, the graph in this case is a complete graph K_W with the edge weights being integers. (As an aside, the NP-completeness of the DOP implies the NP-completeness of the MWHPP even for this special case.)

We now give an example for bi-directional ring with $N = 7$. The Γ matrix obtained by the RWA algorithm and the graph generated from Γ is shown in Fig. 5.6(a) and (b), respectively. The numbers on the edges of the graph in Fig. 5.6(b) denote the weights. The bold path shows the Minimum Weight Hamiltonian Path calculated on this graph with a total weight of 15. Therefore, the minimum number of bands for the bi-directional ring of 7 nodes is $15 + 7 = 22$.

$$\mathbf{\Gamma} = \begin{pmatrix} 1 & 1 & 0 & 0 & 1 & 0 & 0 \\ 1 & 0 & 1 & 0 & 1 & 1 & 0 \\ 0 & 1 & 1 & 0 & 0 & 1 & 0 \\ 1 & 0 & 0 & 1 & 1 & 0 & 1 \\ 0 & 1 & 0 & 1 & 0 & 1 & 1 \\ 0 & 0 & 1 & 1 & 0 & 0 & 1 \end{pmatrix}_{6\times 7}$$

(a)

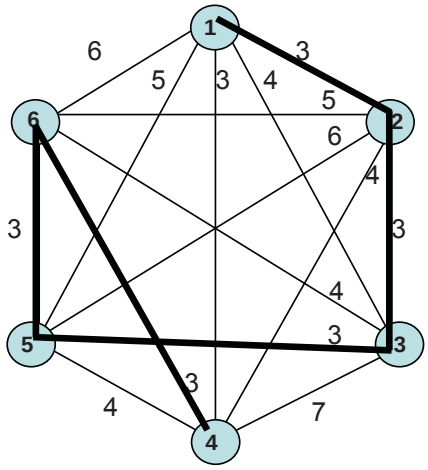

(b)

Figure 5.6: (a) The Γ of a 7-node bi-directional ring. (b) The graph G generated from Γ.

Further, the Minimum Weight Hamiltonian Path Problem can be transformed into the Traveling Salesman Problem (TSP) by adding a dummy node to the graph G and connecting this node to every node in the graph with edges of zero weight. A solution to

the TSP on this new graph G' is a solution to the MWHPP on G. We also note that the Hamming distances obey the triangular inequality which requires that for any i, j, and k, $d(r_i, r_j) + d(r_j, r_k) \geq d(r_i, r_k)$. This inequality is used to derive several approximation algorithms for the TSP. Specific versions of the approximation algorithms applied to the DOP are given in [47]. There is also a greedy heuristic introduced in [47] which is shown to give better results than the approximation algorithms. Several other methods for solving the DOP are summarized in [49]. However, the greedy heuristic of [47] is shown to be the most powerful one with less complexity [49]. Below, we develop our own heuristic algorithm and compare the results with the greedy heuristic and the optimum values for all-to-all traffic in Section 5.3.4. We first introduce our heuristic and then go on to describe the greedy heuristic of [47].

5.2.3.2 Our Heuristic

This is implemented with a recursive function which takes the matrix Γ as input. Given the row vectors of Γ, it takes a pivot vector and moves it to another row only if this reordering reduces the min_total_bands, which is the current minimum value obtained by the algorithm until that point. The output matrix of this reordering is denoted by Γ'. If a reordering occurs, min_total_bands is updated and the same procedure as above is applied to the new reordered matrix by recursively calling the same function with Γ' as the input matrix. All the row vectors r_i ($1 \leq i \leq W$) are used as a pivot vector starting with the first row r_1. When the algorithm stops, the value of min_total_bands gives the minimum total number of bands achieved by this algorithm. We show the outline of this heuristic in Algorithm 5.1. In Algorithm 5.1, calcBands is a function that computes the number of bands in the input matrix.

input : Γ

output: Γ' with reordered rows of Γ

1 *Initialization:* $min\_total\_bands =$ `calcBands` (Γ); $\Gamma' = \Gamma$;

2 `ReorderMatrix` (Γ);

Algorithm 5.1: Pseudocode for the our heuristic.

```
for p ← 1 to W − 1 do
    for i ← p + 1 to W do
        Form Matrix′ by moving r_p to insert after the row r_i
        if calcBands (Matrix′) ≤ min_total_bands then
            min_total_bands = calcBands (Matrix′)
            Γ′ = Matrix
            ReorderMatrix (Matrix)
```

Function `ReorderMatrix(`$Matrix$`)`

5.2.3.3 Greedy Heuristic

In this section, we explain the greedy heuristic introduced in [47]. We can first form the transition matrix Δ of size $W \times W$ whose elements $\delta_{i,j}$ are the Hamming distances between the rows of Γ r_i and r_j. The greedy algorithm initially takes the minimum element in this matrix, which is the pair of rows having the minimum Hamming distance between each other. This pair constitutes the initial sequence of rows. In the next step, it finds the rows having the minimum distances to the rows in the initial sequence. It adds these rows to the two ends of the sequence. At each step, it similarly finds the rows with the minimum distance to the rows at the ends of the sequence and adds these rows to the ends of the sequence. The algorithm stops when every row is included in the sequence.

5.3 Application To All-to-All Traffic

We now apply this problem formulation and the heuristic algorithms to a specific type of deterministic traffic, namely, all-to-all traffic. Recall that in all-to-all traffic, there is exactly one LP between every ordered pair of nodes. This traffic model, though simple, is quite powerful, because if the network is designed for this traffic, then any traffic pattern (with LPS arriving and departing dynamically) can be supported as long as it is a subset of all-to-all traffic, i.e., not more than one LP is required to be provisioned from one node to another node. We also derive a lower bound on the number of bands. We mostly focus on bi-directional rings, and turn to uni-directional rings at the end of this section.

For the bi-directional ring, we adopt the optimal RWA algorithm presented in which uses the minimum number of wavelengths. For simplicity, we assume that the number of nodes in the ring is odd (so that there is exactly one shortest path between any two nodes) and is denoted by N.[3] The optimal algorithm in [46] uses $(N^2-1)/8$ wavelengths for odd N. For reader convenience, we describe this algorithm in Section 5.3.1, because our bound depends on the algorithm. Every wavelength is fully utilized as a result of this algorithm (i.e., all of the wavelengths are busy on all links).

5.3.1 The Optimal RWA Algorithm

The algorithm in [46] works by assigning wavelengths to LPs connecting nodes that are placed on the ring, until all nodes are placed and therefore all LPs are established. Let n_i denote the number of nodes already placed at the beginning of step i. For odd N, this algorithm starts with assigning the wavelength 1 to connect the first three nodes as shown in Fig. 5.7(a) (i.e., $n_0 = 3$). At each step i, two more nodes (denoted by $\alpha_{i,1}$ and $\alpha_{i,2}$) are added to the ring from the previous step at those places of a cut which divides the ring into two sides, one side having exactly one more node than the other. A wavelength is used to connect each node on the right side to $\alpha_{i,1}$ and $\alpha_{i,2}$; the same wavelength also connects $\alpha_{i,1}$ and $\alpha_{i,2}$ to a node on the left side. One more wavelength connects the remaining node on the left side to $\alpha_{i,1}$, $\alpha_{i,2}$; and $\alpha_{i,1}$, $\alpha_{i,2}$ directly to each other (e.g., wavelength 3 in Fig. 5.7(b)). The lightpaths formed at the end of step 1 are shown in Fig. 5.7(b). This procedure of adding two nodes at each step goes on until the required number of nodes N are added to the ring. This algorithm results in the minimum number of wavelengths which is $W = (N^2-1)/8$.

The above RWA algorithm determines the matrix Γ. Let us define π_i as a row (wavelength) of Γ with i 1's, and Π_i as the number of such rows in Γ.

Proposition 5.1. *The output matrix Γ of the optimal RWA algorithm in [46] has $(N-1)/2$ rows with 3 ones, $(N^2-4N+3)/8$ rows with 4 ones. (i.e., $\Pi_3 = (N-1)/2$, $\Pi_4 =$*

[3] For even N, the output of the optimal RWA algorithm have some wavelengths that are not utilized in some of the links, hence some of the switch configurations for those wavelengths are don't cares.

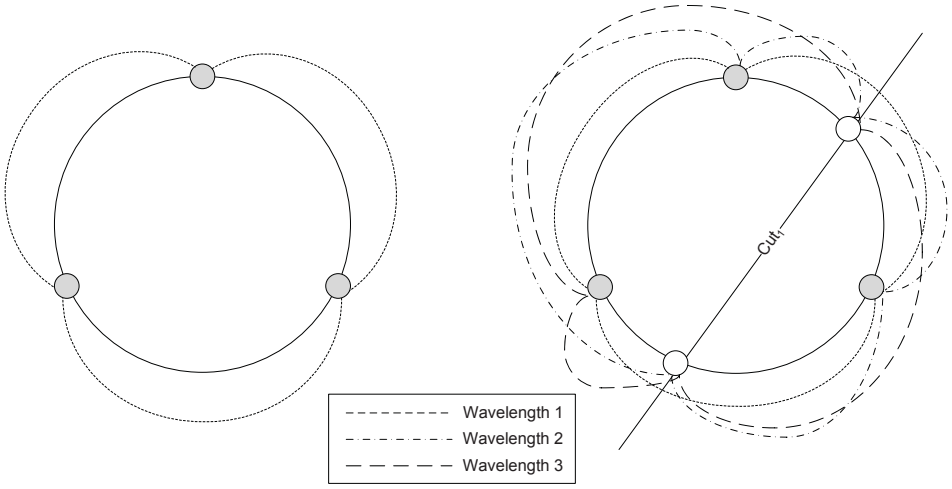

Figure 5.7: Illustration of the optimal RWA algorithm for bi-directional rings: (a) initial three nodes, (b) first step with adding two more nodes.

$(N^2 - 4N + 3)/8$, *and* $\Pi_i = 0 \ \ \forall i \neq 3, 4$*).*

Proof. In the algorithm, initially (i.e., $i = 0$) there are 3 nodes and at each step two more nodes are added. Therefore, there are a total of $(N - 3)/2$ steps. Initially, there are three lightpaths on the first wavelength, hence the first row of Γ is a π_3. At each step $i, i > 0$, there is one new wavelength with three lightpaths (the wavelength used to connect the two new nodes to each other, see wavelength 2 in Fig. 5.7(b)). The number of wavelengths with 3 lightpaths (i.e., the number of rows with three 1's) is $\Pi_3 = \sum_{i=0}^{(N-3)/2} 1 = (N - 1)/2$. At each step i, a single wavelength is used to connect the new nodes to a pair of old nodes on different sides of the cut, thus creating a wavelength with 4 lightpaths (i.e., π_4). Note that at the beginning of step i, there are $2i + 1$ nodes. The number of wavelengths added at step i is $((2i + 1) - 1)/2 = i$ since one new wavelength for a pair of old nodes is used. Therefore, $\Pi_4 = \sum_{i=1}^{(N-3)/2} i = (N^2 - 4N + 3)/8$. To verify the result, we calculate $\Pi_3 + \Pi_4$ to get $(N^2 - 1)/8$ which is the number of wavelengths used by this algorithm. □

We use this proposition in the derivation of the lower bound in Section 5.3.2.

5.3.2 Lower Bound for Bi-directional Rings

Let $t_{i,j}$ be the minimum number of transitions between a row with i ones and a row with j ones. The minimum number of transitions depends on a special property of the Γ matrix. Since it is all-to-all traffic and each pair of nodes is assigned only one wavelength, no two rows can have a sequence starting with a 1 followed by some 0's and ending with a 1, with the 1's exactly in the same positions. For example, Γ cannot have the two rows in (5.3) at the same time because they both contain the sequence $1\ 0\ 1$ at the same positions.

$$\begin{pmatrix} 0 & 1 & 0 & 1 & 1 \\ 1 & 1 & 0 & 1 & 0 \end{pmatrix} \tag{5.3}$$

Using this property, we can find at most how many ones can be at the same positions in any two rows, and hence find the minimum number of bands. We can easily see that between two π_4's, there are at most two 1's at the same positions. The remaining two 1's have to be at different positions, hence there are at least 4 transitions between π_4's (i.e., $t_{4,4} = 4$). If we consider two π_3's, it is trivial to find that the positions of two 1's can remain unchanged resulting in $t_{3,3} = 2$. Knowing that if we have a π_4, we can again at most hold the positions of at most two 1's between a π_4 and π_3. However, in this case the minimum number of transitions is three (i.e., $t_{3,4} = 3$).

Theorem 5.1 (Lower Bound on the Number of Bands in a Bi-directional Ring)**.** *A lower bound on the number of bands in a bi-directional ring with N nodes (N odd) is*

$$L = \frac{N^2 - 7}{2}.$$

Proof. Suppose we are given Π_3 rows with 3 ones and Π_4 rows with 4 ones ($\Pi_3, \Pi_4 > 1$). We want to construct a matrix consisting of these rows with the minimum number of transitions. We start with the initial matrix Γ_1 consisting of only π_4's. We want to insert a row π_3 between the rows of the initial matrix. There are two possible cases of this insertion. The first case is inserting π_3 at the top or bottom of the matrix. The second case is inserting π_3 in between any pair of π_4's. We note that the initial total number of transitions τ_1 in Γ_1 is $(\Pi_4 - 1)t_{4,4} = 4\Pi_4 - 4$. In the first case, the new transition count

becomes $\tau_2 = \tau_1 + t_{3,4} = 4\Pi_4 - 1$. In the second case, with this insertion it removes a transition between a pair of π_4's and adds two transitions between π_4 and π_3. Hence, the new transition count is $\tau_2 = \tau_1 - t_{4,4} + 2t_{3,4} = 4\Pi_4 - 2$. Note that τ_2 obtained in the second case is smaller than in the first case. Suppose we continue with the construction of the matrix as follows.

Suppose that at step i of the construction, we are inserting the i^{th} π_3 into the matrix Γ_i with transition count τ_i and Γ_i has π_4's at the top and bottom. The following cases arise:

1. *Insertion to either top or bottom of* Γ_i: $\tau_{i+1} = \tau_i + t_{3,4} = \tau_i + 3$
2. *Insertion between a pair of* π_4*'s*: $\tau_{i+1} = \tau_i - t_{4,4} + 2t_{3,4} = \tau_i + 2$
3. *Insertion between a pair of* π_3*'s*: $\tau_{i+1} = \tau_i - t_{3,3} + 2t_{3,3} = \tau_i + 2$
4. *Insertion between a* π_3 *and a* π_4: $\tau_{i+1} = \tau_i - t_{3,4} + t_{3,3} + t_{3,4} = \tau_i + 2$

Note that except the first case in which transition count increases by 3, the increment in transition count is 2. Therefore at every step, in order have minimum transition count in the matrix, we can insert π_3 to every position other than top and bottom without a difference in the total transition count. Therefore, Γ_{i+1} will have π_4's at top and bottom. By induction, we say that as long as we have two π_4's at top and bottom, the ordering within the matrix will not matter and will always give the minimum number of transitions. Since the increment of each step on the transition count is 2, the minimum total number of transitions is $\tau = \tau_1 + 2\Pi_3 = 4\Pi_4 + 2\Pi_3 - 4$.

Given that $\Pi_3 = (N-1)/2$ and $\Pi_4 = W - \Pi_3$, where $W = (N^2-1)/8$ by Proposition 5.1 , the minimum total number of transitions is

$$\tau = 4(W - \Pi_3) + 2\Pi_3 - 4 = \frac{N^2-1}{2} - N - 3. \tag{5.4}$$

We then obtain the lower bound as

$$L = \tau + N = \frac{N^2-1}{2} - 3 = \frac{N^2-7}{2}. \tag{5.5}$$

□

5.3.3 Optimal Solution for Uni-directional Rings

For uni-directional rings, a total of $\binom{N}{2}$ wavelengths are required and the same wavelength is used for the lightpaths between nodes s and d (i.e., one LP from s to d and another from d to s). In this case, we do not need to use the methods explained above since an optimal construction of the Γ matrix can be obtained using combinatorial methods. We know that for a uni-directional ring, every row of Γ contains only two 1's. The problem of band minimization can be seen to be identical to the construction of Gray codes of length N with a fixed number of ones. Such Gray codes are also known as Gray codes for combinations [50]. The minimum number of transitions between a pair of rows with two 1's each is 2, since at least one 1 has to be at a different position. A Gray code with this property is obtained by first generating a binary reflected Gray code of size N, and then deleting all the rows with different number of ones than 2. The remaining sequence gives the list of all rows with exactly two 1's in each row [51]. A revolving door algorithm is introduced in [52] which generates the same output codewords with a fixed number of ones. We give an example with $N = 4$ and the binary reflected code generated is shown in Fig. 5.8.

0000	1100
0001	1101
0011	1111
0010	1110
0110	1010
0111	1011
0101	1001
0100	1000

Figure 5.8: Binary reflected gray code of size 4.

When the rows with number of ones other than two are deleted, the rows left behind forms the following matrix:

$$\Gamma = \begin{pmatrix} 0 & 0 & 1 & 1 \\ 0 & 1 & 1 & 0 \\ 0 & 1 & 0 & 1 \\ 1 & 1 & 0 & 0 \\ 1 & 0 & 1 & 0 \\ 1 & 0 & 0 & 1 \end{pmatrix}. \tag{5.6}$$

In this example, the number of transitions between each consecutive row is 2, and therefore the total number of transitions is $5 \times 2 = 10$. In general, the minimum number of transitions obtained by this construction is $\tau = 2(W-1)$ where $W = \binom{N}{2}$. We thus have the following result.

Theorem 5.2. *The total number of bands (switching elements) in a uni-directional ring network that are necessary and sufficient to support all-to-all traffic is* $B = 2(W-1)+N = N^2 - 2$.

5.3.4 Numerical Results

We compare the total number of non-uniform wavebands (i.e., switching elements) calculated by the optimal, greedy, and branch-and-bound algorithms to the total number of switching elements in a wavelength switching architecture (i.e., total number of wavelengths). In a wavelength-switched network, there are W switching elements (one for each wavelength) per node. Therefore, the total number of bands in the network is NW.

First, for a uni-directional ring, the number of wavelengths for all-to-all traffic $W = \binom{N}{2}$, so the number of switches for wavelength-switching is $NW = \frac{N^2(N-1)}{2}$. Compare this with the number of switches with band-switching, which is given by $B = N^2 - 2$ (from Section 5.3.3). Therefore, the reduction in the number of switches (over the entire network) is $N^2\frac{(N-3)}{2} + 2$. For example, a 10-node ring requires $W = 45$ wavelengths, and 450 wavelength switches, but only 98 band switches leading to a 78% reduction in the number of switches. The results get better as the network size increases; for example, a 20-node ring would require 3800 switches with wavelength-switching but only 398 switches

with band switching, a 90% reduction in the number of ports. We show the results for uni-directional ring obtained by the optimal construction method in Table 5.1.

Table 5.1: The number of bands in a uni-directional ring.

N	W	WXC	Non-Uniform BXC	Reduction
2	1	2	2	0%
3	3	9	7	22%
4	6	24	14	42%
5	10	50	23	54%
6	15	90	34	62%
7	21	147	47	68%
8	28	224	62	72%
9	36	324	79	76%
10	45	450	98	78%
11	55	605	119	80%
12	66	792	142	82%
13	78	1014	167	84%
14	91	1274	194	85%
15	105	1575	223	86%
16	120	1920	254	87%
17	136	2312	287	88%
18	153	2754	322	88%
19	171	3249	359	89%
20	190	3800	398	90%
30	435	13050	898	93%
40	780	31200	1598	95%

We next present results for bi-directional ring in Table 5.2. Compared to wavelength-switching (WXC), we see that the reduction in bands is significant starting at 27% for $N = 5$ and increasing with increasing N. Optimal results were obtained (by solving an integer-linear program using ILOG CPLEX 9.0) only until $N = 15$ due to the computation complexity. We also see that Branch-and-bound heuristic and greedy heuristic give very close to optimal results. Additionally, the optimal values are very close to the lower bound. For $N \geq 11$, the greedy heuristic achieves the lower bound and hence gives optimum results. In the same range, the Branch-and-bound heuristic calculates the number of bands as two more than the lower bound. However, for $N = 7$ the Branch-and-bound heuristic achieves the optimum value whereas the greedy heuristic's result is one more than the optimum. The last column shows the further reduction achieved by the greedy heuristic

from the bands in the initial Γ (i.e., the unoptimized Γ resulting from the RWA algorithm).

We can see the percentage reduction in number bands with non-uniform waveband switching in Fig. 5.9. We observe that the reduction percentage increases very fast at the beginning with smaller N and the increase rate slows down at higher values of N.In Fig. 5.9, we also see that the rate of increase is very fast at the beginning and starts to slow down with higher values of N. Compared to the bi-directional ring the reduction in number bands is higher for the uni-directional ring. The difference can be as high as 20% for most values of N.

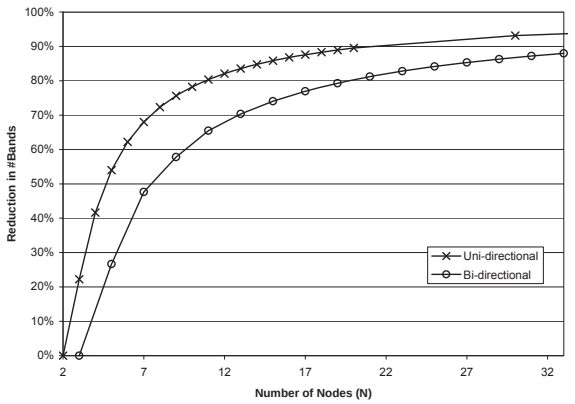

Figure 5.9: The comparison of reduction ratio in number of wavebands for uni-directional and bi-directional ratio.

5.4 Application to Dynamic Stochastic Traffic

In the considered dynamic traffic model, lightpath requests arrive according to a Poisson process and they have exponential holding times, and the load is uniform across all node-pairs. Lightpath establishment requires a wavelength that is available end-to-end with available waveband switches on each node along the route.

We apply the non-uniform bands calculated for deterministic all-to-all traffic to the case of dynamic traffic. The actual number of wavelengths (W_a) in the system can be different from the minimum number of wavelengths required for all-to-all traffic. We assume $W_a \geq W$. For $W_a > W$, the bands calculated can be proportionally expanded depending on the

ratio W_a/W as explained here. Define $x = W_a \mod W$ and $y = \lfloor W_a/W \rfloor$. Given the matrix Γ for all-to-all traffic, x rows of Γ are duplicated y times and $W - x$ rows $y - 1$ times. π_4's have the priority to be among the selected x rows. We call the resulting matrix as Γ_R.

We also compare two cases of non-uniform banding. In the first case, a waveband can only be used to do add/drop or bypass as designated by Γ. We call this case as *fixed* non-uniform wavebands. The second case, in which every band can be configured to do add/drop or bypass on demand (but the band itself is fixed, i.e., at any given time the whole band can be either A/D or B) is just called non-uniform wavebands. We note that in the first case, a lightpath for a source destination pair can only be established at the wavelength(s) that is designated by Γ for that particular pair.

We adapt a first-fit wavelength assignment strategy among the available wavelengths for uniform wavebands and fixed non-uniform banding. For non-uniform wavebands, we modify the first-fit strategy as follows. Let $w_{k,i,j}$ be the k^{th} wavelength for the pair of nodes i and j given that there are $\Omega_{i,j}$ such wavelengths designated in Γ_R. Whenever, there is a lightpath request for the node pair (i, j), it first tries to establish the lightpath on the $w_{k,i,j}$ starting from $k = 1$ to $k = \Omega_{i,j}$. If no such wavelength is available, a first-fit strategy is applied on the remaining wavelengths.

5.4.1 Numerical Results

We compare the performance of non-uniform banding with uniform banding in a 19-node bi-directional ring network in this section. We do not show results for uni-directional rings since they are similar. We ran simulations using 10^6 call arrivals. The load per route and per wavelength is denoted by ρ.

In Fig. 5.10, we plot blocking probability vs. load for $W_a = 90$. The number of non-uniform wavebands calculated for $N = 19$ (see Table 5.2) is 177. We plot the curves for 171 and 190 number of uniform wavebands, corresponding to 9 and 10 wavebands per node with sizes of 10 and 9, respectively. We see that non-uniform wavebands perform better than uniform wavebands (for both 171 and 190 wavebands) for higher loads. For lower

loads (e.g. $\rho = 0.001$), non-uniform wavebands performs the same as uniform with 190 bands. We note that except for lower loads, fixed non-uniform wavebands performs the same as non-uniform wavebands.

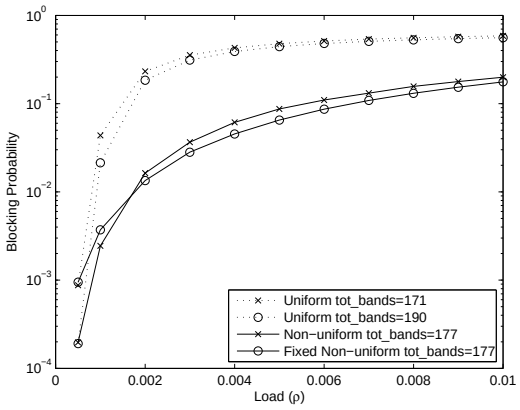

Figure 5.10: Blocking probability vs. load in a 19-node ring for $W_a = 90$.

In Fig. 5.11(a), we plot blocking probability vs. number of uniform wavebands per node for $W_a = 90$. The straight lines correspond to the blocking value obtained with non-uniform wavebands with 9.3 bands per node on average ($b_{max} = 13$, $B = 177$) with different load values. We see that for $\rho = 0.003$, even 18 uniform bands per node ($B = 342$) performs worse than non-uniform banding with half that number of bands per node. For a lower load value ($\rho = 0.001$), the performance of non-uniform banding lies in between the values of uniform banding with 10 and 15 wavebands. With higher loads, more uniform wavebands are required to have the same performance as non-uniform wavebands.

In Fig. 5.11(b), we plot blocking probability vs. number of wavelengths (W_a) for two different load values. For $\rho = 0.001$, for lower W_a, uniform wavebands performs better than non-uniform wavebands. This is due to the fact that, with lower W_a that are closer to W, the probability of a duplicate lightpath (multiple lightpaths on the same route) being blocked is very high since with the non-uniform switch configurations there is a limited set of available wavelengths for any route. However, we see that with higher W_a, non-uniform banding starts to perform better for $W_a > 80$. For $\rho = 0.003$, non-uniform banding starts to perform better than uniform for $W > 45$. In general, the performance of non-uniform banding gets better with higher W_a, whereas the performance of uniform banding gets

worse.

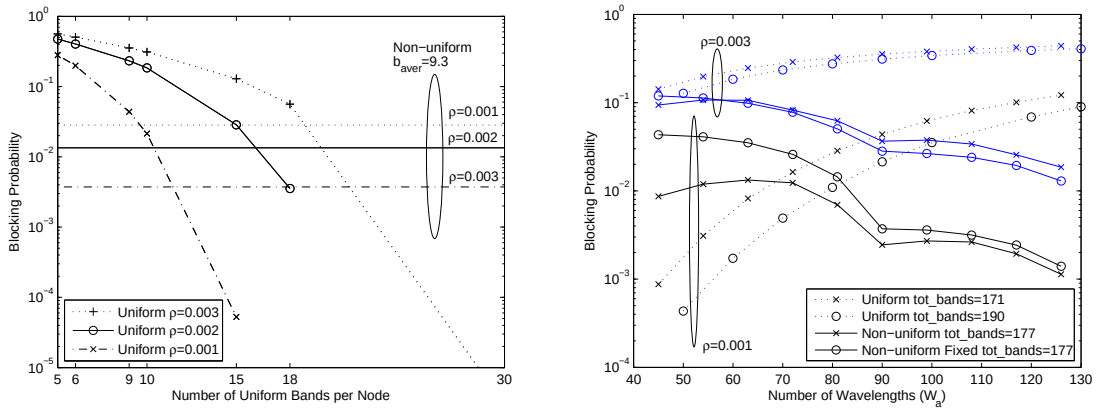

(a) (b)

Figure 5.11: Blocking probability vs. (a) number of uniform wavebands for $W_a = 90$, and (b) number of wavelengths in a 19-node ring.

5.5 Summary

Wavebanding saves port costs in optical crossconnects by grouping together wavelengths and switching them as a band. Optimal ways of waveband switching for ring networks are shown in this chapter. We introduce a novel framework to minimize the number of non-uniform wavebands to support a deterministic traffic in ring networks and presented algorithms that attempted to optimize the number of bands. We then considered all-to-all traffic and obtained a theoretical lower bound for bi-directional rings and an optimal solution for uni-directional rings. The results showed a significant reduction in the number of switches over the entire network. We also evaluated the performance with dynamic stochastic traffic and showed that non-uniform wavebanding is advantageous over uniform wavebanding in most cases in terms of blocking probability metric.

Table 5.2: Results for a bi-directional ring with all-to-all traffic.

N	W	WXC	Non-Uniform BXC					Reduction in #switches			Reduction after Γ
			Lower Bound	Optimal	Our Heuristic	Greedy	Bands in Γ	Optimal	Our Heuristic	Greedy	
5	3	15	9	11	11	11	11	27%	27%	27%	0%
7	6	42	21	22	22	22	27	48%	48%	48%	19%
9	10	90	37	37	37	38	47	59%	59%	58%	19%
11	15	165	57	57	59	57	71	65%	64%	65%	20%
13	21	273	81	81	83	81	99	70%	70%	70%	18%
15	28	420	109		111	109	131		74%	74%	17%
17	36	612	141		143	141	167		77%	77%	16%
19	45	855	177		179	177	207		79%	79%	14%
21	55	1155	217		219	217	251		81%	81%	14%
23	66	1518	261		263	261	299		83%	83%	13%
25	78	1950	309		311	309	351		84%	84%	12%
27	91	2457	361		363	361	407		85%	85%	11%
29	105	3045	417		419	417	467		86%	86%	11%
31	120	3720	477		479	477	531		87%	87%	10%
33	136	4488	541		543	541	599		88%	88%	10%

Chapter 6

Conclusions

While optical networks have been deployed as backbone telecommunication networks for a while, the concept of Reconfigurable Optical Networks has been recently developed in order for network operators to offer more flexible and cheaper service. In this dissertation, we looked into the core of this technology and focused on the specific components which enable it. We asked the question ”How much reconfigurability is sufficient?” and provided an answer for that. After that, we focused on network design to achieve better performance and lower cost.

The optical components required for reconfigurability are Reconfigurable Optical Add/ Drop Multiplexers (ROADMs). These constitute the optical nodes in the network and they regulate the wavelengths that are terminated or bypassed at those nodes. The reconfiguration of the entire network is done by individually adjusting these ROADMs to terminate or add/drop the required set of wavelengths. Each reconfigurable node also requires tunable transponders to convert the optical signal to electrical signal or vice versa. Noting that the tunability of such transponders limits the reconfigurability of a node, our initial question on the sufficient amount of reconfigurability is in this case transformed into ”what size of tuning range is sufficient?”. In order to answer that, we developed an analytical model to calculate the blocking probability which is a common performance metric. Lightpath requests that cannot be established due to insufficient resources (either wavelengths or transponders) are considered blocked and dropped. Our analytical model takes into account the tuning range and the number of transponders other than the number of wavelengths available on each link. We developed a recursive procedure to calculate the blocking for every route in the network. We utilized various probabilistic concepts such as Markovian models to model lightpaths crossing each node. At the end nodes of a route, we model the availability of limited tunable transponders. We confirmed our model by comparing with simulation

results and observed that they matched very well. Our model works with any arbitrary topology. The major conclusion reached is that the blocking probability keeps dropping with increasing values of tuning range only until a certain point and after that point it stays constant. This is the answer we were looking for which points out that we do not need full reconfigurability but limited reconfigurability is sufficient. Numerically, we have shown that a tuning range of 4 to 8 is sufficient in a 32-wavelength system. We also showed that the number of transponders per node is a stronger factor in determining performance.

We then asked if we can improve the performance by choosing wavebands for limited tunable transponders at different nodes. We note that a lightpath can only be established if there are available transponders tunable to one of the end-to-end available wavelengths. If not, the lightpath has to be blocked. We showed that if we choose these wavebands in a fashion that they have the same wavebands at every node, the blocking is significantly reduced for lightly loaded networks. We then applied the waveband assignment problem for the case of non-uniform traffic. In such a traffic scenario, the routes with higher loads are given priority to be assigned wavebands for the transponders at their terminal nodes. We formulated this as an optimization problem with the objective to minimize the maximum load on the common links shared by such highly loaded routes. We developed optimal and near-optimal (but more computationally efficient) solutions by which we showed the blocking can be reduced significantly using several traffic scenarios. We concluded that highest improvement is achieved with fixed transponders and limited tunable transponders with small tuning range. A limited reconfigurable ROADM designed specifically for the chosen wavebands of transponders was also proposed with fewer number of switching ports.

We also investigated a method called *multihopping* to improve the performance of limited reconfigurable optical networks. It is done by dropping a wavelength at a ROADM, and after conversion to electric signal by a transponder we add the signal on another wavelength using another transponder (i.e., O-E-O conversion). We developed a graph formulation to solve the alternate multihop routing problem when limited tunable transponders are used. The algorithm chooses the best route with the most available transponders along. The results show that this method efficiently utilizes the resources of the network and re-

duces the blocking compared to alternate routing without multihopping and fixed routing schemes. We also analyzed waveband assignment policies together with multihopping to decide which one is more effective on the performance. Results show that most improvement was obtained by the transponder waveband assignment policies.

Last but not the least, we studied the *waveband switching* method to reduce the switching costs of the network. In waveband switching, we group wavelengths into wavebands as much as possible and switch these wavelengths as a single waveband. We provided solutions to do waveband switching optimally in ring networks. The objective of the optimization problem was to reduce the number of bands in the network and hence reduce the sizes of the switches. Our results show that the sizes of switches can be reduced by a large amount using waveband switching compared to wavelength switching.

Overall, this dissertation provides a detailed analysis on the performance of reconfigurable optical networks and investigates several design methods to improve the performance and reduce the cost. Results presented for the proposed techniques confirm that these objectives were met.

Bibliography

[1] K. Tse, "AT&T's photonic network," in *Proc. OFC/NFOEC*, March 2008.

[2] L. Eldada *et al.*, "40-channel ultra-low-power compact PLC-based ROADM subsystem," in *Proc. OFC*, March 2006.

[3] J. Tang and K. Shore, "Wavelength-routing capability of reconfigurable optical add/drop multiplexers in dynamic optical networks," *IEEE/OSA J. Lightwave Tech.*, vol. 24, no. 11, pp. 4296–4303, Nov. 2006.

[4] M. Mezhoudi *et al.*, "The value of multiple degree roadms on metropolitan network economics," in *Proc. OFC*, March 2006.

[5] B. P. Keyworth, "ROADM subsystems and technologies," in *Proc. OFC*, March 2005.

[6] K. Grobe, "Applications of roadms and control planes in metro and regional networks," in *Proc. OFC*, March 2007.

[7] C. A. Sayeed *et al.*, "Hybrid low loss architecture for reconfigurable optical add/drop multiplexer," in *Proc. Globecom*, November 2006.

[8] R. Ramaswami and K. N. Sivarajan, *Optical Networks: A Practical Perspective*. Morgan Kaufmann, 1998.

[9] L. Parascbis, O. Gerstel, and R. Ramaswami, "Evaluation of tunable laser applications in metropolitan networks," in *Proc. OFC*, Feb. 2004.

[10] Finisar. [Online]. Available: http://www.finisar.com

[11] L. Noirie, M. Vigoureux, and E. Dotaro, "Impact of intermediate traffic grouping on the dimensioning of multi-granularity optical networks," in *Proc. OFC*, Mar. 2001.

[12] X. Cao, V. Anand, and C. Qiao, "A study of waveband switching with multilayer multigranular optical cross-connects," *IEEE J. Sel. Areas Commun.*, vol. 21, no. 7, pp. 1081–1095, Sep. 2003.

[13] P. Ho and H. Mouftah, "Routing and wavelength assignment with multigranularity traffic in optical networks," *IEEE/OSA J. Lightwave Tech.*, vol. 20, no. 8, pp. 1292–1303, Aug. 2002.

[14] M. Lee, J. Yu, Y. Kim, C. Kang, and J. Park, "Design of hierarchical crossconnect WDM networks employing a two-stage multiplexing scheme of waveband and wavelength," *IEEE J. Sel. Areas Commun.*, vol. 20, no. 1, pp. 166–171, Jan. 2002.

[15] X. Cao, V. Anand, and C. Qiao, "Waveband switching for dynamic traffic demands in multigranular optical networks," *IEEE/ACM Trans. Netw.*, vol. 15, no. 4, pp. 957–968, Aug. 2007.

[16] M. Li, W. Yao, and B. Ramamurthy, "A novel cost-efficient on-line intermediate waveband-switching scheme in WDM mesh networks," in *Proc. IEEE Globecom*, Nov./Dec. 2005, pp. 2019–2023.

[17] Y. Suemura, I. Nishioka, Y. Maeno, S. Araki, R. Izmailov, and S. Ganguly, "Hierarchical routing in layered ring and mesh optical networks," in *Proc. ICC*, Apr. 2002, pp. 2727–2733.

[18] R. Izmailov, S. Ganguly, V. Kleptsyn, and A. Varsou, "Non-uniform waveband hierarchy in hybrid optical networks," in *Proc. IEEE Infocom*, San Francisco, CA, Mar. 2003, pp. 1344–1354.

[19] L. Chen, P. Saengudomlert, and E. Modiano, "Uniform vs. non-uniform band switching in WDM networks," in *Proc. BroadNets*, Oct. 2005, pp. 204–213.

[20] T. Hsieh, N. Barakat, and E. H. Sargent, "Banding in optical add-drop multiplexers in WDM networks: Preserving agility while minimizing cost," in *Proc. ICC*, June 2003, pp. 1397–1401.

[21] H. Zhu and B. Mukherjee, "Online connection provisioning in metro optical WDM networks using reconfigurable OADMs," *IEEE/OSA J. Lightwave Tech.*, vol. 23, no. 10, pp. 2893–2901, Oct. 2005.

[22] G. Shen *et al.*, "The impact of number of transceivers and their tunabilities on WDM network performance," *IEEE Commun. Lett.*, vol. 4, no. 11, pp. 366–368, Nov. 2000.

[23] G. Shen, S. Bose, T. Cheng, C. Lu, and T. Chai, "The impact of the number of add/drop ports in wavelength routing all-optical networks," *Optical Networks Magazine*, pp. 112–122, Sep./Oct. 2003.

[24] B. Schein and E. Modiano, "Quantifying the benefit of configurability in circuit-switched WDM ring networks with limited ports per node," *IEEE/OSA J. Lightwave Tech.*, vol. 19, no. 6, pp. 821–829, June 2001.

[25] R. A. Barry and P. A. Humblet, "Models of blocking probability in all-optical networks with and without wavelength changers," *IEEE J. Select. Areas Commun.*, vol. 14, no. 5, pp. 858–867, June 1996.

[26] A. Birman, "Computing approximate blocking probabilities for a class of all-optical networks," *IEEE J. Select. Areas Commun.*, vol. 14, no. 5, pp. 852–857, June 1996.

[27] S. Subramaniam, M. Azizoğlu, and A. K. Somani, "All-optical networks with sparse wavelength conversion," *IEEE/ACM Trans. Networking*, vol. 4, no. 4, pp. 544–557, Aug. 1996.

[28] B. Ramamurthy and B. Mukherjee, "Wavelength conversion in WDM networking," *IEEE J. Select. Areas Commun.*, vol. 16, no. 7, pp. 1061–1073, Sep. 1998.

[29] Y. Zhu, G. N. Rouskas, and H. Perros, "Blocking in wavelength routing networks, part I: The single path case," in *Proc. Infocom*, March 1999, pp. 321–328.

[30] A. Sridharan and K. N. Sivarajan, "Blocking in all-optical networks," in *Proc. Infocom*, March 2000, pp. 910–919.

[31] V. Tamilraj, S. Subramaniam, K. Sivalingam, and H. Krishnamurthy, "Performance evaluation of optical cross-connect architectures with tunable transceivers," in *Proc. ONDM*, Feb. 2005, pp. 477–82.

[32] B. Mukherjee, D. Banerjee, S. Ramamurthy, and A. Mukherjee, "Some principles for designing a wide-area wdm optical network," *IEEE/ACM Trans. Netw.*, vol. 4, no. 5, pp. 684–696, Oct. 1996.

[33] Ilog cplex. [Online]. Available: http://www.ilog.com/products/cplex/

[34] R. Izmailov, A. Kolarov, R. Fan, and S. Araki, "Hierarchical optical switching: A node-level analysis," in *Proc. HPSR*, May 2002, pp. 309–313.

[35] X. Chu and B. Li, "Dynamic routing and wavelength assignment in the presence of wavelength conversion for all-optical networks," *IEEE/ACM Trans. Networking*, vol. 13, no. 3, pp. 704–714, Jun. 2005.

[36] T. Ye *et al.*, "On-line integrated routing in dynamic multifiber IP/WDM networks," *IEEE J. Select. Areas Commun.*, vol. 22, no. 9, pp. 1681–1691, Nov. 2004.

[37] H. Zang, J. Jue, and B. Mukherjee, "A review of routing and wavelength assignment approaches for wavelength-routed optical WDM networks," *Optical Networks Magazine*, vol. 1, no. 1, Jan. 2000.

[38] R. Ramaswami and K. N. Sivarajan, *Optical Networks: A Practical Perspective*. Morgan Kaufmann, 2001.

[39] J. Simmons, *Optical Network Design and Planning*. Springer Verlag, 2008.

[40] T. Wang, P. N. Ji, L. Zong, and O. Matsuta, "Flexible band tunable add/drop multiplexer and modular optical node architecture," U.S. Patent 0 281 558, Dec. 22, 2005.

[41] P. Ho, H. Mouftah, and J.Wu, "A novel design of optical cross-connects with multi-granularity provisioning support for the next-generation internet," in *Proc. IEEE ICC*, May 2003, pp. 582–5875.

[42] B. Lekkala and B. Ramamurthy, "Discontinuous waveband switching in WDM optical networks," in *Proc. IEEE EIT'05*, May 2005.

[43] L. Chen, P. Saengudomlert, and E. Modiano, "Uniform vs. non-uniform band switching in WDM networks," *The International Journal of Computer and Telecommunications Networking*, vol. 50, no. 2, pp. 149–167, Feb. 2006.

[44] M. Al-naimi and S. Subramaniam, "Wavelength assignment in optical networks with limited reconfigurability," in *Proc. Globecom*, Nov 2007.

[45] O. Turkcu and S. Subramaniam, "Blocking in reconfigurable optical networks," in *Proc. Infocom*, May 2007.

[46] G. Ellinas, K. Balat, and G.-K. Chang, "A novel wavelength assignment algorithm for 4-fiber WDM self-healing rings," in *Proc. ICC*, June 1998, pp. 197–201.

[47] R. Murgai, M. Fujita, and S. Krishnan, "Data sequencing for minimum-transition transmission," in *Proc. IFIP Intl Conf. on VLSI*, Gramado, RS, Brasil, Aug. 1997, pp. 365–376.

[48] N. Drechsler and R. Drechsler, "Exploiting don't cares during data sequencing using genetic algorithms," in *ASP Design Automation Conf*, 1999, pp. 303–306.

[49] D. Logofatu and R. Drechsler, "Efficient evolutionary approaches for the data ordering problem with inversion," in *Lecture Notes in Computer Science*, vol. 3907. Springer Berlin / Heidelberg, Mar. 2004, pp. 320–331.

[50] C. Savage, "A survey of combinatorial gray codes," *SIAM Review*, vol. 39, no. 4, pp. 605–629, Dec. 1997.

[51] J. R. Bitner, G. Ehrlich, and E. M. Reingold, "Efficient generation of the binary reflected gray code and its applications," *Commun. ACM*, vol. 19, no. 9, pp. 517–521, 1976.

[52] A. Nijenhuis and H. S. Will, *Combinatorial Algorithms: For Computers and Hard Calculators*. Orlando, FL, USA: Academic Press, Inc., 1978.